Development of a Convective Cloud Field Model based upon Principles of Self-Organization

Dissertation
zur Erlangung des Doktorgrades
der Naturwissenschaften
im Fachbereich Geowissenschaften
der Universität Hamburg

vorgelegt von

Frank Josef Nober
aus Hattingen

Hamburg

2003

Als Dissertation angenommen vom Fachbereich Geowissenschaften
der Universität Hamburg

auf Grund der Gutachten von Herrn Priv. Doz. Dr. H.-F. Graf
und Herrn Prof. Dr. H. Graßl

Hamburg, den 16.04.2003

Prof. Dr. U. Bismayer
Dekan des Fachbereichs Geowissenschaften

Abstract The parameterization of cumulus convection is still one of the great challenges in global climate modeling. After several decades of climate research and simulation of global climate, there is no satisfactory treatment of cumulus clouds in today's GCMs (General Circulation Models). In fact, the entire "cloud description" in large scale models remains an unsolved problem.
This work attempts to describe essential statistical characteristics of convective cloud fields in GCMs. In the first chapter, as a motivation, a concrete example is given for the importance of a real physical description of convection in global climate models. Since the climate system is a highly non-linear system, even a small change in the latent heat release due to convective clouds can lead to large scale effects in the global circulation.
In the further chapters we propose a new Convective Cloud Field Model (CCFM). Chapter 2 gives, both a mathematical and conceptual description of the model based on fundamentals of population dynamics. First model results are presented. Since the model proposed in chapter 2 is by far too time consuming for larger global climate simulations, we have developed a reduced and effective model version which is described in chapter 3. This reduced model, although much less complex regarding to the numerical cost, shows a very similar behavior to the full model. Both model versions are compared with LES model simulations. Since we intended to run the reduced model in a global GCM mode we give in chapter 4 some basic results of global experiments done with the reduced model. We show also some statistical cloud field data provided by our model. Finally, we end up with chapter 5. Here we give our concluding remarks, some concrete perspectives on how to use our model for future research, and a more general prospective.

Jeder Mensch, seine Thätigkeit sei noch so sehr durch die Anforderungen des bürgerlichen Lebens auf einen bestimmten Kreis von Geschäften gewiesen, hat doch eine Seite, nach welcher er sich zur Natur verhält, und wäre es auch nur die, nach der er sie gewähren lässt, und wer kann sich ihr entziehen! Wenn Wochenlang der Himmel mit einem einförmigen Grau bedeckt ist, so werden am Ende auch wir trübe, wenn es endlich oben wieder hell wird, werden auch wir heiter. So sind wir ein treuer Spiegel des Himmels über uns, wir gehen ein in seine Launen, und jeder ist in diesem Sinne nicht nur ein Meteorologe, sondern so zu sagen die Meteorologie selbst. Aber dies passive Ergeben macht bald dem Bedürfniss Platz, die Sprache zu verstehen, in der die Natur zu uns redet, in dem Wechsel das Bestehende, in der scheinbaren Willkühr das Gesetz nachzuweisen. Denn wenn es überhaupt Aufgabe der Naturwissenschaft ist, in den besonderen Erscheinungen das Allgemeine aufzuzeigen, wir mögen es Kraft, Gesetz, Gattung oder wie wir wollen nennen, so scheint es natürlich auch in diesen Theile der Physik dieselbe Behandlungsart gelten zu machen, welche sich für andere Zweige der Wissenschaft als tüchtig bewährt hat.

Heinrich Wilhelm Dove (1803-1879)
in "Meteorologische Untersuchungen"
Berlin, 1837.

Contents

Chapter 1

Motivation

Sensitivity of the global circulation to the suppression of precipitation by anthropogenic aerosols [1]

Abstract From recent satellite observations it is evident that an increase in cloud condensation nuclei, for instance due to biomass burning, can substantially reduce rain efficiency of convective clouds. This is potentially important for the global climate since the release of latent heat due to condensation of water vapour and fallout of rain from cumulus convection is the most important source for available potential energy in the free troposphere. Furthermore, cumulus convection is a key process in controlling the water vapour content of the atmosphere. The sensitivity of the global climate with respect to alteration of rain efficiency of convective clouds due to the suppression of drop coalescence by anthropogenic aerosols is studied by using the atmospheric general circulation model ECHAM4. This paper presents results from a 15 year sensitivity study considering the aerosol effect on warm precipitation formation. Effects on ice processes are not yet included, and therefore the results likely underestimate the magnitude of the full effects due to suppression of precipitation. The instantaneous forcing is locally large (up to 100% reduction of precipitation and the related latent heat release) but confined to small areas leading to small large scale mean anomalies in the convective heating and therefore the vertical temperature gradient. We found a definite perturbation of the global circulation, showing distinct sensitivity to the impact of aerosols on suppressing rainfall.

1.1 Introduction

Cumulus convection is a key process in atmospheric dynamics. Atmospheric convection can be interpreted as a heat engine which transports energy from the heat source

[1] This chapter has been accepted for publication in *Global and Planetary Change*

at the surface to the heat sink in the free troposphere. Since the energy source of this convective heat engine is located at higher pressure than the sink, the system is capable of performing mechanical work by driving the most important features of atmospheric dynamics (i.e. the Walker and Hadley circulation). Therefore, convection is strongly linked to all dynamical processes via energy supply for the global circulation.

Understanding cumulus convection and representing it in an adequate way in atmospheric general circulation models (A-GCM) is therefore of paramount importance for climate simulation and prediction. In the context of A-GCMs, cumulus convection is not only interesting because of its importance for the climate system, but also because of its difficult treatment. Large scale numerical models, like A-GCMs, have grid cells with horizontal resolutions on the order of hundreds of kilometers, whereas single cumuli have diameters on the order of 1 - 10 km. Cumulus convection is therefore a typical sub grid-scale process which cannot be resolved explicitly. The representation of this unresolvable process is called cumulus parameterization and normally is based upon the resolved mean values of the grid.

While nature makes no principle distinction between the enormous variety of different cloud realizations in terms that they all obey the same physical laws of thermodynamics and fluid dynamics, models do so. A typical distinction (as realized in ECHAM4) [*Roeckner et al.*, 1996] consists of a stratiform cloud scheme and a cumulus convection scheme [*Tiedtke*, 1989]. The stratiform cloud scheme calculates the grid mean cloud cover fraction and is therefore responsible for the link between the hydrological cycle and radiation. Cumulus convection is associated with cumulus clouds which in general are smaller in their horizontal extent than stratiform clouds, but are much more developed in the vertical direction. Cumulus convection, in models as in ECHAM4, normally is not directly connected to radiation, assuming that cloud cover associated with cumulus clouds fills only a small fraction of a grid cell. In contrast to stratiform clouds, convection denotes strong vertical transport. During vertical mixing the release of latent heat by condensation of water vapour to cloud droplets and the fallout as rain is the most important source for available potential energy in the atmosphere.
Most current cumulus convection parameterizations in A-GCMs are based on a mass flux formulation [*Tiedtke*, 1989, *Arakawa and Schubert*, 1974]. Depending on different closure assumptions the schemes determine upward and downward mass fluxes which are responsible for the vertical transport of energy and humidity. While the treatment of microphysics in stratiform cloud schemes is essentially more sophisticated [*Lohmann and Feichter*, 1997, *Roelofs et al., 1998*, *Lohmann, et al.*, 1999], the representation of microphysics in convective clouds, especially the generation of rainfall, is quite simple at the moment. One reason for this imbalance might

be that, from the modelers point of view, cloud microphysics seems to have the largest impact on the model behavior via the connection to radiation. One result of this paper is that this is not true in general. In the past, the sensitivity of convection schemes to different microphysical formulations and its further impact on the model climate was not object of extended research [*Emanuel et al.*, 1998]. In the present study we will focus on this issue in a simplified, observation - based manner.

The investigation of aerosols and their direct and indirect effects on global climate is considered one of the most important issues in recent climate research due to their potential to partly reduce the effects of increasing greenhouse gases.
Aerosols interact in different ways with the climate system: The direct aerosol effects (scattering and absorption of solar and terrestrial radiation) and the indirect aerosol effects (modification of cloud radiative properties). Both classes can be subdivided according to the underlying physical mechanism:

Direct: - Back scattering of solar radiation due to aerosols leads to a reduction of net incoming solar radiation and therefore to a cooling of the climate system [*Penner et al.*, 1998, *Tegen et al.*, 1996, *Hobbs et al.*, 1997].
- Some aerosols, like black carbon absorb solar radiation, thereby heating the aerosol laden atmospheric layer. This can result either in a local reduction of cloud cover or can inhibit new cloud formation. This process was termed the "semi-direct" aerosol effect [*Hansen et al.*, 1997, *Ackerman et al.*, 2000].

Indirect: - The indirect effects of aerosols all are related to changes of the cloud droplet spectrum (in general, more and smaller cloud droplets due to high availability of aerosols which act as cloud condensation nuclei). This can influence the cloud albedo (first indirect effect) [*Lohmann and Feichter*, 1997, *Lohmann et al.*, 2000, *Twomey*, 1977], cloud lifetime (second indirect effect) [*Lohmann and Feichter*, 1997, *Albrecht*, 1989] and the precipitation formation process (and the related release of latent heat) especially in deep convective clouds which was first observed by [*Rosenfeld and Lensky*, 1998, *Rosenfeld*, 1999, *Rosenfeld*, 2000 a, *Rosenfeld and Woodley*, 2000] and modeled e.g. by [*Graf et al.*, 2001, *Khain et al.*, 2001].
We want to point out that the latter aerosol effect on convective heating (ACOH) is of totally different nature than the other mentioned indirect effects. The first and second indirect effect are caused via the connection between (layered) clouds and radiation, whereas ACOH works on the interrelation between convective clouds and the dynamics of atmospheric circulation.
The physical mechanism leading to the last mentioned indirect effect can be described as follows:

If a large number of CCN is available (e.g. in plumes from forest fires or large cities), clouds contain more and smaller droplets than those clouds which form in clean air. This, in principle, is the difference between continental clouds (more CCN) and maritime clouds (less CCN). In terms of the cloud droplet spectrum, maritime clouds have a broad spectrum with larger droplets, while continental cloud droplet spectra are narrow and their centres are shifted towards smaller radii.
High concentrations of CCN, and therefore a high cloud droplet number concentration (CDNC), reduce the diffusional droplet growth. Droplet sizes which are large enough for an efficient growth via droplet collision cannot be reached. Growth by collision of droplets in turn is the dominant growth process in warm clouds. As a result the production of warm rain (only the liquid water phase is involved) is strongly reduced or even stopped. In addition, the high amount of small droplets can also suppress the rain production in the mixed phase (water and ice). Freezing of small droplets is a very inefficient process and collision efficiencies between ice crystals and small droplets are negligible [*Pruppacher and Klett*, 1997]. If additionally the radius of the largest cloud droplets is reduced below the threshold of 12μ, which is required for primary and secondary ice generation [*Mossop and Hallet*, 1974, *Rangno and Hobbs*, 1994], the Bergeron - Findeisen process cannot play the major role for precipitation formation as it normally does. The reduction of these two leading precipitation formation processes (collision growth and Bergeron - Findeisen process) finally results in enhanced detrainment of cloud water and ice at cloud tops [*Khain et al.*, 2001].

Early observations concerning the effect of reduced rain due to a large amount of aerosols in the atmosphere e.g. from cities or industrial sources were reported up to 30 years ago [*Warner*, 1968, *Graf and Gräfe.*,1979]. Recently, these observations have been confirmed by remote sensing [*Rosenfeld and Lensky*, 1998, *Rosenfeld*, 1999, *Rosenfeld*, 2000 a, *Rosenfeld and Woodley*, 2000]. Using data from TRMM (Tropical Rainfall Measuring Mission), AVHRR/NOAA (Advanced Very High Resolution Radiometer / National Oceanic and Atmospheric Administration) and the AARRP (Applied Atmospheric Research Resources Project) it could be clearly demonstrated that under the effect of smoke tropical clouds tend to show a decreased effectivity of converting cloud droplets into rain. The auto conversion process is suppressed and rain is formed only after the glaciation process started. This modification of cloud properties is found to be highly efficient reducing the rain formation from single clouds by up to 100%, depending on whether the freezing level is reached or not.
This effect of suppression of precipitation due to high aerosol concentrations could be clearly verified by numerical simulations with a high resolution, cloud resolving model [*Textor et al.*, 2000].

Many A-GCM studies have been related to the direct and indirect aerosol effects focusing on stratiform clouds [*Lohmann and Feichter*, 1997, *Roelofs et al., 1998*,

Penner et al., 1998, *Lohmann et al.*, 2000, *Rotstayn et al.*, 2000], but very little work has been done concerning the aerosol effect on convective heating (ACOH).
[*Graf et al.*, 2001] were the first to study concerning the ACOH but it represented aerosol emissions only by prescribed monthly varying data without interaction with model dynamics and transport. The present study is much more realistic since we include a full representation of the aerosol cycle which takes into account transport, washout and ageing of aerosols. For more details see section 2.
The most important aerosol source in regions where convective precipitation predominates (i.e. the tropics, ITCZ) is biomass burning. The ACOH is therefore to a large degree caused by the biomass burning effect on convective clouds. This motivates to focus our attention on these regions and seasons when biomass burning occurs. Because of the increasing population on Earth, especially in tropical regions, biomass burning is clearly enhanced during the last 100 years, however, the change in this type of land use is not very well known and requires further investigation.

Summarizing, the ACOH provides a possible link between the microscale (cloud microphysics) and the global scale (energy supply for the global circulation due to convection). This gives reason to investigate the sensitivity of an AGCM to the ACOH.

1.2 Model Description and Experiments

We examine the reduction of warm precipitation formation for convective clouds. For this reason we performed a 15 year numerical experiment consisting of a control run and an experiment run using the ECHAM4 A-GCM.
The dynamical core and some parts of model physics in the ECHAM model were developed at the European Centre for Medium-Range Weather Forecasts (ECMWF). The prognostic variables are vorticity, divergence, temperature, logarithm of surface pressure, the mass mixing ratio of water vapour, cloud liquid water and cloud ice. The model equations for these variables are solved on 19 vertical levels in a hybrid p-σ-system by using a spectral transformation method with a triangular truncation. The physical processes are evaluated at grid points of a gaussian grid. For time integration a semi - implicit leapfrog scheme is used [*Roeckner et al.*, 1996]. Cumulus convection is represented by a mass flux scheme. This scheme calculates convective updraft and downdraft with respect to entrainment and detrainment [*Tiedtke*, 1989]. An adjustment closure based on the convective available potential energy (CAPE) is used [*Nordeng*, 1994].
Our control run (CTR) was carried out with ECHAM4 (T30 resolution, time step 30 minutes, using a prescribed climatology SST) including an extensive stratiform cloud scheme [*Lohmann, et al.*, 1999] and, in addition, an

aerosol life cycle for sulfate [*Kettle et al.*, 1996, *Spiro et al.*, 1992, *Graf et al.*, 1997, *Hao et al.*, 1990, *Benkovitz et al.*, 1994], black carbon [*Liousse et al.*, 1996], organic carbon [*Liousse et al.*, 1996, *Guenther et al.*, 1995], dust and sea salt aerosols. Dust and sea salt are prescribed as three dimensional monthly mean data.

Transport, dry and wet deposition and chemical transformations of the sulfur constituents are calculated on line with the GCM. Prognostic variables are dimethyl sulfide and sulfur dioxide as gases and sulfate as an aerosol. Transport of these species due to advection, vertical diffusion and convection is treated in the same way as the transport of water vapour.
Prognostic equations are solved for hydrophilic and hydrophobic organic and black carbon, respectively. A special fraction of newly emitted carbonaceous aerosol is hydrophobic. These aerosols become hydrophilic after the typical exponential aging time of 40 hours.
The aerosol lifetime is governed by deposition (wet and dry). Precipitation scavenging of hydrophilic carbon (dust and sea salt also) is calculated explicitly with respect to the model's local precipitation.
Prognostic variables of the cloud scheme are cloud liquid water/ice and the cloud droplet number. The scheme takes into account condensational growth of droplets, depositional growth of ice crystals, homogeneous, heterogeneous and contact freezing of cloud droplets, auto conversion of cloud droplets, aggregation of ice crystals, accretion of cloud ice and cloud droplets by snow, of cloud droplets by rain, evaporation of cloud liquid water and rain, sublimation of cloud ice and snow and melting of cloud ice and snow.
The nucleation rate of new cloud droplets is based on the total number of hygroscopic aerosols, aerosol composition, size spectrum of aerosols and the updraft velocity. Aerosol size and composition are considered in a factor α which is obtained from a microphysical model and additionally depends on the geometric standard deviation of an initially preexisting log-normal aerosol size distribution, the mode radius and the aerosol composition. It is parameterized as a function of updraft velocity and the mass of sulfate aerosols assuming internally mixed aerosols.

The assumption of an internally mixed aerosol is part of the droplet formation parameterization in the cloud scheme. In contrast to this, an external mixture is used for calculating the aerosol optical depth. Since optical properties of aerosol particles and cloud droplets are calculated in this scheme the direct aerosol effect and the indirect cloud albedo effect are included automatically. Additionally, if the droplets are smaller, the formation of precipitation is less efficient. Therefore, the residence time of clouds with small droplets may be increased (indirect cloud lifetime effect).
Details of the cloud and aerosol scheme and the applied parameterizations can be found in [*Lohmann, et al.*, 1999].

In our experiment run (EXP) we applied a similar microphysical scheme also for the convective clouds. Using the cloud droplet number concentration (CDNC) for convective clouds, we modified the standard convective mass flux scheme used in ECHAM4 as described below.
In the control run convective precipitation forms if the convective layer is at least 150 hPa deep. In this case, the precipitation formation depends linearly on the liquid water content and on one empirical constant which controls the conversion rate of cloud droplets to rain drops.
The equation is (q_r: rain, q_l: liquid water content):

$$q_r = q_l * const. \tag{1.1}$$

The approach of our experiment was to introduce a dependency of this conversion rate on temperature and on CDNC at cloud base.
When $T > 263K$ and $CDNC|_{cloudbase} > 750\#/cm^3$ we reduced the formation of new rain to 25% of the original value, while we totally inhibit formation of new rain when $T > 263K$ and $CDNC|_{cloudbase} > 1000\#/cm^3$. That means we introduced a function $f(T, CDNC)$ with:

$$\begin{aligned} f(T,CDNC) = 1.0 \quad if \quad & CDNC < 750\#/cm^3 \\ or \quad & T < 263K \\ f(T,CDNC) = 0.25 \quad if \quad 1000\#/cm^3 > & CDNC > 750\#/cm^3 \\ and \quad & T > 263K \\ f(T,CDNC) = 0.0 \quad if \quad 1000\#/cm^3 < & CDNC \\ and \quad & T > 263K \end{aligned} \tag{1.2}$$

and modified the rain formation to:

$$q_r = q_l * const. * f(T, CDNC) \tag{1.3}$$

These values of temperature and CDNC were taken from satellite data and aircraft observations [*Lahav and Rosenfeld*, 2000].
However, having the temperature threshold of $T = 263$ K, we did not take into account the slower freezing rate and decreased formation of precipitation through the mixed and ice phase. This modification, although very simple, is based on observations and

simulations with cloud resolving models. We applied such a moderate modification in order to avoid a totally different behavior of the model (e.g. leaving its equilibrium).

1.3 Results

Convection is one of the most important processes in the climate system. It provides the energy for planetary wave excitation at least in the tropics and drives the main circulation systems (Walker and Hadley circulation) on our planet. For that reason convection is closely linked to all other processes in the climate system.
In order to isolate the first order effects of the ACOH without the feedback of the whole dynamical system, we performed a single time step analysis in addition to the main 15 year experiment. We present therefore two different kinds of results:

- A single time step analysis which shows the instantaneous convective forcing due to the ACOH. In this experiment we can identify the locations and the strength of ACOH. The convective forcing due to ACOH pushes the model off its basic state due to its impact on large scale circulation (see the later discussion). This interaction of the ACOH and the climate system is prevented in the single time step analysis.

- An ensemble experiment, where the full interaction between ACOH and the rest of model dynamics is allowed.

The difference between the single time step experiment and the main experiment is important. Once the main experiment is running at least a few time steps, it is no longer reasonable to compare one by one a single model column from the control and the experiment run at a special time step. In this case, it is possible and to be expected that the meteorological situation is much different. Because of the feedback effect of the whole model dynamics (which we need of course to find the effect on the circulation), it is not possible to compare the same meteorological situation with and without ACOH.
This is possible in the single time step experiment because there is no feedback of the climate system.
To get a better feeling of the distribution of the ACOH events and to compare single convective events with the same surroundings (vertical profiles for moisture, temperature, etc.) but with ACOH and without we used this single time step experiment.

1.3.1 Single Time step Analysis

We integrated a control (CTR_S) and an experiment (EXP_S) version of ECHAM4 by preventing any dynamical response to the ACOH (i.e. calculating at each time step the control and the modified version, saving the difference and continue only with the control). Depending on the special situation (i.e. the vertical profiles of the surrounding atmosphere) in EXP_S we find (as expected) in general a reduction of convective precipitation (and the related quantities like latent heat release) as well as a different vertical redistribution of those quantities compared to CTR_S where the aerosol concentration is high. The result in each case is a modification of the vertical stability compared to the CTR_S.

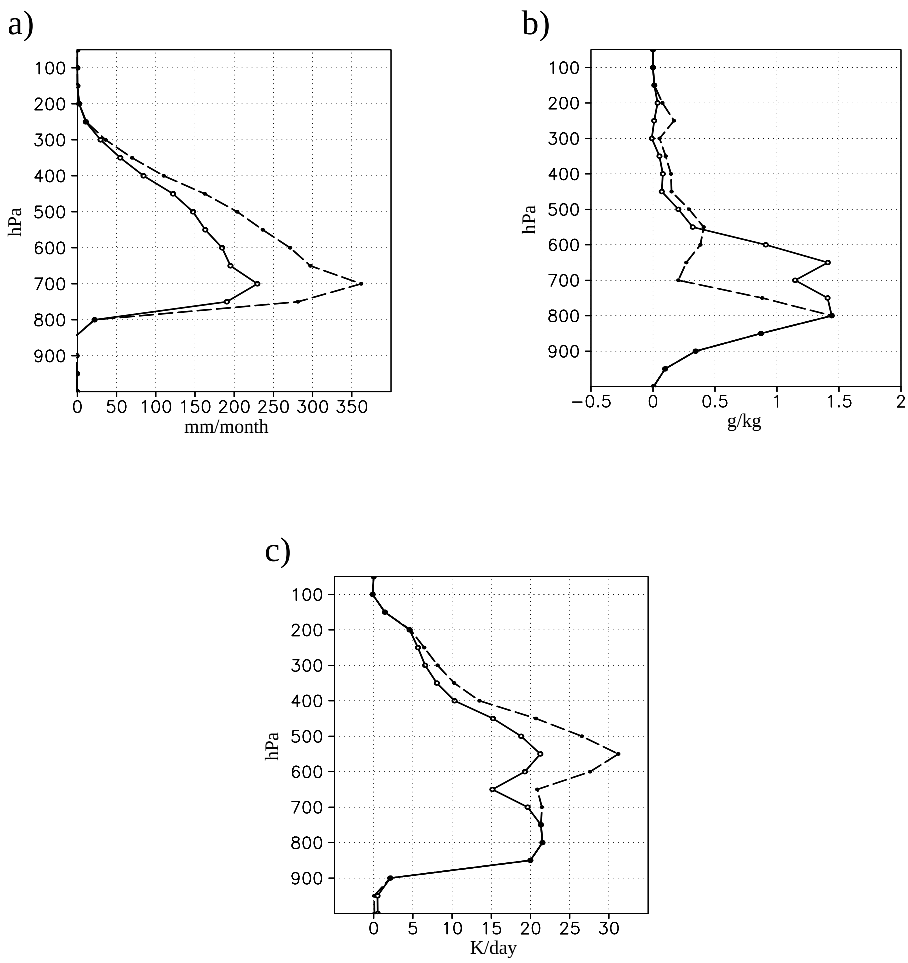

Figure 1.1: a) Precipitation formation, b) Cloud water content, c) Heating rates; solid line: simulation with aerosol effect; dashed line: control simulation

It should be pointed out that the ACOH does not necessarily lead to less convective rain. The reduction of rain efficiency in the lower troposphere (T > 263 K) enhances the cloud liquid water content which in turn potentially leads (depending on the special situation and the convective mass flux) to more precipitation from higher altitudes.

In Figure 1.1 a-c the vertical profile of precipitation formation (a), cloud water content (b) and release of latent heat due to precipitation formation (c) are presented. These data are from one model column in the tropics (longitude=15^o, latitude=-9^o) and one time step where the ACOH comes into force. In the EXP_S version we have less formation of new precipitation (1a) and therefore a higher cloud water content (1b). As a result the release of latent heat to the surrounding is weaker (1c).

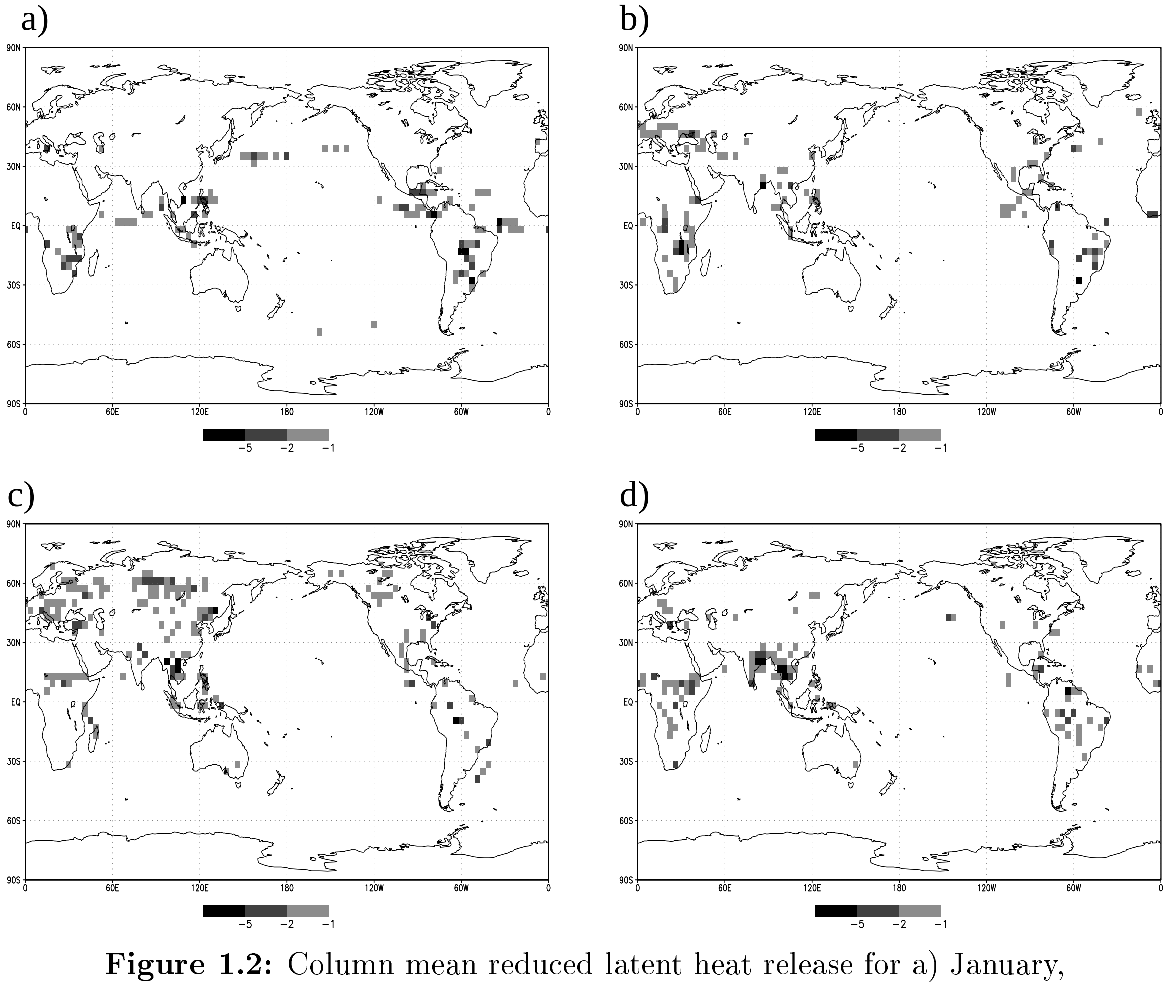

Figure 1.2: Column mean reduced latent heat release for a) January, b) April, c) July, d) October $[W/m^2]$

Figure 1.2 a-d shows exemplarily for January, April, July and October the geographic distribution of the column mean reduced latent heat release due to the ACOH (10 day mean). Each shaded grid point in Figures 1.2 a-d represents at least one event where the ACOH was active. The geographic distribution can be well understood by combining Figure 1.3 a-d and Figure 1.4 a-d. Figures 1.3 a-d show the convective precipitation (10 day mean as in Figures 1.2 a-d) while Figures 1.4 a-d show the total number of aerosols. It is notable that in the tropics (the region which is most interesting and important in terms of convection) the most important source for these aerosols is biomass burning. Therefore the highest aerosol concentrations can be found over parts of Africa, South America, Indonesia, India and China. But Figures 1.4 a-d show also the possibility of large scale transport which can lead to remarkable high aerosol concentrations over the oceans.

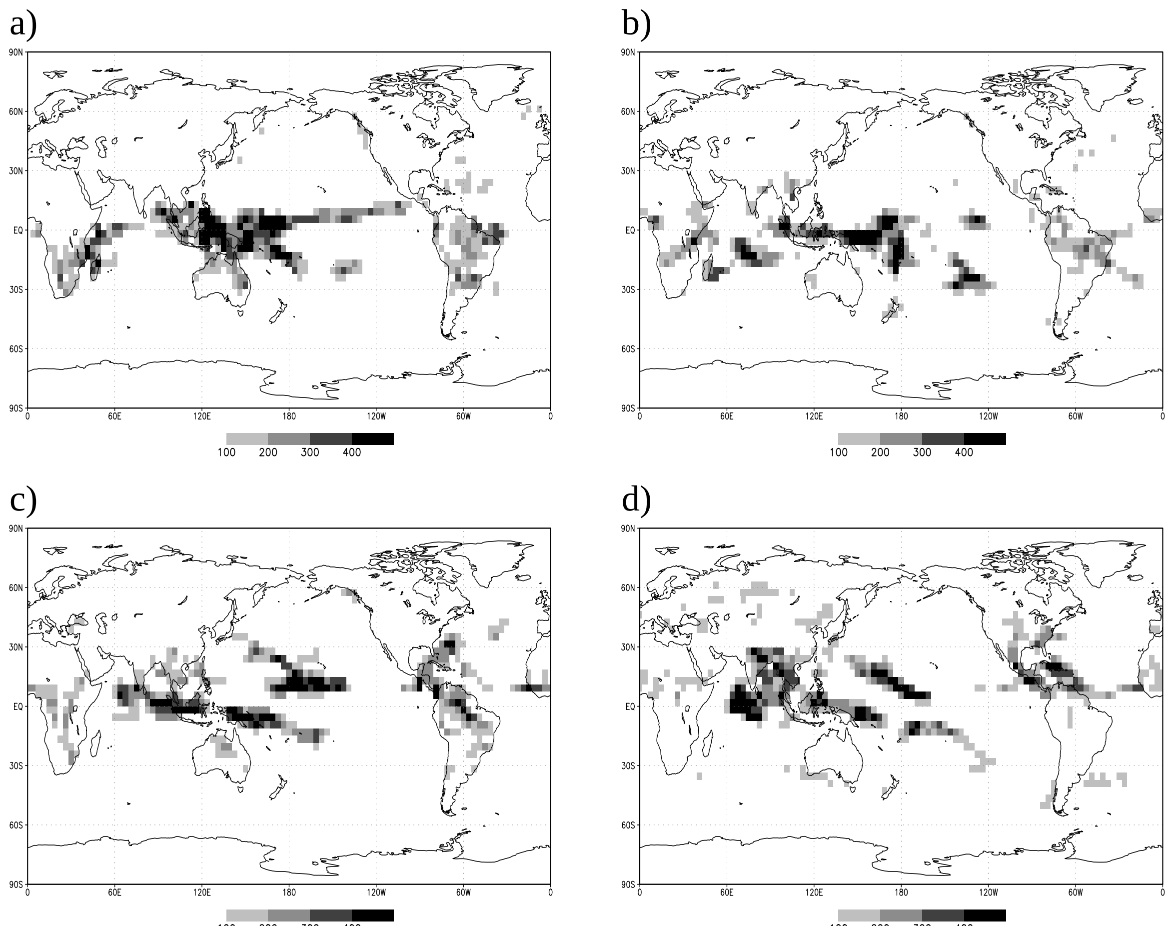

Figure 1.3: Convective precipitation a) January, b) April, c) July, d) October $[mm/month]$

Because both, the occurrence of convective precipitation and high aerosol/CCN concentrations are a necessary condition for the ACOH, Figures 1.2 a-d are a kind of "product" of Figures 1.3 a-d and Figures 1.4 a-d. We want to point out that there is an anti - correlation between burning season (high emissions) and wet season (high precipitation rates) in most parts of the tropics. This determines to a large degree the probability for the ACOH and leads to a strong spatial and temporal fluctuation of the forcing (Figures 1.2 a-d).

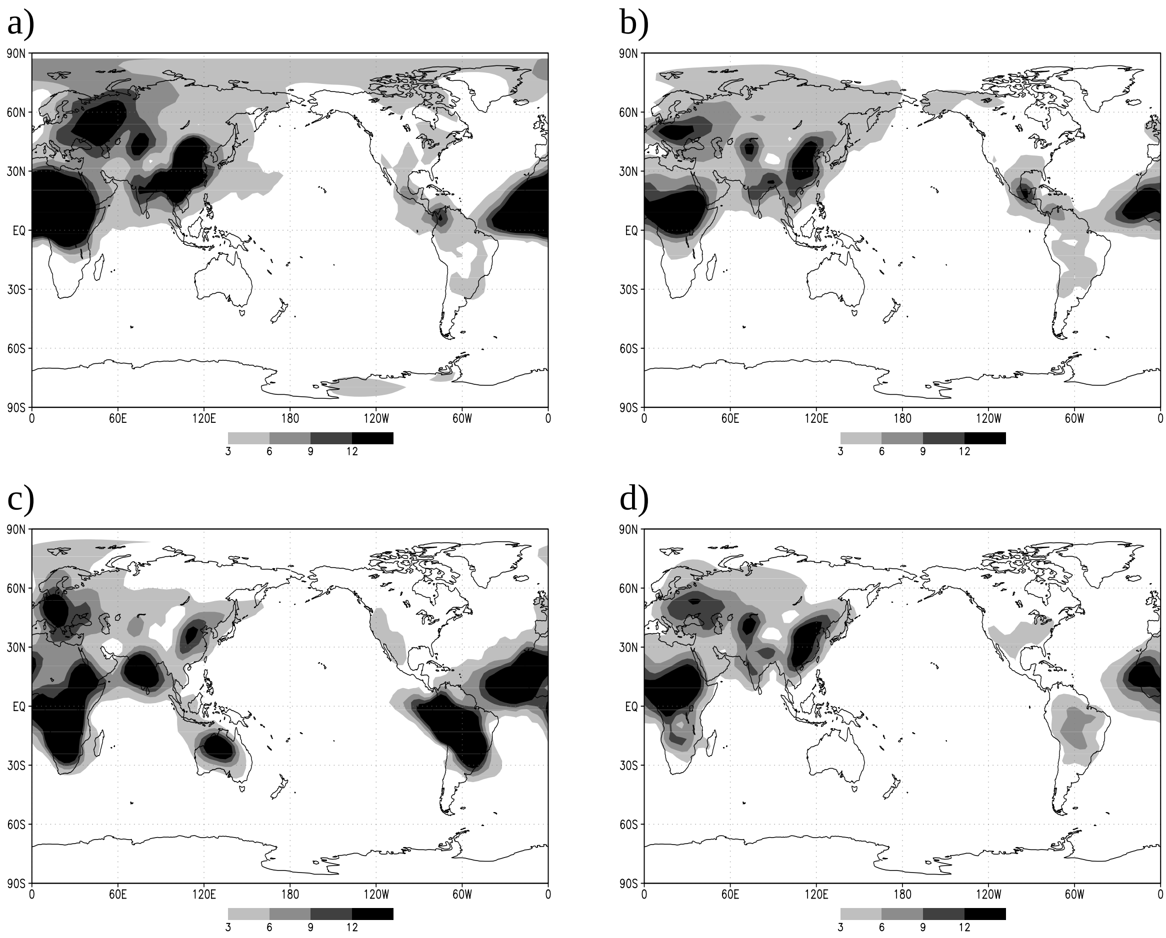

Figure 1.4: Aerosol distribution 900 hPa level a) January, b) April, c) July, d) October $[\# * 10^3/m^3]$

Considering one time step and one model column (see Figure 1.1 a-c) the reduction of precipitation (and all related quantities) is in the order of 10 percent but can also reach (depending on the vertical stability of the atmosphere and the vertical extent of the convective layer) 100 percent (complete suppression of precipitation). However, the number of affected model columns (ACOH events) per time step is very small (of the order of 1 to 10). As a result the global average of the forcing, as shown in Figure 1.2 a-e, over a longer time (10 days) is very small (order of 0.1 to 1 percent). Later on we will refer to the difference between EXP_S and CTR_S as the *origin effect* of ACOH.

1.3.2 Ensemble Experiment

Considering the main 15 year experiment we want again to point out that differences between EXP and CTR are the results of the origin effect as shown in Figure 1.1 and 1.2 and the response of the whole dynamical system to these origin effects. As a consequence of the manifold of atmospheric processes it is not easy, if not impossible, to separate them.
The description of the results of our simulation will begin with the quantity which is directly affected by the ACOH: precipitation. In Figure 1.5 a-d we present the global precipitation for all four seasons (average over three months). Values of the control run are represented by isolines, while total anomalies are shaded.

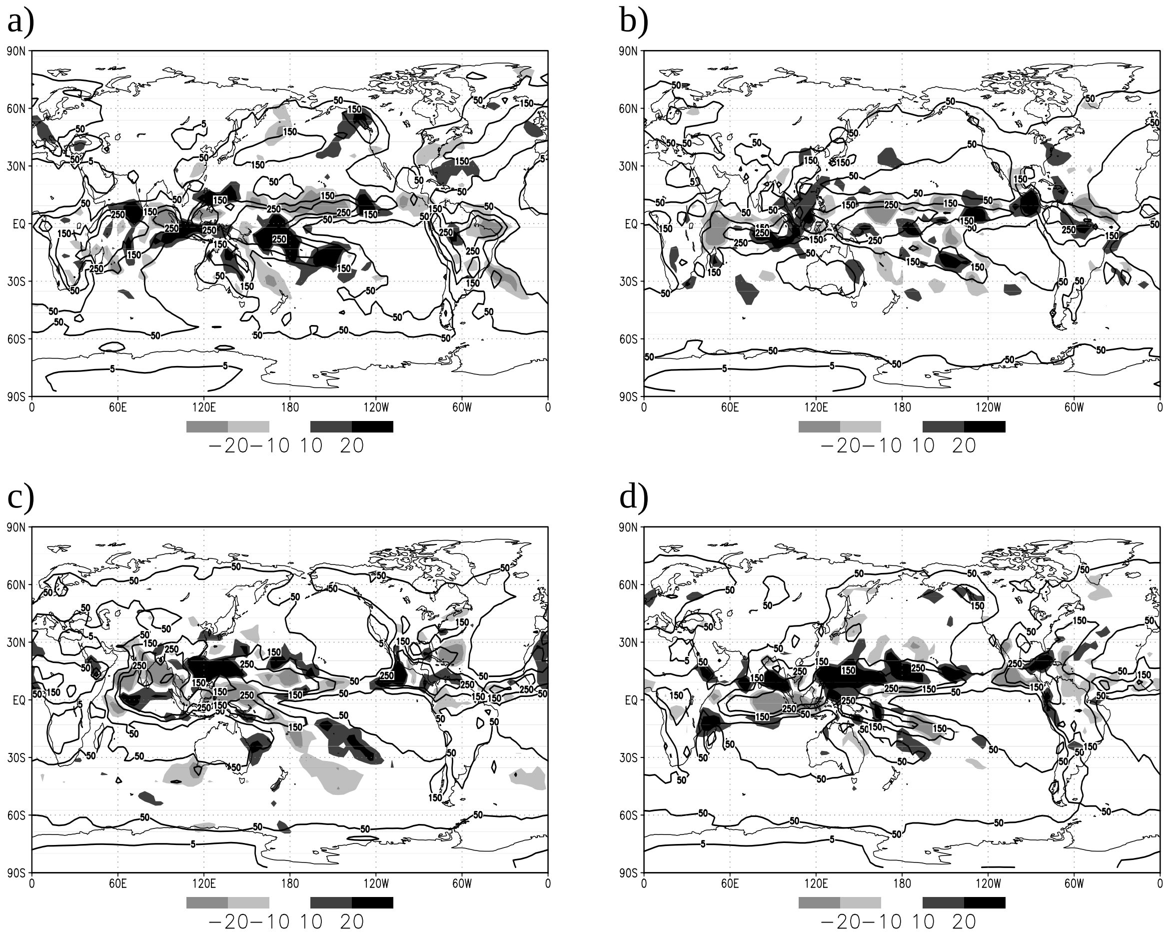

Figure 1.5: Precipitation, Anomalies: Shadings, Control run: Contour lines a) DJF, b) MAM, c) JJA, d) SON [$mm/month$]

In all our Figures total anomaly means the average of EXP minus the average of CTR. First we will focus our attention on the control run values to consider the

principle global distribution of precipitation. In each season we can clearly identify the Inter Tropical Convergence Zone (ITCZ). The ITCZ marks the region with the strongest (predominantly convective) precipitation rates and therefore the strongest diabatic heating due to the release of latent heat in the troposphere. It shows a clear annual cycle which is caused by the annual march of the sun. During the DJF season the ITCZ is shifted to the south while in the JJA season to the north. In the latter season (JJA) the strong maximum over parts of the Indian Ocean, India, the Bay of Bengal indicates the monsoon.
Surprisingly the anomalies (shadings) in Figure 1.5 are not restricted to the regions which are most probably affected by the ACOH (Figure 1.2) but are distributed rather randomly over the tropics. Large anomalies are visible in the whole Pacific and the Indian Ocean. It is evident from the Figures 1.2 a-d that these anomalies can not be explained as a direct response to the ACOH (the origin effect) but only as an indirect dynamical feedback of the climate system.

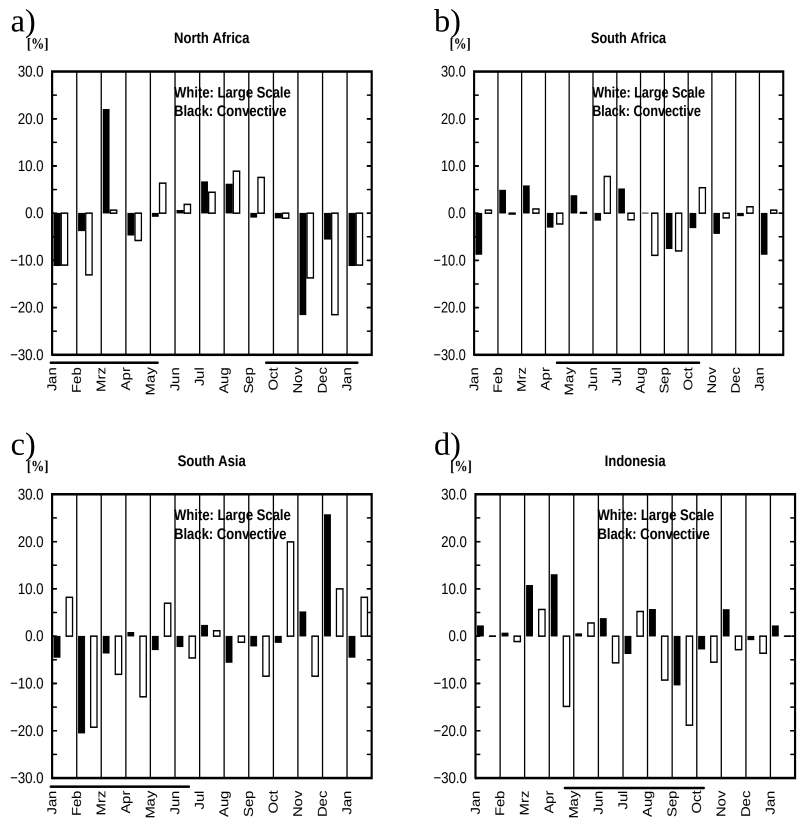

Figure 1.6: Percentage precipitation change for different regions indicated in Figure 1.6 h)

To analyze the precipitation anomalies in more detail, we focus on some specific regions which are known to be important sources for aerosols from biomass burning.

Since we used a relatively coarse resolution (T30) in our simulation, which corresponds to a nominal resolution of $3.75^o * 3.75^o$ in gaussian grid space, it is not recommended to look at too small regions. We consider therefore as the main regions: Northern and southern parts of Africa, South Asia, Indonesia, Brazil, North Pacific and South Pacific (Figure 1.6 a-g). To identify the regions on a global map see Figure 1.6 h.

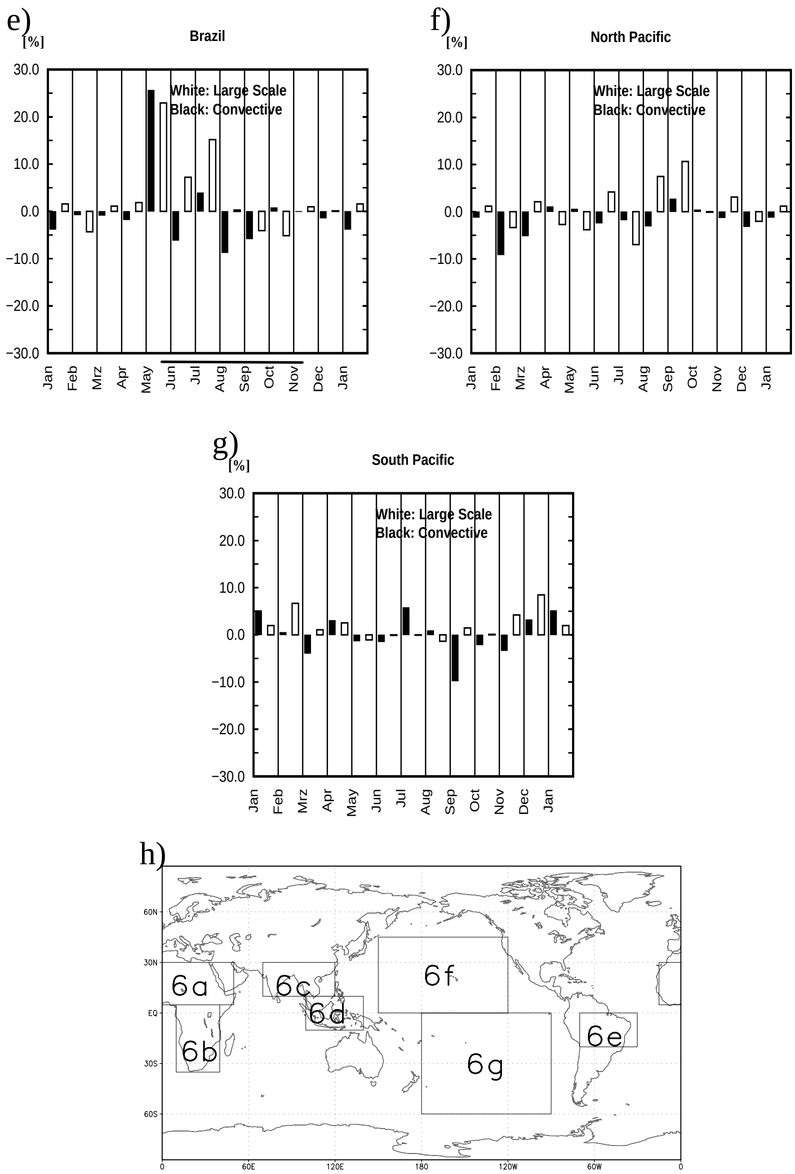

Figure 1.6: Percentage precipitation change for different regions indicated in Figure 1.6 h)

In these Figures the percentage change of large scale and convective precipitation at monthly mean basis averaged over the region is shown. The time of strongest fire activity in each region is indicated by a horizontal line as the burning season. Naturally there is no burning season in the two Pacific regions. If there would be no interaction between the changes in fallout of convective precipitation and the rest of the atmosphere (as in the single time step analysis) we would expect slightly less rain during the burning season in the shown regions and no change during the rest of the year. However, this is not the case. We find precipitation anomalies (positive and negative) during the whole year up to 25%, but there is no principal difference in the distribution of positive and negative anomalies between the burning season and the rest of the year. Only in the northern part of Africa and South Asia there is a small shift towards less convective precipitation in the burning season (including months with opposite behavior e.g. March for Africa). However, this shift also cannot be a pure and direct result of the ACOH. Otherwise there should be no change in large scale precipitation at the same time and region, which is not the case. Considering e.g. Indonesia or the southern part of Africa we find only randomly distributed positive and negative anomalies in both convective and large scale precipitation. Only in Brazil (June, August, September) there is a signal which looks like a direct result of the ACOH.

Considering the possible relations between convective and large scale precipitation anomalies for a special month we can distinguish four different cases:
a) more convective and more large scale precipitation
b) less or unchanged convective and more large scale precipitation
c) more convective and less or unchanged large scale precipitation
d) less or unchanged convective and less or unchanged large scale precipitation

All these cases can be found in Figures 1.6 a-g, but only case b) is a possible direct result of ACOH (and can be found in the single time step analysis). The reduction of convective precipitation formation at a special time step and model column leads to an increase of the remaining water vapour content in the same (or the neighboring) model column in the next few time steps after convection occurs. This in turn results in more stratiform clouds and potentially can cause more large scale precipitation.

Considering again Figures 1.6 a-g, we find that the months with the largest anomalies (where the large scale or convective anomaly exceeds at least 20%) do not belong to case b) but to the other cases. Case a) we can find in the northern part of Africa (March), South Asia (December) and Brazil (May). Case d) can be observed in the northern part of Africa (November, December) and South Asia (February). Case c) finally can be found in Indonesia (April) (anomalies do not reach the 20% level).

Figures 1.6 f and 1.6 g play a special role in this analysis. Here it is self-evident that the shown anomalies must be caused by indirect effects and not directly by the

ACOH. The anomalies are not as high as in the other regions but this is at least in part due to the large size of both regions (the anomalies partly average out). In some parts of the ITCZ and the South Pacific Convergence Zone (SPCZ) the precipitation anomalies reach sometimes up to 20% in remarkably large areas.

In all these cases the reason for the anomalies must be a perturbation of the general atmospheric situation. This means that the influence on the climate system due to the ACOH is not restricted in time and space, but is a scale overlapping effect which has its origin at the local scale but shows its impact on the global scale. Before we will consider the global scale and the related structures of circulation, we will discuss the possible ways of interaction between local disturbances of convection and the large scale. Doing that, we have to mention the energy and water the budget which are coupled to each other:
Convection, because of its ability to very effectively transport high amounts of energy and momentum from low to high altitudes is, at least in the tropics, the leading process which is responsible for planetary wave excitation. Due to this process even local anomalies of convection can propagate through the atmosphere and influence the global scale.
Further, perturbations in the convection can affect the radiation budget:

If less convective precipitation is formed, more cloud water will remain in the model column which will either be transported to higher altitudes or remain at lower levels in the troposphere. In each case the probability for stratiform clouds will be enhanced in the model column. This results in enhanced stratiform cloud cover, which in turn has a great impact on the grid mean albedo and the radiation. Increase in stratiform cloud cover can also result in more large scale precipitation. In the case of deep convection an increase in detrainment of convective cloud water at high altitudes will result in more non - precipitating ice clouds. The stored water can then be transported over large distances (including several phase changes) before leaving the atmosphere. Finally, a single and strong reduction of convective precipitation will also reduce the soil water content which in turn results in less evaporation during the next time steps. Large scale rising or sinking motion driven by the planetary scale effect of ACOH (e.g. changes of the Walker circulation) can also lead to more or less layered clouds via changes in the relative humidity.
These examples are only a short list of some possible physical interrelationships between convection and the rest of model physics. More complex interactions occur.
Given these possible ways for the ACOH to affect the large scale we will now consider the velocity potential field in Figure 1.7 a-d. The Figures show the control values (isolines) and the absolute anomalies (EXP - CTR: shadings) of velocity potential at 200hPa minus the 900hPa level. Negative values for isolines indicate ascending and positive descending air motions. A simple comparison with the global precipitation

distribution shows that ascend of air is driven by convective activity (i.e. deposition of latent heat, transport of moist static energy) in South East Asia. In this region the predominantly convective precipitation rate often exceeds 400 mm/month (monthly mean).

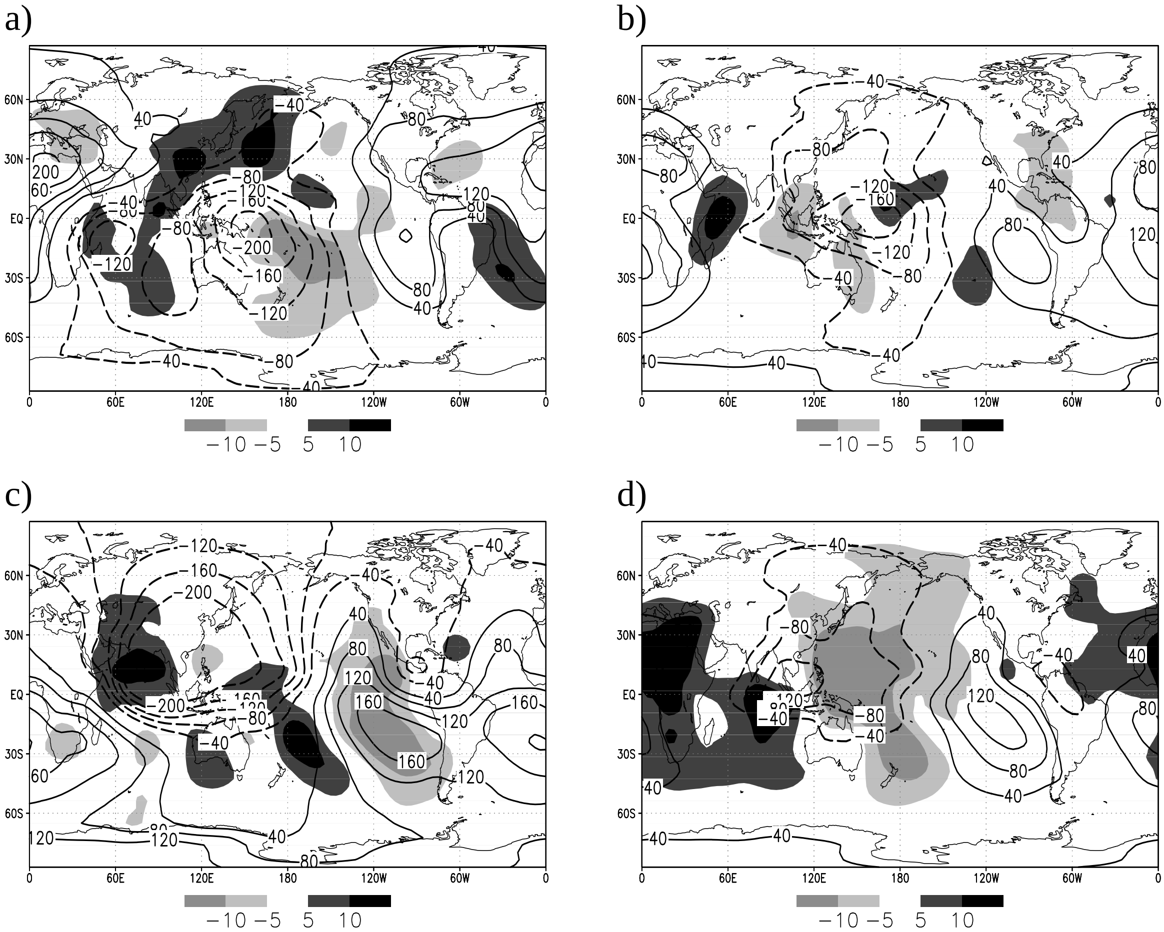

Figure: 1.7 Velocity Potential 200 hPa level minus 900 hPa level; Contour lines: Control run, Shadings: Anomaly; a) DJF, b) MAM, c) JJA, d) SON $[m^2/s * 10^5]$

Figure 1.7 a-d provides basic insights in the structure of the Walker circulation which consists of an ascending branch over the West Pacific (in northern winter) or South Asia (in northern summer) and a descending branch over the east Pacific. Depending on the season, the cell is more (DJF, JJA) or less (MAM, SON) developed. The anomalies (shadings) in velocity potential (Figure 1.7 a-d) are consistent with the precipitation anomalies in Figure 1.5 a-d. It is evident from these two sets of pictures that an increase in precipitation is accompanied with a negative anomaly in the velocity potential and vice versa, a decrease in precipitation with a positive anomaly in velocity potential. Therefore more precipitation causes an amplification of the Walker circulation when located in the active branch of the Walker cell. This is more or less so in the DJF, MAM and SON seasons.

DJF: In this season we can find a positive precipitation anomaly (Figure 1.5 a) in the southern central Pacific which covers nearly the whole Southern Pacific Convergence Zone. Larger negative anomalies can be found at the ITCZ in the Central Pacific, to the west of Sumatra in the Indian Ocean, in the region of the North West Pacific and the north eastern Pacific basin and off the north eastern coast of Brasil, as well as in some parts of the southern Atlantic. In principle all these features can be found again in the velocity potential (Figure 1.7 a). The enormous advantage of the latter quantity in comparison to precipitation is that the field is much smoother and not as patchy as the precipitation distribution. In Figure 1.7 a we have a negative velocity potential anomaly in the Central Pacific corresponding to a stronger Walker circulation. The positive anomalies in the North West Pacific, over China, parts of the Indian Ocean and east of South Africa in the South Atlantic complete the picture and indicate less ascent or more subsidence depending on whether the background control field is negative or positive. Because the anomalies are much weaker in MAM season we will leave out this season and discuss the JJA season.

JJA: In this season we find, contrary to DJF and SON (described below), a weakening of the Walker circulation. This is caused by a negative precipitation anomaly of the summer monsoon over India, the Arabian Sea and the Bay of Bengal and in the South - West Pacific (and the related positive anomaly on the velocity potential). A direct consequence of this weakening of the active branch of the Walker cell is the negative velocity potential anomaly in the passive branch in the East Pacific.

SON: Here we find a large negative anomaly in the West and South West Pacific in the velocity potential (Figure 1.7d) which corresponds to more precipitation in that region (Figure 1.5d). Positive anomalies of the velocity potential are located over the Central Indian Ocean and nearly over the whole African continent. The dipole structure of the anomaly over the Indian Ocean and West Pacific indicates a shift of the core of the ascending branch of the Walker cell to the north west.

As a further consequence of the perturbation of large scale features of atmospheric dynamics we only want to mention some effects at higher latitudes. Therefore we show in Figure 1.8 a-d the geopotential at 500 hPa level for the four seasons (contour lines: anomalies; shadings: t-test with significance 80% and 90%).

We find larger anomalies over the Asian Continent (in DJF and less strong in JJA) and Europe (MAM and JJA). In JJA the anomalies are concentrated in the southern hemisphere while in DJF the northern hemisphere is more affected. Because there is definitive no direct forcing in DJF (northern higher latitudes) and JJA (southern higher latitudes) Figures 1.8 a and 1.8 c support the assumption that the geopotential field reflect perturbations which are transferred via the Hadley circulation (specially due to the leading branch on the winter hemisphere).

To summarize the effects on the Walker and Hadley circulation, we note that we can only describe the anomalies and that we are not able to give a satisfying and closed explanation. Since every positive anomaly in velocity potential causes a negative one (and vice versa) for reasons of continuity, it is impossible to decide what is the reason and what the result.

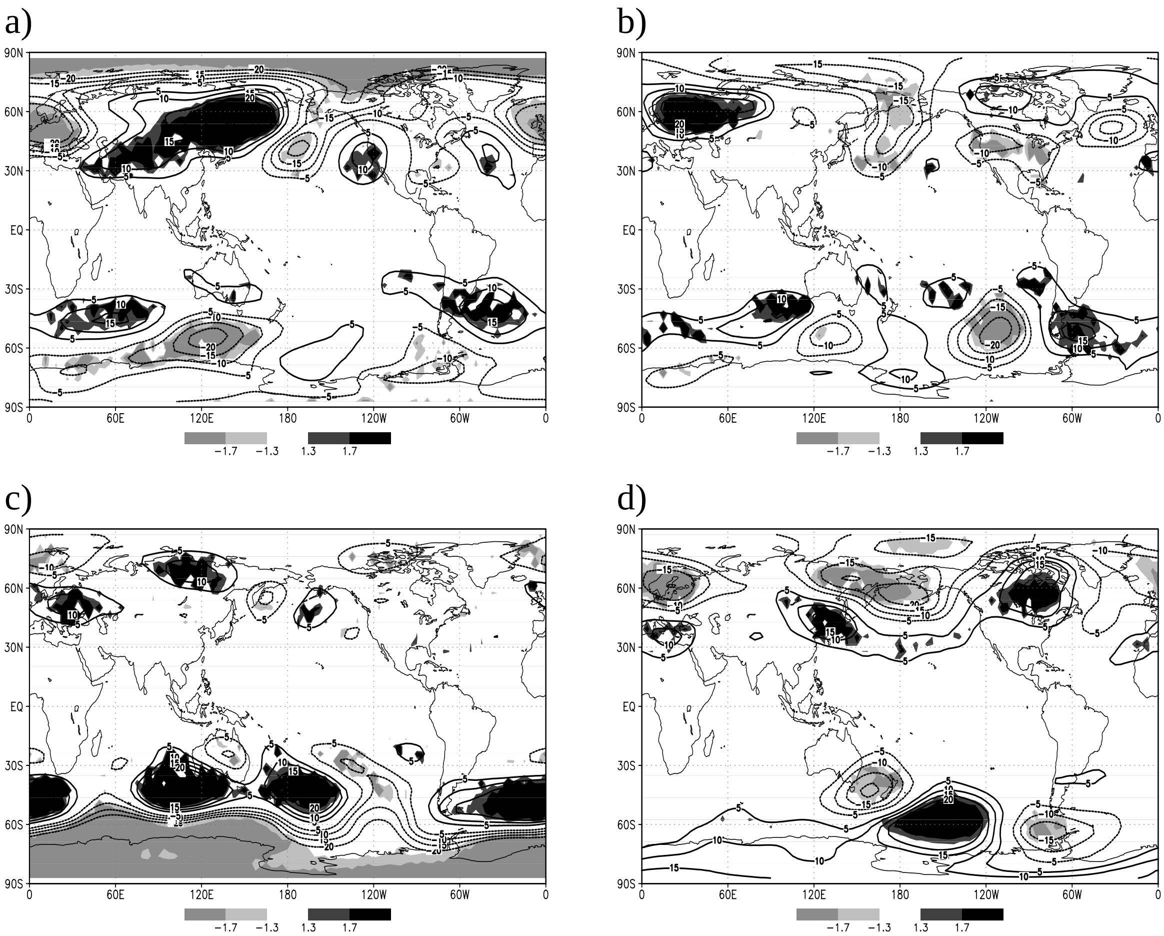

Figure 1.8: Geopotential 500 hPa; Contour lines: Anomaly, Shading: T-test 80 % and 90 % Significance, a) DJF, b) MAM, c) JJA, d) SON [gpm]

It is appropriate to compare our results with results from numerical studies about the aerosol effect on stratiform clouds. Because of the different temporal and spatial distribution of convective clouds and stratiform clouds (stratiform clouds are much more uniformly distributed than convection) aerosol effects on stratiform clouds in general lead to remarkable effects on cloud cover, liquid water path and radiation. While [*Lohmann et al.*, 2000] e.g. found for the indirect effect of sulfate and carbonaceous aerosols on stratiform clouds a global radiative forcing in the range from $-1.1W/m^2$ to $-1.5W/m^2$, there is no significant signal for the globally averaged radiation budget in our simulation but the shown circulation anomalies. This underlines the different nature of both effects.

1.4 Discussion

Discussing the results it is at first important to give a statement about the statistical significance of the shown anomalies. To test the significance we applied a common t-test as well as some other distribution independent tests (Siegel and Tukey, Kolmogoroff and Smirnoff). Most meteorological quantities like precipitation do not follow a normal distribution which is an assumption for the application of a t-test. Because of the small ensemble and the weak forcing, it should be no surprise that the observed anomalies are at the lower boundary of significance. Depending on the statistical method only a few months in Figure 1.6 a-g show significant values. However, at least the months where the anomalies reach the 20 % level (and which only were discussed in more detail) are conceived as statistically significant.

The same problem appears for the velocity potential. In terms of a common t-test the shaded area is to a large degree significant on the 80 % and 90 % confidence level. This is a weak signal and the reason why we do not go into detail by analyzing the exact structure of the anomalies. However, the difference between ensemble average values in EXP and CTR exceeds up to three standard deviations of CTR (shaded area at least about one standard deviation), which is sufficient to attract our attention.
Because of this problem of statistical data analysis we want to underline, that the result of our simulation is not the detailed structure of anomalies on local, regional and global scales, but only the proof of the existence of those anomalies on all scales. This shows the large sensitivity of the global circulation to the ACOH.
The Figures 1.2 a-d show the rarity of ACOH events. One should remember the strong coupling between the aerosol concentration (which is one of the controlling input parameters for our ACOH parameterization) and convection itself. Convection (and the fallout of rain from convective clouds) is the most effective process to remove aerosols from the atmosphere due to rainout and washout. Thus, even in regions with high aerosol emissions (see Figure 1.4 a-b) one should not expect ACOH events at every time when convection occurs. Once convection is active the aerosol loading in the

atmosphere is strongly reduced. This in turn reduces the probability for ACOH during the next time steps, until again a higher aerosol concentration is accumulated in the model column.

The fundamental reason for the shown response to such a localized and spatially and temporally highly variable forcing (Figure 1.2 a-d) is, that a key process in atmospheric dynamics is modified. In addition, the forcing takes place at some neuralgic regions which are known to be important for the state of general circulation. For this reason these regions (i.e. mainly the tropical regions with deep convection: Indonesia, Amazon and Congo Basin) were called "centres d'action" [*de Bort*, 1880] or "strategic points of world weather" [*Walker*, 1924].

1.5 Conclusions

An A-GCM study concerning the sensitivity of the global climate to the suppression of warm precipitation formation in convective clouds is presented. The experiment was divided into two parts: The main 15 year experiment allows the whole dynamics to respond to a modified convective forcing, and an additional experiment with single time step analysis which allows to locate and to measure the origin effect of aerosols on convective clouds. The main experiment provides a wide variety of effects and anomalies at the local and the regional scale (cloud cover, temperature, precipitation) and the global scale. The simulation confirms therefore the statement that microphysical effects of aerosols on precipitation formation in convective clouds is potentially of great importance for climate change on the global scale. The concrete results of our simulation should not be taken as the final answer to the question how the ACOH works on global dynamics, but rather as an estimate of its strength. There is need for further investigations of the ACOH. These should focus more on the transient behavior of the model and the process how a perturbation of convective activity propagates through the atmosphere and finally dissipates. In contrast to the present simulation these further experiments require a much more detailed description of microphysical processes in convective clouds to justify an extensive and detailed analysis of their results. Our modification of convection, and therefore our treatment of the microphysical effect was rather simple in order to make no principle changes of the standard convection scheme. Our study suggests that it is potentially of great importance to include more comprehensive microphysics in convection schemes. There might be a benefit for transient components of tropical circulation and the statistics of planetary wave excitation. If this would be true there is a good chance to improve the general behavior of A-GCMs and their ability to reproduce past and current climate as well as to predict future climate changes. Recapitulating, the ACOH is a very interesting effect which couples the microscale (cloud microphysics) directly to the global scale (global circulation). It

(ACOH) is a distinct example that even the large scale atmospheric dynamic depends on ostensibly negligible and local phenomena.

Chapter 2

The Convective Cloud Field Model

Abstract A cumulus cloud field model has been coupled to an atmospheric general circulation model (AGCM). The results, which show a good performance of the model within the AGCM and a qualitatively good agreement to observation concerning the statistical information of cloud fields are presented in this paper. While most of the current cumulus convection parameterizations are formulated as mass flux schemes (determine the overall mass flux of all cumulus clouds in one AGCM grid column), the presented cloud field model determines for each AGCM grid column (where convection takes place) an explicit spectrum of different clouds. Therefore, the information about the actual cumulus convection state in a grid column is not restricted to an averaged mass flux but includes the number of different cloud types which in principle are able to develop under the given atmospheric conditions. The degree to which part each cloud type participates in the whole cloud field is determined by the cloud field model with respect to the special vertical state in the grid column. The choice of the cloud model to define the different cloud types is very flexible. Very simple cloud models are possible but also more complex ones that describe more realistic clouds (including dynamic and microphysical information) than simple mass flux approaches do. The cloud field model takes into account the interaction between all non-convective processes calculated by the AGCM and (which makes the procedure self consistent) the cloud-cloud interaction between each cloud type and each other. The final calculation of the cloud field is done following an approach from population dynamics. The tests of the model in the ECHAM5 AGCM (running in single column mode) show that the model produces reliable convective feedbacks (i.e. integral convective heating, convective transport, etc.). The additional information of the cloud field structure (power law behavior of cloud size distribution, cloud tops for each cloud type, cloud cover, etc.) shows also a principle consistency with observations.

2.1 Introduction

Cumulus convection, or more general, the treatment of clouds which is forced by local vertical instability, is one of the major problems in global climate modeling [*Emanuel*, 1994]. A reasonable treatment of the physical process associated with convective clouds is of great importance for many (all) other physical processes in a AGCM. Convection controls to a large degree the vertical transport of moisture, chemical tracers, energy and momentum. When precipitation forms in convective clouds, the net release (due to condensation of water vapour to cloud droplets and afterwards raindrops) leads to a supply of available potential energy in the free atmosphere. This couples convection to the large scale dynamics. Cumulus convection not only takes part directly at the global energy and water cycle (transport), but also indirectly:
The outflow of cloud water at the tops of convective clouds often leads to layered clouds. In this case convection leads not only to a redistribution of moisture and energy within cumulus towers itself, but also to a decoupling of these quantities from their primary sources. Layered clouds in turn have great importance in the radiation budget of the Earth. Since the problem of cumulus convection parameterization has been recognized to be such an important module of climate models, it has been widely studied in the past and is still a current question and point of interest in climate modeling [*Emanuel and Raymond*, 1993]. Different attempts and strategies have been followed doing this. To classify the model presented in this work according to these attempts, a short overview shall be given.

2.1.1 Different Convection Parameterizations in Climate Models

Kuo - Type - representation

This approach [*Kuo*, 1965, *Kuo*, 1974] reflects the idea that the water substance follows a statistical equilibrium. Therefore, convection is assumed to consume water and not energy. There is a significant problem in this representation: Convection in nature is always caused by an instable temperature profile and therefore by a state that is not in its entropy maximum. The supply of moisture by the macrofluid system without any accompanying production of instability can not force convection. This parameterization is therefore in a major point unphysical [*Emanuel and Raymond*, 1993].

Classical convective adjustment

The underlying principle for adjustment schemes is that convection is a response to instability [*Betts*, 1986, *Betts and Miller*, 1986]. Therefore, these schemes have a better physical basis than Kuo - type - schemes. An instable temperature profile is adjusted back towards a profile that is neutral or nearly neutral to convection. The main drawback of this approach is that these parameterizations make no attempts to consider the physical properties of the physical entities which are responsible for the adjustment (clouds) to calculate the adjustment effect.

Convection schemes based on cloud models

There are a number of convection schemes based on cloud models of different complexity. In principle, these schemes are also adjustment schemes with the important difference that a cloud model is used to calculate the response to instability. The cloud models (one dimensional cloud, mass flux or parcel models) are used to produce vertical profiles of heating and moistening by convective clouds. The model presented in this paper belongs to this group. Among several specific details, the two main differences between the schemes lie in the used cloud model (complexity, microphysics, downdrafts) and the manner in which the convective response is coupled to the resolved large scale variables (closure). Schemes which are comparable in a conceptual sense with the presented one are: [*Arakawa and Schubert*, 1974, *Anthes*, 1977, *Kain and Fritsch*, 1990, *Kreitzberg and Perkey*, 1976, *Kreitzberg and Perkey*, 1977]
We will refer later in this work in more detail to these schemes when discussing the concept of our scheme.

2.1.2 General Requirements to Convection Parameterizations

The variety of different cumulus convection parameterizations currently used in AGCMs and which show a good performance depending on the focal point of analysis reflects one important point:
The problem to describe the behavior of cumulus clouds on the typical scale of current horizontal AGCM resolution is in principle not exactly solvable. The scales of AGCM resolution (horizontal and less extreme vertical) and the typical cumulus cloud scale differ in such a way that there is a significant lack of information to determine an exact cloud state for an AGCM column. The mathematical problem is therefore extremely under-determined.

To motivate our approach we recall the basic requirements to a convective parameterization and point out the difficulties that appear.

The need to parameterize convection

Convection is a typical sub-grid process in current AGCMs. While the typical horizontal model resolution is on the order of 100 km, the typical cloud scale is about 1 - 10 km. This shows that a global climate model is not able to resolve convective clouds in terms of grid mean variables. So there is need to parameterize this effect. Parameterization does not mean to describe a physical process by solving the basic equations for this process, but to construct a sub model that should describe basic features of the real process using generalized physical degrees of freedom of the system.

Characterization of a convective parameterization

In general, such a sub-model is a statistical description of the real process. The accuracy of this description has to satisfy the demands of other processes calculated in the climate model. A well defined sub-model should contain an exact definition of the actual degrees of freedom which describes the convective state in a column. This is important since it helps to define the limits of such a parameterization. Limits are also given by the fact, if and how the model reacts on an external forcing. Is the response of a model strictly given by the forcing or is there the possibility for an internal organization of the response?

Budget Equations

For completeness we give a short description how the convective parameterization is usually incorporated in the large scale processes of an AGCM. The fundamental paradigm that makes it possible to think of a convection parameterization is (and it is by no means assured that this is true), that there exists a well defined ensemble of convective clouds on the scale of GCM resolution that is large enough to be treated as a statistical object. The direct consequence of this idea is that, if the paradigm is true, there must be a separation of scales (temporal and spatial):
The scale of large scale motion which force the convective process and the scale of local and spontaneous convection that reacts as fast on the large scale forcing that every time, on GCM resolution scale, a good equilibrium between both processes exists. This leads to the result that in all mass flux schemes the contribution of convection to the overall transport of heat/moisture etc. is written in a simple vertical eddy flux term. We will give a short outline of the usual mathematical procedure. Reynolds [*Reynolds*, 1901] introduced the division of each model variable Ψ into a resolved, slowly varying component $\overline{\Psi}$, and a sub-grid fast fluctuating deviation from this grid mean value Ψ'. Each variable can be written in the form:

$$\Psi = \overline{\Psi} + \Psi' \tag{2.1}$$

The budget equations for temperature and moisture are given in the form:

$$\overline{\frac{\partial T}{\partial t}} = \overline{\nabla \cdot \underline{v}T} + \overline{\frac{\partial wT}{\partial z}} = \frac{L(\overline{c-e})}{c_p} - Q_R \tag{2.2}$$

$$\overline{\frac{\partial q}{\partial t}} + \overline{\nabla \cdot \underline{v}q} + \overline{\frac{\partial wq}{\partial z}} = -(\overline{c-e}) \tag{2.3}$$

The symbols have their standard meteorological meaning given in the appendix. All terms in these two equations contain in general contributions from the resolved processes and the unresolved sub-grid processes. So, before they can be used in a numerical model some mathematical conversions must be applied. Therefore we use the Reynolds averaging assumptions [*Reynolds*, 1901]:

$$\begin{aligned} \overline{\overline{\Psi}} &= \overline{\Psi} \\ \overline{\Psi'} &= 0 \\ \overline{\overline{\Psi}\Psi'} &= 0 \\ \overline{\frac{\partial \Psi}{\partial x}} &= \frac{\partial \overline{\Psi}}{\partial x} \end{aligned} \tag{2.4}$$

With these averaging assumptions the budget equations for temperature and moisture can be written in a much more transparent form: time derivatives can be written as finite differences of only resolved model variables, horizontal and vertical fluxes can be divided into resolved components and unresolved eddy components. These fluxes become:

$$\overline{\nabla \cdot \underline{v}\Psi} = \nabla \cdot \overline{\underline{v}}\overline{\Psi} + \nabla\overline{\underline{v}'\Psi'} \tag{2.5}$$

$$\overline{\frac{\partial w\Psi}{\partial z}} = \frac{\partial \overline{w}\overline{\Psi}}{\partial z} + \frac{\partial \overline{w'\Psi'}}{\partial z} \tag{2.6}$$

where Ψ represents temperature and moisture, respectively. On the right hand sides of these equations we find now the resolved component (first term) and the sub-grid or Reynolds stress component (second) term. Finally our budget equations have the form [*Reynolds*, 1901]:

$$\frac{\partial \overline{T}}{\partial t} + \nabla \cdot \underline{\overline{v}}\overline{T} + \frac{\partial \overline{w}\overline{T}}{\partial z} = \frac{K(\overline{c-e})}{c_p} - \frac{\partial \overline{w'T'}}{\partial z} - Q_R \tag{2.7}$$

$$\frac{\partial \overline{q}}{\partial t} + \nabla \cdot \underline{\overline{v}}\overline{q} + \frac{\partial \overline{w}\overline{q}}{\partial z} = -(\overline{c-e}) - \frac{\partial \overline{w'q'}}{\partial z} \tag{2.8}$$

In this form we find all resolved terms on the left hand sides and the sub-grid terms or eddy flux terms on the right hand sides. The parameterization problem is then basically to find the terms $\frac{\partial \overline{w'\Psi'}}{\partial z}$, c, and e.

Convection parameterization and statistics

As mentioned before in general, a parameterization needs a statistical basis. Comparing the different scales (horizontal resolution of AGCMs and cloud scale) it is obvious that in general a grid column contains more than one cloud and additionally more than one cloud type. In case of strong convective activity we can estimate to find about 1000 up to 10000 clouds per grid column (resolution dependent). This seems to be very much. In fact it is not in a statistical thermodynamic sense! Remembering that a typical thermodynamic system for which statistics is valid without dispute contains on the order of 10^{23} particles, it is questionable to apply a statistical method to the convection problem. Convection is a typical phenomenon that falls into the gap between deterministic and stochastic tractability.

However, each representation which is currently in use makes use of a statistical approach and so does the presented scheme. The essential assumption to ascribe a sub grid process like cumulus convection to the resolved system is that both processes are in a statistical equilibrium. This important insight in the convection parameterization problem was first made by [*Arakawa and Schubert*, 1974]:
To the extent convection can be diagnosed from the large scale macro fluid flow, its energy must be in a state of statistical equilibrium with that flow.
This statement reflects the chance to parameterize convection but also, and more important, the limits to resolve sub grid structures of convective cloud fields.

2.1.3 Sub-grid Variability

One, if not the most important, point in each convection parameterization is to consider sub-grid structures in cloud fields. Since there are only mean profiles for temperature, humidity, etc. available, this is no trivial or straightforward task! However, studies and efforts [*Gedney and Valdes*, 2000, *Lin and Neelin*, 2000, *Graf et al.*, 2001] show that even small changes in the convective forcing can lead to large effects in the structure of global circulation and/or precipitation. Additionally, more and more studies are carried out to investigate questions like cloud microphysical effects on global circulation (see chapter 1. for aerosols and precipitation, lifetime of clouds, ice formation, etc.), transport of chemical tracers, radiation and clouds and many other problems. These problems are highly coupled to convection and sub-grid structures of cloud fields. This shows the need to have as much information as possible about the convective state in a grid column. This information must be based on a physical model for the structure of convective cloud fields. Different strategies have been followed to reach this aim. We concentrate on convective schemes that are based on cloud models. Schemes without any cloud or parcel model have nearly no chance to resolve sub-grid structures.

Prescribed implicit cloud spectrum

Many schemes represent convective sub-grid variability using prescribed parameters. In general, these schemes determine one averaged mass flux per grid column which represents all clouds present in a grid column. A typical cloud model (mass flux model) used for this type of calculation contains one or more parameters (e.g. entrainment, detrainment, overshooting, mixing) which implicitly describe a spectrum of different clouds (different dynamic, different vertical extent). The general structure of such a spectrum is fixed since the parameters are fixed. So, there is no direct consequence of different vertical profiles on the general structure of cloud fields. The schemes are tuned to reproduce a small number of observations in special regions and special meteorological situations and /or to reproduce a satisfactory result of global circulation/precipitation. The disadvantage of such schemes is that one set of parameters can hardly be valid for the wide variety of different convective regimes. The advantage is that they are the only schemes that are fast enough to work as operational schemes for long climate runs in AGCMs.

Interactive explicit cloud spectrum

A more sophisticated way to consider sub-grid variability is to introduce explicitly different cloud types at one time step for one grid column. This was first done by [*Arakawa and Schubert*, 1974]. For the detailed description of this method see [*Arakawa and Schubert*, 1974, *Lord et al.*, 1982]. Also other authors followed the "explicit" way. The main advantage of this approach, compared to the "implicit" one, is that one describes in more detail the different behavior of the different cloud types (microphysics, dynamic). Additionally it is possible to calculate interactions between different cloud types. In this case the cloud spectrum is not fixed to some parameters. Far from it! The spectrum is a result of different possible cloud types that are able to develop in the given vertical situation and the effect that each cloud type has on its environment. The presented model follows strictly this way. It is more complex and detailed than other explicit schemes but this at the expense of computer time. It is not designed to work operationally as a standard convection scheme for long climate runs but as a tool to get insights in the structure of cloud fields. More than other schemes, it follows the paradigm of self-organization and self-consistency.

2.2 Organization and Self-Organization

The formation of organized and self-organized structures (in physics, biology and chemistry) has become one of the most challenging problems in science in the last few decades. Numerous examples of these systems have been studied extensively in different fields. Since the pathbreaking book "Synergetics" [*Haken* , 1977, *Haken* , 1983], the question if and how structure formation arises in nature has become a physically and mathematically well based sub-discipline in many parts of natural science. One general result of these proceedings has been that even very complex systems (systems with a large number of degrees of freedom and dynamics which are too complex to be exactly solvable) tend to show a relatively simple behavior. Maybe the most prominent examples are the Laser and the Benard-convection [*Haken* , 1977, *Haken* , 1983]. Both systems show enormous complexity and it is much too difficult to write down the exact leading physical equations and solve them. But from a convenient point of view they seem to loose this complexity and show a more abstract but clear and ordered behavior. A common feature of these systems is the force that drives them towards this special behavior. Because it approaches the special problem of this paper (atmospheric convection) we focus on the phenomena of Benard-convection. It is one of the problems that have fascinated physicists for a long time. The system is characterized by complete disorder while residing in thermal equilibrium. But when pushed away from this equilibrium it can show a highly pronounced order. The physical situation is very simple: An infinitely extended horizontal fluid layer is heated from below. Consequently a temperature gradient is maintained. If this gradient exceeds a certain threshold, very regular convection starts. The heated system "fluid" is pumped with high quality energy which reduces the entropy of the system. It is the actual meaning of the second law of thermodynamic, that each free system tries to achieve the state of maximum entropy as fast as possible. This is the basic reason for the occurrence of highly ordered convection cells as seen in the Benard-experiment. The affinity between the highly idealized Benard-experiment and real atmospheric convection becomes clear now. The real atmospheric situation may be seen as a very crude realization of Benard's problem. Atmospheric instability may be created by the manifold of atmospheric processes (heating from the ground due to direct radiation absorption by the soil, radiative cooling in high atmospheric levels, advection, etc.). If the rate of instability creation does not reach a certain threshold it can be reduced fast enough due to vertical diffusion. But if this threshold is reached convection starts. Convective clouds form. In general, atmospheric convection does not show such a regular pattern as the Benard-convection does. Nevertheless, there are impressing situations (cold arctic air outflow) where real cloud fields show a fine regularity. What effectively happens when convective clouds form is the following: Nature finds an instable situation far from its state of maximum entropy. The fastest way to re-establish a stable situation (a situation of maximum entropy) is to form clouds. These clouds, although they are much more complicated than the simple convective cells in the Benard-experiment, play the same role as these. The important difference between Benard-convection and atmospheric convection is that the later one underlies many more dependencies: The temperature gradient (which is the measure for instability) is not as regular, wind shear and the large scale flow may inhibit the formation of simple cloud structures, orographic structures determine to a large degree if and how convection starts, and, as a major point, the effect of humidity due to phase changes. The physical problem we want to describe is a self-organization system. Considering an atmospheric column, as we have to describe it in an AGCM, the situation is as follows: There is a forcing term, which is actually given by every process that can create instability. And we have cloud-cloud interaction. When convection starts, normally not only one cloud forms. Different clouds develop, modify their surroundings - reduce instability - and affect each other. The resulting cloud field is due to self-organization of different clouds. The main difference between the presented Convective Cloud Field Model (CCFM) and common mass flux approaches is the following:

Mass flux schemes describe the integrated effect of a whole cloud ensemble. In these schemes there is no such thing as a single cloud! The entire effect of a cloud ensemble, including the cloud - cloud interactions has to be described by empirical parameters. Basically this is an important advantage and at the same time an important disadvantage:

The use of empirical parameters leads to very efficient numerical codes. Therefore, mass flux schemes can be used for long time simulations of global climate. On the other hand, these parameters are not able to represent the complete phase space of possible cloud configurations. Convection parameterization schemes based on a mass flux approach in general are tuned to simulate a few convective cases in a satisfying way. Using such parameterizations in a global model implies that it works reasonablly in all meteorological situations that appear in the model climate. As proven in many studies, this is not the case.

The transition from a mass flux approach to our cloud field approach is somewhat analogous to the transition from phenomenological thermodynamics to statistical thermodynamics. A mass flux scheme provides ensemble quantities (mass flux, heating rates, precipitation, etc.) that refer to some degree to pressure, density, temperature

in the phenomenological thermodynamic. Mass flux schemes describe the macro state of the cloud ensemble! Our model provides distribution functions of clouds analogous to e.g. the Maxwell-Boltzmann distribution in statistical thermodynamics. These distribution functions indicate to what degree the different clouds contribute to the ensemble. Especially cloud - cloud interactions are included in the model not due to empirical parameters, rather due to a theoretical model. The Convective Cloud Field Model describes the micro state of the cloud ensemble in a statistical sense.
This is the basic idea which we want to pursue in this work.

2.2.1 Classical Population Dynamics

The situation we want to discuss is the competition of n different species for m different food resources. Let us begin with the simplest example where $m = n = 1$. The equation that can describe basic features of this state is known as Verhulst equation. It is given by:

$$\frac{dn}{dt} = \alpha_1 n - \alpha_2 n^2 \tag{2.9}$$

where n is the number of species. In this equation we have a growth term $\alpha_1 n, \alpha_1 > 0$ which reflects the increase of the species due to food supply and reproduction. If this would be everything ($\alpha_2 = 0$) we would end up with the solution $n(t) = n_0 \exp(\alpha_1 t)$ which describes exponential growth and therefore can never describe a realistic situation since an infinite increase of a population is not possible. To prevent this unrealistic behavior Verhulst introduced a depletion term $(-\alpha_2 n^2, \alpha_2 > 0)$. This term leads to a limited increase. n grows until an equilibrium between growth and depletion is established. A solution of the Verhulst equation is given in Figure 2.1.

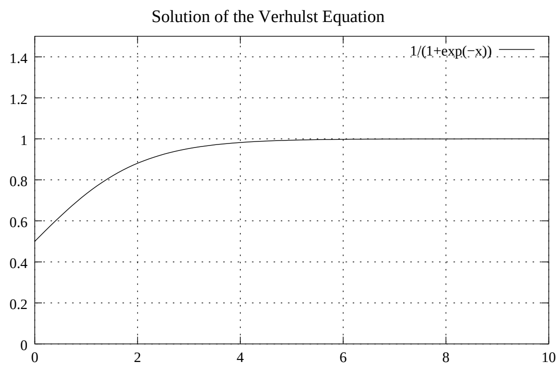

Figure 2.1 : Solution of the Verhulst equation
Asymptotic state is $n = 1$; x-axis: time , y-axis: population

A generalization of this equation is the so called Lotka-Volterra equation:

$$\frac{dn_i}{dt} = n_i F_i + \sum_{j=1}^{N} K_{ij} n_i n_j \tag{2.10}$$

This system of coupled differential equations was introduced by Volterra as a model for the competition of N different biological species [*Lotka*, 1925, *Volterra*, 1931, *Murray*, 1993]. F_i is a parameter depending on the environment and on the species number i. It describes the support of species number i due to external processes. $\mathcal{K}_{i,j\in 1,\ldots,N}$ is the interaction matrix. The coefficient K_{ij} describes the interaction between species i and j. Or more precisely, since the matrix is not necessarily diagonal, it describes the effect of species j on species i. Depending on the signs of the interaction coefficients the system is called a cooperative ($K_{ij} \geq 0$), a competitive ($K_{ij} \leq 0$), or a prey - predator one ($K_{ij}K_{ji} \leq 0$). The various systems have been extensively analyzed. They have proven their ability to describe at least some features of a variety of complex systems. In the following we would like to apply this approach to the problem of cloud-field-development.

2.2.2 Cloud Population and Cloud Field Development

In this section we show how the self-organization of a cloud field can be treated as a mathematical system. Before describing the full mathematical procedure we will expose the analogies between a typical biological system of N-different species which are in competition for different food sources and a cloud field. We will use the following nomenclature (cloud type, cloud class, cloud spectrum). Consider a given meteorological situation in a certain atmospheric column. This case refers to a specific grid column in an AGCM at a specific time step. The meteorological situation is then defined by a set of vertical profiles (temperature, humidity, etc.). Some situations may be possible where all clouds in such an area are very similar (cloud base, top, dynamic). In this case we would speak of one realized cloud type. However, in more complex situations we will generally find very different clouds. Small clouds, high clouds, clouds with a different dynamic. In this case we can classify the clouds according to a proper attribute. This can be the cloud top, cloud radius, or something else. The variety of all clouds form the cloud spectrum can be expressed as a function of the above mentioned attribute. Since it is a numerical problem to describe a continuous cloud spectrum we have to discretize it and consider a limited number of cloud types. These types or classes describe in each case identical clouds with a well defined physical structure. The analogy that we proclaim is to treat different cloud types as different species. Biological species as described by equation 2.10 are in competition ($K_{ij} \geq 0, F_i \geq 0$) for an external food supply rate. In such a simple model the supply of food is the reason for a species to survive or grow. The analogy to convective clouds is straightforward: The reason for convective clouds to form is atmospheric instability. Instability can be vertically distributed in very different ways. Since each cloud type has then a different environment (because of different vertical extent), it has a different "food-supply" due to non-convective atmospheric processes. Additionally, each cloud type acts on its environment in a well defined way and tends to reduce instability. Therefore each cloud tends to reduce somehow the "food-supply" for all other cloud types (K_{ij}) including itself (K_{ii}). This is the general idea behind our model which shall be introduced in detail in the following sections.

2.3 Model Description

A significant feature of the model is its modular structure. This makes the model very flexible and allows easy changes of the separate components. In principle we have three main parts in the model: The heart is a one dimensional cloud model. This is used to define the cloud types which are able to develop under a given meteorological situation. The next step is to define the cloud forcing and the cloud-cloud- interaction coefficients for these special clouds and the special meteorological situation. The last step is to use a master equation to calculate the development and the final state of the cloud spectrum. We want to point out that we think that each of these three parts should (and will) be object of our further investigations. The program structure is shown in Figure 2.2.

The proposed model follows the idea of quasi-equilibrium that was first formulated by [*Arakawa and Schubert*, 1974]. This idea defines to a large degree how the convective scheme has to be inserted into the hosting GCM. Since we tested the model in ECHAM-AGCM [*Roeckner et al.*, 1996] we confine our explanation to this model. However, there may be no principal differences to other AGCMs.

When the physics is activated in ECHAM it follows a certain sequence: Radiation, vertical diffusion, gravity waves, convection, stratiform clouds. We assume the following idealized but not too artificial situation: Let the vertical profile in a special grid column be a neutral one. Then the physical processes, which are specified before convection, (namely radiation) are able to create some instability. Therefore, at the time convection is activated there are probably two sets of vertical profiles available: A neutral one from the last time step (which we call TM for temperature and HM for humidity) and an instable one which is just the sum of TM and HM and the tendencies of the current time step. We call them T and H. So we have a stable situation and an instable situation. This is all the information we get from the GCM. The manner in which instability is vertically distributed will determine the cloud spectrum.

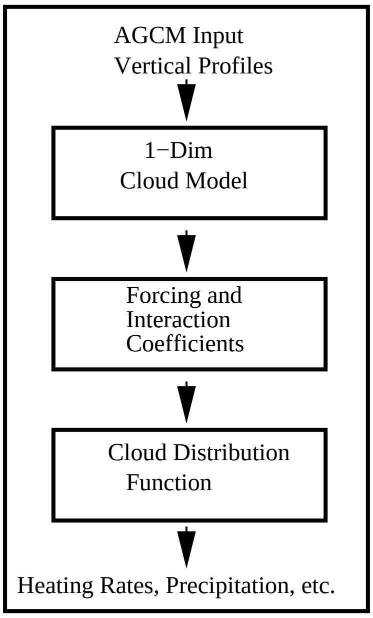

Figure 2.2 : Program structure

One - Dimensional Cloud Model

The used one-dimensional cloud model is based on the concept of a computer model developed in the late 1960's at the Pennsylvania State University [*Weinstein and MacCready*, 1969]. From today's view it is a very simple model and it is far from being comparable with the performance of current three - dimensional cloud resolving models. However, we think it is a good choice to use it as a part of our model since it needs very little computational resources but allows for more microphysical and dynamical calculations than many of the current convection schemes. The model is a steady state Lagrangian solution of a set of equations for temperature, cloud radius, vertical velocity, cloud water/ice and rain water/ice. The thermodynamic and dynamic calculations are numerical analogies of the classical parcel method with entrainment. The equations are based on the first law of thermodynamics and the vertical equation of motion. Cloud microphysical calculations follow the well known parameterization developed by Kessler [*Kessler*, 1969]. The equations are given by:

$$\frac{dT}{dz} = [-\frac{g}{c_p}(1+\frac{Lq_s}{RT}) - \mu\frac{L}{c_p}(q-q_e) + \frac{L_f Q}{c_p dz} + \frac{L_s(\Delta q_s)_{w\rightarrow i}}{c_p dz}]/(1+\frac{\epsilon L^2 q_s}{c_p RT^2}) \quad (2.11)$$

$$q_s = \frac{\epsilon e_s}{p - e_s}; \frac{1}{e_s}\frac{de_s}{dT} = \frac{\epsilon L}{RT^2} \quad (2.12)$$

$$\frac{1}{2}\frac{dw^2}{dz} = g(\frac{T_v - T_{ve}}{T_{ve}} - Q) - \frac{\mu w^2}{2} \quad (2.13)$$

$$Q = Q_c + Q_h \quad (2.14)$$

$$\frac{dQ_c}{dz} = -\frac{dq_s}{dz} - \mu(q - q_e + Q) - \frac{K_1}{w}(Q_c - A) - \frac{K_2}{(w - V_t)}\rho^{-0.875} Q_c Q_h^{0.875} \quad (2.15)$$

$$\frac{dQ_h}{dz} = \frac{K_1}{w}(Q_c - A) + \frac{K_2}{(w - V_t)}\rho^{-0.875} Q_c Q_h^{0.875} \quad (2.16)$$

$$V_t = 130 D_0^{0.5} \quad (2.17)$$

$$D_0^{0.5} = K_3 Q_h^{0.125} \quad (2.18)$$

$$\frac{d(lnR)}{dz} = 0.5[\frac{d(lnw)}{dz} + \frac{d(ln\rho)}{dz}] \quad (2.19)$$

To run the model requires a set of vertical profiles (temperature, humidity) and initial values for cloud base radius and cloud base vertical velocity. The indefiniteness of these two parameters opens the possibility for creating a cloud spectrum. As mentioned before, the first step is to define, for a special grid column and at a special time step, a spectrum of different clouds which in principle are able to develop under the given meteorological situation. Therefore we take the instable set of profiles (provided by ECHAM4), since this set is susceptible for convection, and run the one-dimensional model several times with different initial values for cloud base radius and cloud base upward velocity. Practically, this is done by choosing for both quantities an upper and a lower boundary and an increment. Let us assume that we have K initial radii ($r_{min}, r_{min} + \Delta r, ..., r_{min} + \Delta r(K-1)$) and L initial vertical velocities ($w_{min}, w_{min} + \Delta w, ..., w_{min} + \Delta w(L-1)$). So we end up with $K \cdot L$ different couples of initial conditions that lead to $K \cdot L$ different cloud types. Each cloud type is completely defined by the output-profiles of the one-dimensional model. The difference in these cloud types depends on the increment of r and w and on the special meteorological situation. We show in Figure 2.3 several different cases of cloud vertical velocity profiles as orientation to the variety of resulting cloud types arising from different meteorological situations. While referring to the Figure we would like to discuss briefly the possible cases:

In Figure 2.3 a-h we initialized 50 different cloud types. The initial updraft velocity was fixed (2m/s) while the initial cloud radius started with 500m and an increment of 50m. This increment is much smaller than that we used finally in the model (and the cloud type number is much higher). However, these pictures give an impressive illustration how the 1-dim model reacts to different vertical environments and how the cloud types differ with respect to different initial radii. Figure 2.3 a-c show three typical convective regimes with increasing complexity. In picture a) we have a very clear situation. There is a continuous spectrum of possible cloud types (cloud base at about 1km) beginning with small clouds (not much more than 1km deep) up to considerably deep clouds rising up to about 6 km altitude (5 km deep). There is no gap in this case, or, in other words, all cloud thicknesses from 1-5km are in principle possible in this situation. The situation in picture 2.3 b) is a bit more complicated. Here we have no continuous spectrum of possible cloud tops but a two level situation. The cloud base is at about 500 m. There are about 10 cloud types that reach the height between 2000 m and 2700 m. In the vertical temperature profile here we find a small inversion. This inversion is responsible for the fact that the smaller clouds (clouds with smaller initial radius) cannot grow to higher altitudes but stop at this height. However, there is a threshold for the initial radius of cloud types above which the clouds are able to overcome this inversion. These clouds again form a continuous spectrum with tops ranging from 6000 m up to 8000 m. The mechanism that determines this relation between cloud initial radius and maximum cloud height lies in the entrainment rate $\mu = \frac{C}{R}$. For small clouds μ becomes very large. This means that there is a very efficient dilution of buoyant cloud air with colder environmental air. This process disrupts the ascending motion. The picture also shows very impressively, how different the dynamical structure of the different cloud types can be. This information of the vertical velocity profile can be very useful for more detailed microphysical parameterizations or e.g. for lightning in clouds. In picture c) the situation is again more complex. Here we have a clear three level situation. Cloud tops can be found at 2000 m, 6000 m and 10000 m. Additionally we find in this situation a good example for the typical overshooting of deep convective clouds:

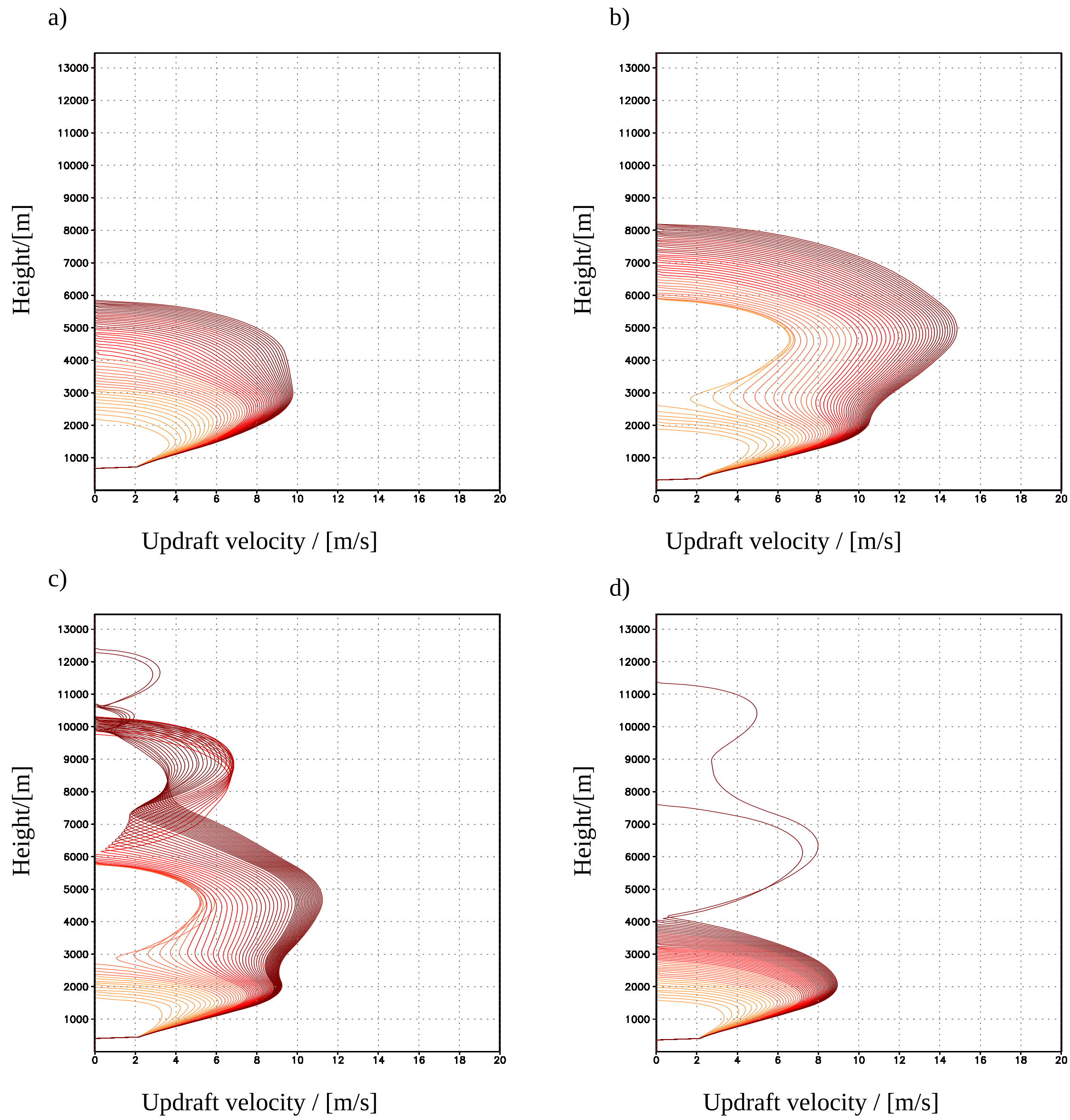

Figure 2.3 a-d : Cloud updraft velocity for different vertical situations
Different colours indicate different initial cloud base radii:
yellow: $500m \leq R_{ini} < 1000m$; orange: $1000m \leq R_{ini} < 1500m$;
light red: $1500m \leq R_{ini} < 2000m$; red: $2000m \leq R_{ini} < 2500m$;
dark red: $2500m \leq R_{ini} < 3000m$

A few clouds reach about 10500m while two cloud types can develop up to 12500m. The picture shows of course also that this overshooting is a very sensible process. It may depend on the accuracy of the cloud model calculation and the vertical resolution. However, case c) is a typical example for what happens in the model in deep convective regimes. Overshooting in nature is a critical phenomenon and so it is in the model. Therefore, we are surprised to find this behavior in the model.

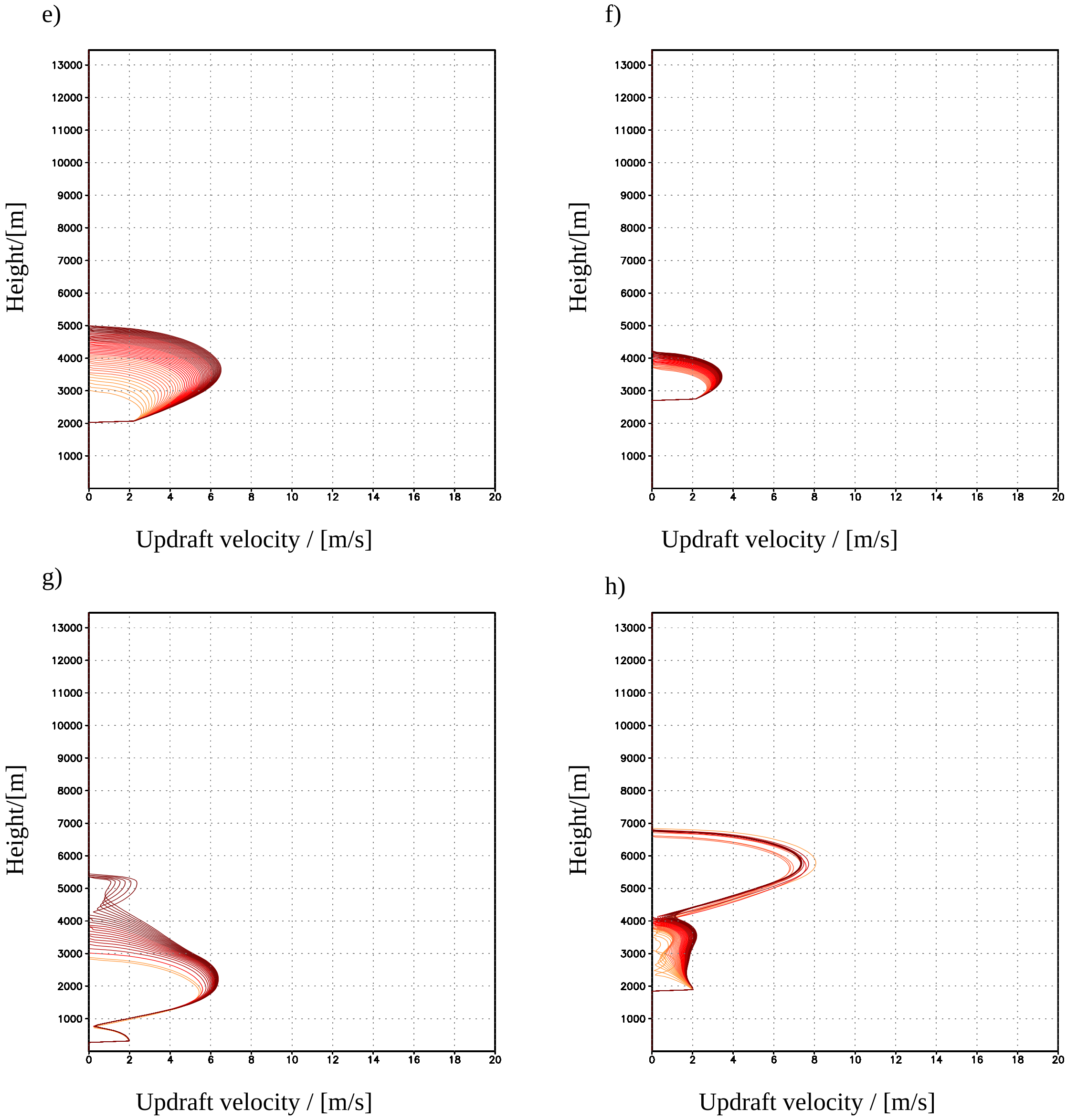

Figure 2.3 e-h : Cloud updraft velocity for different vertical situations
Different colours indicate different initial cloud base radii:
yellow: $500m \leq R_{ini} < 1000m$; orange: $1000m \leq R_{ini} < 1500m$;
light red: $1500m \leq R_{ini} < 2000m$; red: $2000m \leq R_{ini} < 2500m$;
dark red: $2500m \leq R_{ini} < 3000m$

Case d) is in principle the same as case c). But here we see that the threshold for initial cloud radius to overcome the inversions has changed. In fact we have here a stronger inversion than in case c). Most of the cloud types have tops below 4000m. Only two reach about 7500 m and 11500 m.

The pictures 2.3 e-h show no absolute new information. But, they give some more examples of the possible convective regimes. Cases e) and f) show two examples for higher cloud bases. In both cases the cloud type spectrum is as simple as in case a). Case f) is a very special situation where this spectrum is so extremely narrow that nearly all cloud types are equal. The last two pictures g) and h) show a nearly inverse dynamical structure of each other. Very intensive updrafts in the lower part of the clouds and less intensive updrafts in the upper part in picture g) and the other way round in picture h).

Each single picture in Figure 2.3 shows for a special time step and a special grid column the clouds that in principle are able to develop. This should not be confused with the cloud spectrum we want to calculate. The information of Figure 2.3 should be taken as follows: The meteorological situation in each of these cases is instable. Otherwise no clouds would form. Our aim is to abolish this instability, as it is the aim of each convection scheme. But in our scheme we are only allowed to use these clouds and nothing else! It is comparable, not in a strict mathematical sense but more in an intuitive way, to a base of a vector space. The single clouds constitute the base of this vector space. Our aim is now to determine a vector which is actually the resulting cloud field that describes the spectrum of clouds realized by nature to relax the instable situation to a neutral one. This is done by using the Lotka-Volterra equation. However, to use this equation we first have to define interaction coefficients between clouds and external processes and between the clouds themselfes.

The CAPE formalism

To formulate our model concept we make extensive use of the CAPE (Convective Available Potential Energy) formalism. Although this is widely used, we give a short introduction.
The onset of convection, whether in an idealized laboratory experiment or in the atmosphere, is always caused by a specific stratification of air/fluid - masses. In fact, the shape of the temperature profile is the first order criterion that determines whether convection appears or not. The buoyancy force that acts on a vertically replaced air parcel is given by:

$$B = g\frac{T_p - T}{T} \tag{2.20}$$

where T is the temperature of the environment and T_p the temperature of the air parcel. The temperature of such a vertically replaced air parcel follows a dry or moist adiabatic (in the saturated case) temperature gradient. Therefore, an air parcel that is lifted upwards and finds a colder environment, is conditionally unstable. Exactly that is the case when the one-dimensional cloud model is working. The potential energy (instability) that is consumed by such a cloud is given by the vertical integral of buoyancy force from cloud base up to the level where buoyancy is zero (Level of Neutral Buoyancy) LNB. Above that point the cloud parcel finds a stable stratification which stops and inverts its vertical acceleration, and therefore defines the cloud top. The energy converted by a cloud in a given environment is scaled with the CAPE given by:

$$CAPE = \int_{base}^{LNB} B dz \tag{2.21}$$

Cloud forcing

After having defined the cloud classes in the first part, now we need information which cloud types are actually forced or supported by external processes. To get this, we need to make some important definitions and conventions. As mentioned before, we have two sets of vertical profiles available when running the convection scheme. We called them (TM,HM) for the neutral one from the last time step and (T,H) for the potentially instable one, which is the sum of (T,H) and the associated tendencies of all other physical processes which are called before convection. Since we have run the cloud model in the instable environment (T,H) (we need to do it in the instable one since we need clouds), we have a third set of profiles (for each cloud type separately) available which is the in-cloud-temperature T_{c_i} of cloud type number i. We now define the "cloud potential energy content" by

$$CAPE_i(T) = g\int_{Base_i}^{LNB_i} \frac{T_{c_i} - T}{T} dz \tag{2.22}$$

and

$$CAPE_i(TM) = g\int_{Base_i}^{LNB_i} \frac{T_{c_i} - TM}{TM} dz \tag{2.23}$$

where $T = TM + T_{tend}\Delta t$, $Base_i$ is the base of cloud type i and LNB_i the Level of Neutral Buoyancy of cloud type i. The relative change of the "cloud potential energy content" due to all non-convective processes during the current time step can be expressed therefore as

$$F_i = \frac{CAPE_i(T) - CAPE_i(TM)}{CAPE_i(TM)\Delta t} \tag{2.24}$$

It may be helpful to note that $F_i CAPE_i(TM)$ can be understood as the time derivative of $CAPE_i(TM)$ with respect to the effect of all non-convective processes.

$$CAPE_i(TM)F_i = \frac{CAPE_i(T) - CAPE_i(TM)}{\Delta t} = \frac{CAPE_i(TM + T_{tend}\Delta t) - CAPE_i(T)}{\Delta t} \tag{2.25}$$

with

$$\frac{dCAPE_i(TM)}{dT} = \lim_{\Delta t \to 0} \{\frac{CAPE_i(TM + T_{tend}\Delta t) - CAPE_i(TM)}{\Delta t}\} \tag{2.26}$$

Cloud-Cloud Interaction

The cloud-cloud interaction is treated similar to the cloud forcing due to external processes. It is done as follows: First we calculate the effect of each cloud type on the environment (T,H). We call the resulting profiles (T_j,H_j), where j is the index that indicates the cloud types. As in the former section we are interested in the effect of the change in the vertical profiles on the cloud potential energy. According to equation 2.22 and 2.23 we define:

$$CAPE_i(T_j) = g \int_{Base_i}^{LNB_i} \frac{T_{c_i} - T_j}{T_j} dz \tag{2.27}$$

where $T_j = T + T_{tend_j}\Delta t$ and T_{tend_j} is the tendency due to the effect of cloud type j on the temperature profile T.

The relative change of cloud potential energy of cloud type i due to the effect of cloud type j is therefore:

$$K_{ij} = \frac{CAPE_i(T_j) - CAPE_i(T)}{CAPE_i(T)\Delta t} \tag{2.28}$$

$K_{ij}CAPE_i(T)$ is again the time derivative of $CAPE_i(T)$ with respect to the effect of cloud j.

$$\frac{dCAPE_i(T)}{dt} = \lim_{\Delta t \to 0} \frac{CAPE(T + T_{tend_j}\Delta t) - CAPE_i(T)}{\Delta t} \tag{2.29}$$

It is evident that the definition of F_i and K_{ij} causes some problems when trying to explain it mathematically exact. $CAPE_i(T)$ is based on an exact definition since T_{c_i} is created by running the cloud model in the environment (T,H). This is different for $CAPE_i(TM)$ and $CAPE_i(T_j)$. Here we compare T_{c_i} with TM and T_j. However, the difference between T and TM/T_j is not too large, so that the procedure is acceptable. The exact way would be to run the cloud model not only N-times (N different cloud types) with the profile T, but also N-times for TM and N-times for each of the N different T_j. We would end up with $(2N + N^2)$ times to run the cloud model instead of N times in the current procedure. Although we choose a fast and simple 1-dim model this would exceed a tolerable quantum of computer time requirement. Tests show that the numerical difference between the "N" solution and the "$2N + N^2$" solution is not too large. However, we recognize that this inconsistency might be a starting point for criticism of the model concept.

Lotka-Volterra Equation

Now we are prepared to formulate our master-equation to calculate the resulting cloud spectrum. The Lotka-Volterra equation is given by [*Lotka*, 1925, *Volterra*, 1931, *Murray*, 1993]:

$$\frac{dn_i}{dt} = \sum_{j=1}^{N}[K_{ij}n_in_j] + F_in_i \tag{2.30}$$

Aside from the fact that this equation is probably the simplest one to describe the self-organization of a system of N-different components, we would like to elucidate this approach. With our definitions of the K_{ij} and the F_i we have two parts in this equation:
The part (F_in_i) represents the external forcing on the cloud field. The relative ratio of the different components $(F_i, i = 1, ..., N)$ shows which cloud types are favoured by the non-convective forcing. The n_i in this part reflects that this forcing is assumed to be proportional to the actual cloud type amount of each cloud type. Perhaps the more interesting part is $(\sum_{j=1}^{N}[K_{ij}n_in_j])$. K_{ij} is the effect of cloud type j on cloud type i. Analogous to the first part, this coefficient is multiplied by n_i and additionally by n_j

since the effect of cloud type j on i is assumed to increase linearly with the amount of cloud type j.

It is possible to give a first characterization of the equation by recalling the definition of F_i and K_{ij} and discussing some physical basics:

Clouds are assumed to reduce instability or, in other words, to consume convective available potential energy. Therefore $CAPE_i(T_j)$ is in general smaller than $CAPE_i(T)$ since T_j is already a bit stabilized due to cloud type j. As a consequence K_{ij} is in general negative. The non-convective processes are only important for us if they produce instability. Then $CAPE_i(T)$ is larger than $CAPE_i(TM)$ and therefore F_i is positive. If, for a special cloud type, F_i is negative (or zero) which could be possible, this cloud type has no chance to be a member cloud field.

Thus, in the model we assume that $K_{ij} < 0$ and $F_i > 0$. If $F_k \leq 0$ we can ignore this special cloud type k which reduces the degrees of freedom for the Lotka-Volterra equation by one dimension.

The technical procedure is as follows: After running the cloud model N-times and after calculating the F_i and K_{ij} we search for the positive F_i. In general we have $M < N$ positive F_i which potentially helps to save computer time. We choose an initial condition $n_i(0)$ and solve the set of differential equations of dimension m by iteration until a satisfying equilibrium is reached. Here is one crucial factor:
- initial conditions

Initial conditions: The model has no a priori values for the initial conditions. Therefore we have to choose a starting vector $n_i(0)$. This choice is not without problems since it is known that different initial conditions in general lead to different solutions in the field of coupled differential equations. And indeed that is the case here. The solutions for various initial vectors $n_i(0)$ are different, but in the context of convection parameterisation, which is to calculate principal structures of convective cloud fields, not too different.
To be more precise:

The principle structure of the resulting cloud spectrum, we call it "macro-solution", differs only gradually for different initial conditions. The "micro-solutions" do! However, this is not too bad, since the overall cloud spectrum, integrated mass fluxes, heating rates, precipitation fields remain unchanged. We think the difference in the "micro-solutions" is no deficit of our model. It reflects that the available information is just too small to predict an exact cloud state!

There are different ways to treat equation 2.30 and to extract a suitable cloud spectrum from the solution.

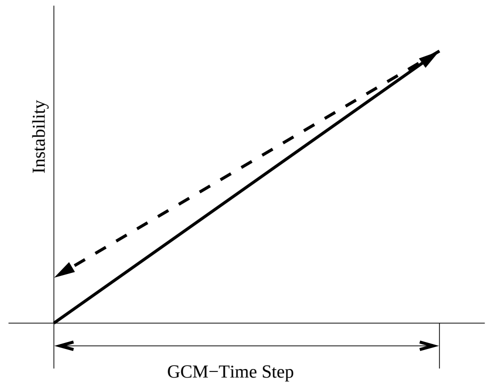

Figure 2.4 a) : Removing instability (schematic description)

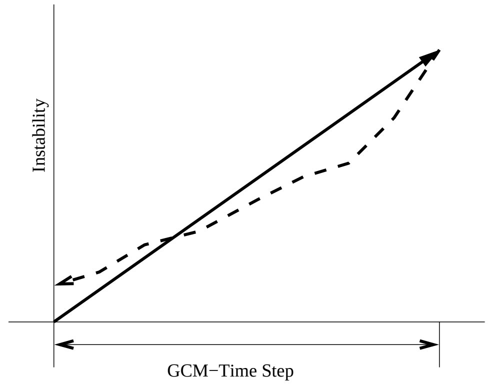

Figure 2.4 b) : Removing instability (schematic description)

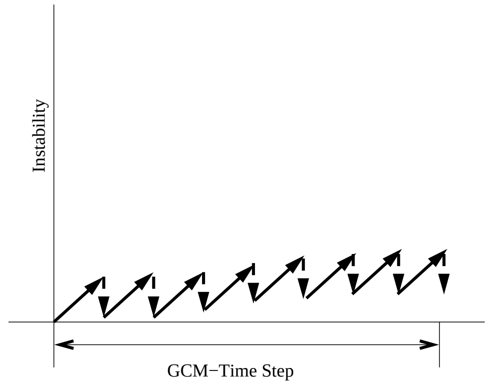

Figure 2.4 c) : Removing instability (schematic description)

The first one is the common way to treat convection. In Figure 2.4 (a) we describe the procedure in a schematic way. On the abscissa we have the time (actually one GCM time step), while the ordinate represents a (qualitative measure) for instability. During one time step external processes are able to create instability (solid line). When convection starts, it finds this instable situation and tries to remove it (dashed line). In general this is done in a perfect way. Therefore, the end point of the dashed line is not necessarily the same as the starting point of the solid line.

One of our questions was to investigate if it makes an important difference to subdivide (within the convection scheme) the GCM - time step into finer ones. For this procedure there are two strategies:
- One can just use the rates of instability creation and proceed in each sub-time step as in the the main time step without subdivision (b).
- The other way is to start at the same point as in case (a) but to recalculate the cloud spectrum several times (c).
It is obvious that the cases (b) and (c) become equal to case (a) if there is no subdivision of the main GCM time step.

For each sub-timestep (including the case were ($\Delta t_{sub} = \Delta t_{GCM}$) we have to solve equation 2.30 until an equilibrium is reached. Since there is no exact definition of a numerical equilibrium we have to stop the iteration when the solution converged within a certain accuracy.

Currently we follow case (a) as most convection parameterizations do. However, the model is constructed in a way that allows to switch very easyly between a, b, and c. Especially when introducing a more sophisticated cloud model (probably a time dependent one) it will become very interesting to change either to (b) or to (c).

Cloud Spectrum

As previously mentioned, we try to investigate principle structures of convective cloud fields. This statement implies that we have reasons to believe that there are fundamental and invariant structures to find. And indeed, besides theoretical and philosophical concepts (Section 2.2), there are sustainable observational indications that such an invariant in the cloud field organization may exist. This is the power law behavior of the cloud spectrum when it is expressed as a function of cloud radius. Since the work from [*Cahalan and Joseph*, 1989] also other authors found comparable results that show that such a power law behavior seems to be a general feature of convective cloud fields [*Benner and Curry*, 1998, *Weger et al.*, 1992, *Zhu et al.*, 1992, *Weger et al.*, 1993]. In principle, our model and the calculated cloud spectra show such a behavior (see later in this chapter). The results are not as accurate as those from satellite, but this should not be expected, keeping in mind how simple and idealized our model is.

2.4 Model Validation

Although the proposed model is actually not a pure convection scheme but a cloud field model, it can be used like a convection parameterization within an AGCM. As input it needs vertical profiles of temperature and humidity and as output it returns information about heating rates, integrated mass fluxes, tracer transport, precipitation and moisture transport, and detrained cloud water (important as source for cloud water in stratiform clouds). We use the ECHAM4-GCM as environment for our model.

GCM-Physics

The dynamical core of the ECHAM model has been adopted from the European Centre for Medium Range Weather Forecasts (ECMWF) model [*Roeckner et al.*, 1996]. Vorticity, divergence, temperature, surface pressure, and mass mixing ratios of water vapour and total cloud water/ice are treated as prognostic variables. The master equations are solved on a vertical hybrid $p - \sigma -$ system (19 - level) using the spectral transformation method with a triangular truncation. The truncation wave number can be selected (21,30,42,63,106). In this work we used the coarse resolutions T21 and T30. All physical parameterizations are calculated at grid points of a Gaussian grid. Wave numbers T21 and T30 correspond to a resolution of $5.6^0 \times 5.6^0$ and $3.75^0 \times 3.75^0$. For the time integration a semi-implicit leapfrog scheme is used. The time step depends on the resolution (40 min for T21 and 30 min for T30). Physical parameterizations exist for horizontal diffusion, surface fluxes and vertical diffusion, land surface processes, gravity wave drag, cumulus convection, stratiform clouds and radiation. Because the cloud parameterizations are more relevant for our work than the others, we focus in the following on cumulus and stratiform clouds.

<u>ECHAM4 standard convection:</u> The ECHAM standard convection is based on the widely used bulk mass flux concept of [*Tiedtke*, 1989]. The original Tiedtke scheme has been changed to include some suggestions of [*Nordeng*, 1994]. The changes include organized entrainment/detrainment and the mass-flux closure (adjustment type instead of moisture convergence for deep cumulus). Cloud water that may detrain at the tops of cumulus clouds is used as a source for cloud water in stratiform clouds. This comprises an important link between the two cloud parameterizations.

<u>Stratiform clouds in ECHAM4:</u> In this scheme mass mixing ratios of water vapour and cloud water are calculated. Cloud microphysical terms are condensation of water vapour, evaporation of cloud water, precipitation formation, sedimentation of ice crystals, and evaporation of precipitation in unsaturated air. Since real clouds normally are smaller than grid cells of an AGCM, it is sufficient that the grid mean relative humidity

exceeds a threshold which is smaller than than 100% to form clouds. In contrast to the convective cloud scheme the stratiform scheme calculates a cloud cover fraction.

Single Column Mode

The proposed version of our convective cloud field model is too time consuming to run it in an AGCM in a global mode. This is a disadvantage but not too bad. The model is explicitly developed not to work as a real convection scheme but to gain insights in cloud field organization and structure. To test the model and obtain an evaluation if it is capable to describe convective clouds, it is sufficient to run it in a single column mode in an AGCM. Therefore, we used the single column mode of ECHAM4 to run our cloud model at some representative points on the globe. These grid points were chosen to cover at least the extreme cases of the wide variety of different convective regimes. The column version of ECHAM4 is not a separate model, but the full model including all physics parameterizations of ECHAM4. The difference is that this model - mode considers only the vertical axis, whereas horizontal processes and tendencies have to be provided by a preceding 3D-model run. The detailed procedure is as follows: First a global run with the ECHAM4 standard configuration (including the convection) is performed. The "boundary forcing" for a special grid point is written into a forcing file. The next step is to run time series at these special grid points. This can be done in two different ways: We can simply switch on our model but just in passive, diagnostic mode. In this case, the standard convection scheme is still working and determines the model. Our model is just called at each time step and calculates a cloud configuration, and the related quantities (e.g. heating rates, precipitation). Here we can see for each time step separately what happens in our model and how it reacts on a given forcing (which is still determined by the standard convection). The other way is to switch off the standard convection scheme and to couple our model completely to the ECHAM4 physics, and to allow feedback of our model to the main model. In this case the standard convection has no effect within the column calculation which is now completely determined by our model. Nevertheless, it is still present since the boundary forcing was calculated with ECHAM4 standard physics. This is an inconsistency but acceptable since at this step of the model evaluation we are only interested in the principle model performance and not in details of the interaction between convection and the full model integrated over a longer time. This shall be part of further investigations.
Before starting final tests of the model we first have to fix some essential internal model parameters. These are namely the internal vertical resolution and the number of different cloud types. In both cases again we have to compromise between numerical accuracy and computational efficiency.

Vertical Resolution

A convection parameterization tries primarily to overcome the deficits of a low horizontal resolution. Likewise, the coarse vertical resolution seems to be a smaller problem. Most convection schemes work with the vertical resolution of the whole GCM (ECHAM4 standard: 19 levels from 1000 hPa to 10 hPa) or with interpolated values on "half- levels". This is sufficient since mass-flux models are designed to be content with such coarse resolutions. 1-dim cloud models, as the one used in this work, demand a finer resolution since the microphysical and dynamical calculations are more sensitive. Therefore, we interpolate the ECHAM4 standard vertical resolution on a finer vertical grid before starting the cloud model and cloud spectrum calculation. Also the calculation of the interaction coefficients F_i and K_{ij} is performed on this finer grid since this stabilized the numerical procedure.

Cloud Types

It is obvious that the idea behind the model is to have as many different cloud types as possible. However, there are limiting factors that one should not omit. The first point is the computational demand and the numerical accuracy of the Lotka-Volterra equation iteration. With increasing number of cloud types this part of the model becomes more and more problematical and time consuming. The second point is that a reasonable choice of the cloud type number (actually the increments Δr and Δw) is naturally coupled to the vertical resolution. It would be wasteful to use a relatively low vertical resolution and a relatively high cloud type number (with small increments) so that there is effectively no resolvable difference between clouds with similar initial conditions. The problem is of course to fix the term "relative" in this relationship. A good way is to invest more in the vertical resolution and less in the cloud type number. In this case one has more details of the possible cloud types and more precise F_i and K_{ij} which aids the cloud spectrum calculation. A third point for cloud type number fixing is the sensitivity of the 1-dim cloud model to variations of $r_{initial}$ and $w_{initial}$.

It turns out that variations in $r_{initial}$ are much more important for a large spectrum of possible clouds than variations in $w_{initial}$. This is of course under the condition that a sufficiently large value for $w_{initial}$ is chosen. The reason is shown by a simple energetic assessment of the situation:
$w_{initial}$ is only necessary to give the cloud a small initial momentum. Compared to the buoyancy that is typically involved in convective events, the initial momentum is small. After a short time the information about $w_{initial}$ is forgotten by the cloud, whereas the value $r_{initial}$ is responsible for the dilution of cloud air by environmental air. The larger r, the smaller is this dilution based on the cloud area.

However, there are of course thresholds for $w_{initial}$ that have to be exceeded.

Otherwise no clouds will develop at all.

Typical combinations for initial conditions that we used in this work are: 1-2 different $w_{initial}$ and 20-50 different $r_{initial}$.
$w_{initial}$ is always chosen to be in the range of 1 - 2 m/s.
$r_{initial}$ is in the range from 100 m up to 3000 m.

It turns out that in nearly all cases this combination leads to a reasonable spectrum of possible clouds.

2.4.1 Qualitative Validation

According to J. Mitchell [*Mitchell*, 1999] there is no generally accepted theory against which to test current cloud parameterizations. This statement becomes obvious when analyzing the problem:
Parameterizations (not only cloud parameterizations) have to represent the effects of a physical process. This proposition seems to be self evident. However, the point is to define exactly which process! It is by no means the real natural process, but the part that is given to this process within a numerical model. This is the fundamental difference between resolved and unresolved processes. Resolved processes can be identified to a much higher degree with the real process they are describing, while unresolved, parameterized processes cannot. The problem becomes worse when replacing a parameterization in a well tuned model by a new one. There is no chance to end up with satisfying results when the new parameterization does not fit to the model tuning. Therefore, the first step of a validation of our model can only be a qualitative one. This is what we present in this section: A comparison of the convective feedback of our model with the ECHAM standard convection scheme. Additionally, we give a short comparison of cloud field structure information with observations. Both comparisons have only qualitative character, since we use our model only in a diagnostic way, which means that we run the ECHAM model in its standard setup and calculate online, but without any feedback to the model dynamics of our model (just doing the diagnostics). This procedure is not necessaryly harmful, since we want to focus on the convective feedback on a single time step and single column basis. The questions are:
a) Is the convective feedback of similar nature as the standard convection scheme?
and
b) Do the diagnosed cloud field structures show a typical shape as observed in nature?
While the first question can be affirmed, the second one needs some more discussion. In the experimental setup we choose in this section, it is questionable to look for detailed structures in the feedback of the cloud field model. To run the ECHAM model in a single column mode, it is first necessary to perform a global run to provide the boundary and surface flux data for the single column considered afterwards. Since we

are currently not able to do this global run with our model, we have to use the ECHAM standard configuration. So, the forcing term, especially the created instability which forces the convection and determines the cloud structure, is given by the ECHAM standard setup including the standard convection scheme. This causes, as discussed before, an inconsistency. Therefore, the cloud distribution function only in part reflects the expected power law behavior.

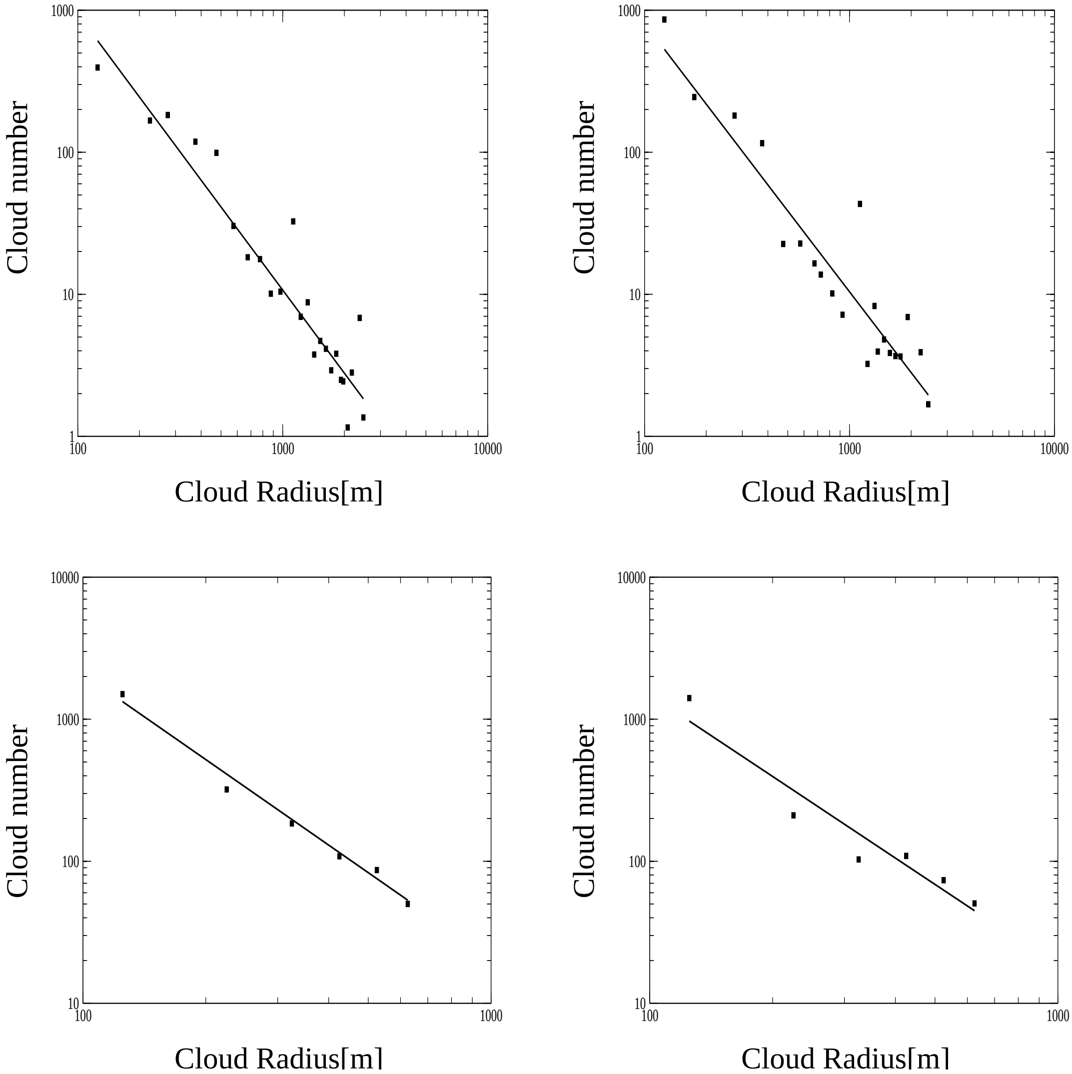

Figure 2.5 : Cloud distribution functions at different time steps

In Figure 2.5 some examples for this cloud distribution are shown. We recognize, at these time steps, a general power law structure in this curve. However, the slope is not in a satisfying agreement to observations. Typically these values are in a range from -1.5 to -2.5 [*Benner and Curry*, 1998, *Weger et al.*, 1992, *Zhu et al.*, 1992, *Weger et al.*, 1993]. We find CDF's in our model with slopes in the range from -1.5 to -5. We will come back to this problem in the next section. Although we do not want to look in too great a detail at model performance, we of course must look at the general convective feedback. In Figure 2.6 we show convective mass fluxes for different time steps. We can identify the updraft mass flux from the Tiedtke scheme and the updraft mass flux (integrated over the whole cloud ensemble from our scheme).

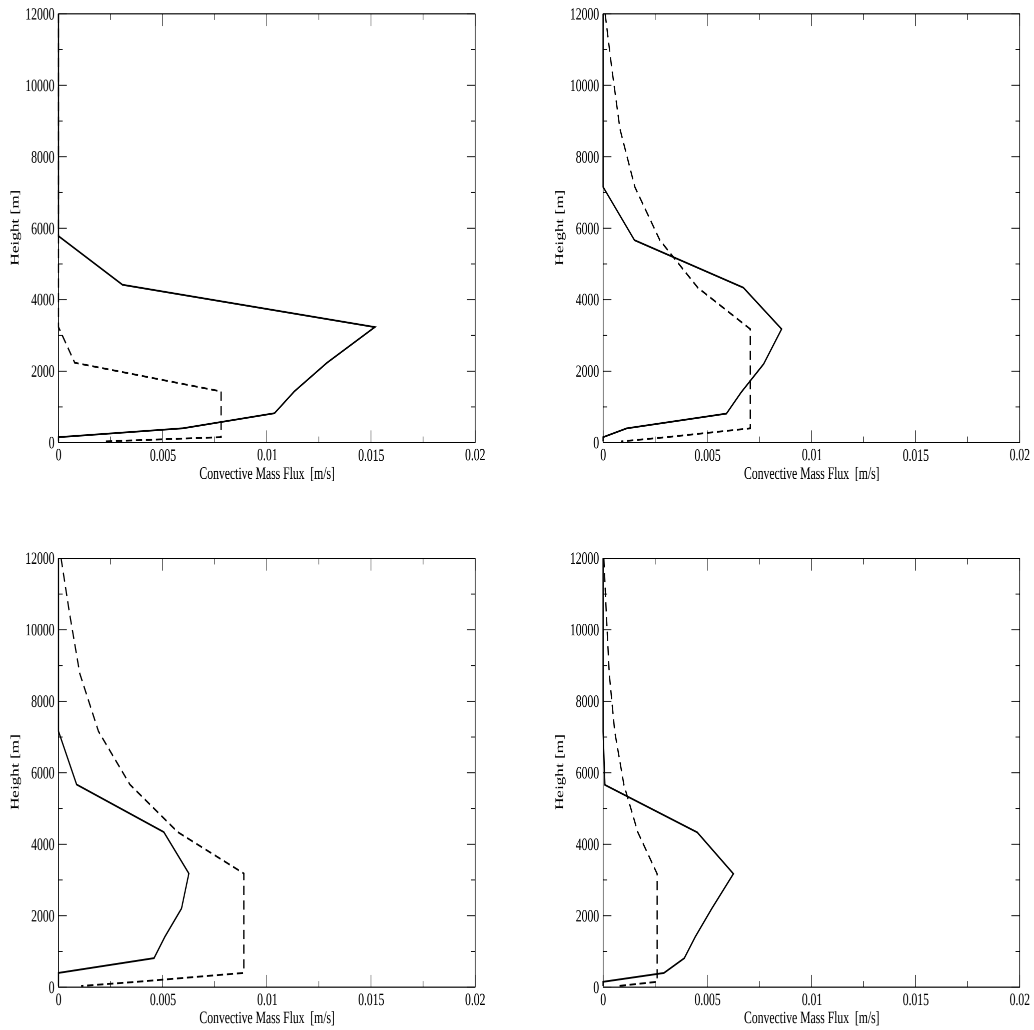

Figure 2.6: Convective Mass Fluxes at different time steps

dashed line: ECHAM standard scheme; solid line CCFM

The overall structure of the fluxes show both, similarities and differences. Important is that the general shape of both mass fluxes is the same. Hence the convective activity described by both schemes is of similar nature and dimension. Values of mass flux differ by a factor up to 5 (in the maximum) but not by orders of magnitude. The type of convection is also similar. In the same situations we have shallow or deep convection, respectively. The similarity of our scheme to the standard scheme is important, since it enables to use our scheme interactively in the GCM. Besides the mentioned similarities we can also identify differences. The main point is here that our scheme produces mass flux profiles which are less smooth and show a higher internal structure. There is no way to decide at this point whether these structures are reasonable or not, but the chance to resolve such structures is given. A more detailed discussion at this stage is dispensable. The major conclusion is: The cloud field model in principle is able to replace a convective scheme.

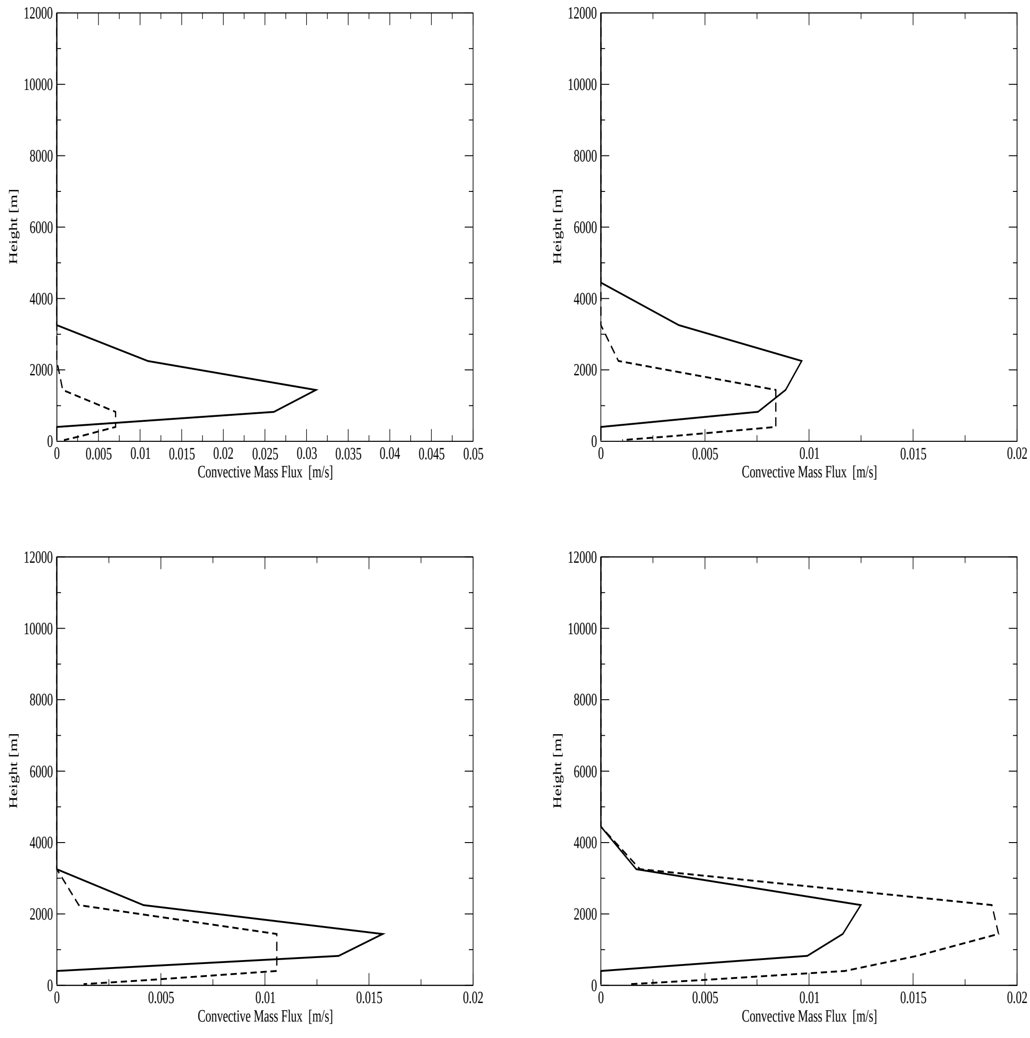

Figure 2.6: Convective Mass Fluxes at different time steps
dashed line: ECHAM standard scheme; solid line CCFM

2.4.2 Quantitative Validation

After this soft test we go ahead to a really acid test for our model. This test, that we call briefly "ARM-case" (Atmospheric Radiation Measurement Program), is part of the "European Project On Cloud Systems In Climate Models" (EUROCS) [*EUROCS*]. In the framework of this project several models of different hierarchies have been tested against observations. The experiment took place at the Southern Great Plains (SGP) ARM site on January 21 1997 [*ARM,EUROCS*]. Observations of this day show shallow cumulus clouds developed at the top of an initially clear convective boundary layer. The non precipitating cumulus cloud field showed a clear diurnal cycle starting around 8.30h local time and disappearing around 17.30h. This case was simulated by a number of LES-models (Large Eddy Simulation). All these models show a quite good performance to simulate both, the temporal structure (diurnal cycle) and the spatial structure (vertical mass fluxes, profiles, cloud distribution). Additionally, several global and meso-scale models were used to run this case in single column mode with prescribed surface and boundary fluxes. While LES models all show a very uniform and satisfying performance close to reality [*Brown et al.*, 2001] the other models do not [*ARM,EUROCS*]. Global as well as meso-scale models have serious problems to simulate a correct diurnal cycle and a reasonable cloud cover fraction and liquid water path.
Since surface and boundary fluxes are prescribed in this setup, we get rid of the problem of model inconsistency and tuning as described in the last section. To take further full advantage of the detailed information about the cloud field diagnosed in our model and to make the simulation as consistent as possible, we do some more changes in the ECHAM model setup:
Since all information needed by the remaining part of the ECHAM model are computed by the cloud field model (especially cloud cover and cloud liquid water path as input variables for the radiation) we switch off all other cloud processes in the ECHAM model and couple our model completely to the ECHAM physics (namely radiation). Figure 2.7 shows the maximum cloud cover for the ARM-case from LES [1], ECHAM standard, and our model.
Another important cloud quantity is shown in Figure 2.8. Here we show, according to Figure 2.7, the vertically integrated cloud water. As clearly to be seen, two key-quantities of the shallow cumulus cloud field can be as well simulated by our model as by the LES model.

[1]LES data and model setup kindly provided by [*Chlond and Müller*]

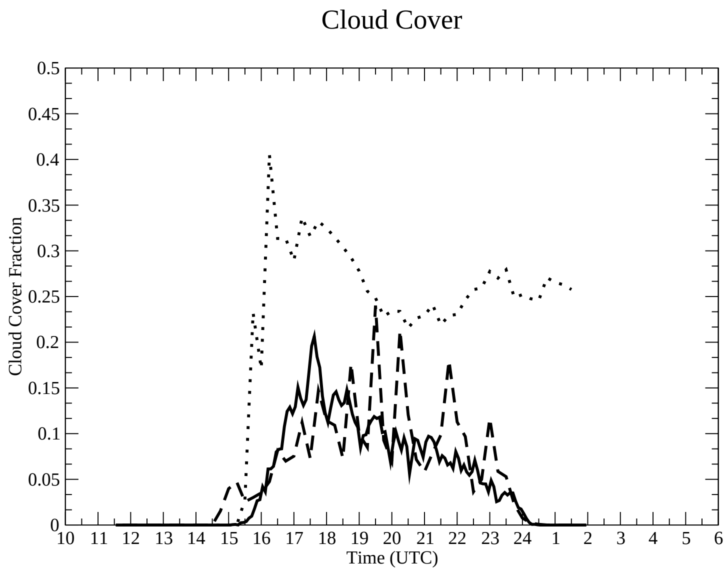

Figure 2.7: Cloud cover for ARM-case; dotted line ECHAM5, solid line LES, dashed line CCFM

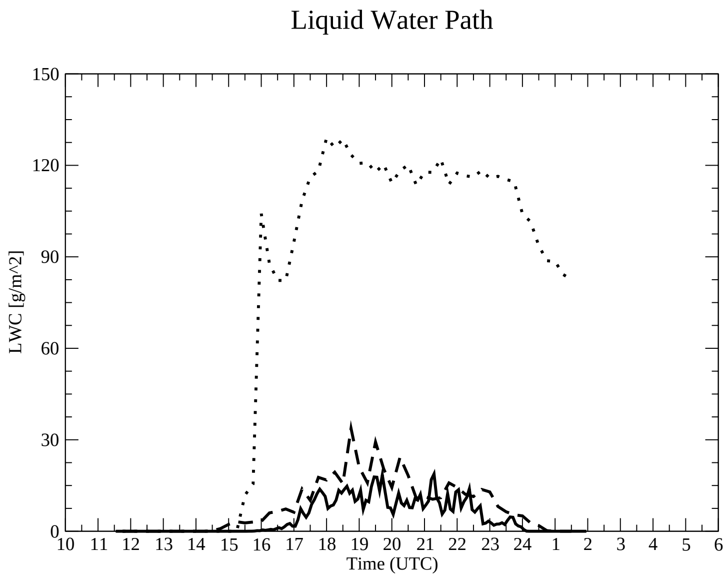

Figure 2.8 : Liquid water path for ARM-case; dotted line ECHAM5, solid line LES, dashed line CCFM

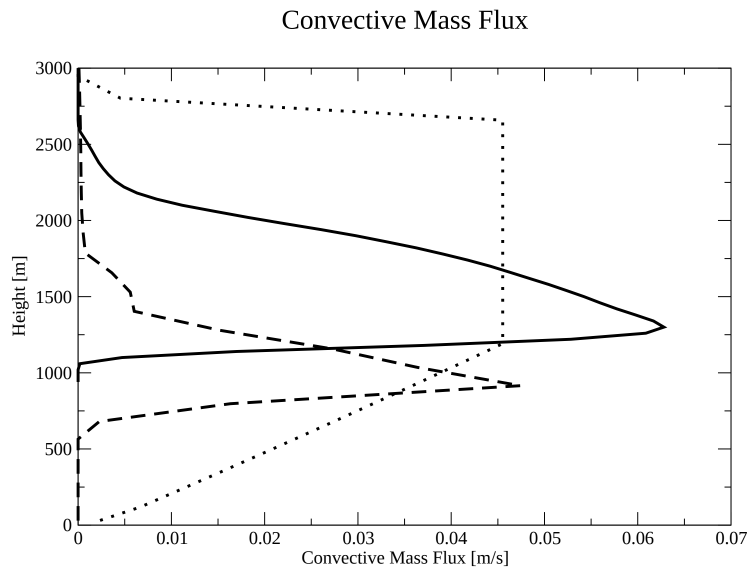

Figure 2.9 : Mass Flux ARM-case 20.00 UTC ; dotted line ECHAM5, solid line LES, dashed line CCFM

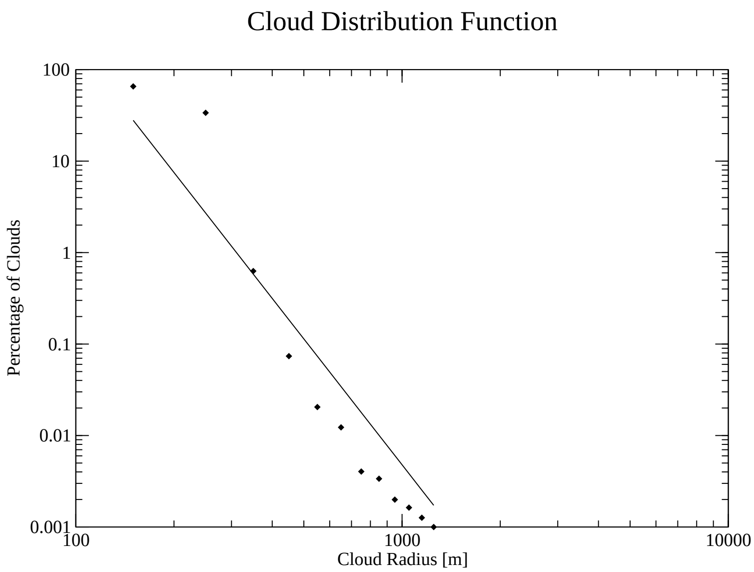

Figure 2.10 : Cloud distribution function from the CCFM

Additionally, Figure 2.9 and Figure 2.10 give information about the vertical structure of the cloud field. While the first one shows the vertical profiles of mass fluxes of LES, ECHAM-standard and our model, the second one shows the cloud distribution function calculated by our model. Both pictures show that the principal structure of the cloud field is quite good. Combining the information of the four Figures, the overall

picture is as follows:
The model produces a diurnal cycle very close to the LES simulations. Cloud cover and liquid water path are much better simulated than in the ECHAM standard configuration. On the other hand, three main discrepancies between the CCFM and the LES model remain:
Onset of convection is about one hour too early. This is probably a triggering problem of our model. A second point is the high noise particularly in the cloud cover curve of the CCFM. This artificial behavior is caused by the fact that there is no memory of the convective cloud state from time step to time step. The third and main point that has to be mentioned is the too low cloud base in our model (Figure 2.9). The mass flux calculated by our model has a fairly god shape compared to the LES model simulation, except the fact that it is shifted by about 500m closer o the ground. Potentially this is caused by the interpolation from the coarse vertical resolution to the finer resolution in the CCFM.
The remaining discrepancies are probably caused to a large degree by the fact, that there is still no real information about the sub-grid variability of temperature and humidity profiles in our model. This shall be discussed in more detail:
The slope of the power-law curve fitted to the cloud distribution function determined by our model is about -4. This is too steep compared with observationas or with the value found in LES simulations for the ARM-case by [*Neggers et al.*, 2001]. All these values are in a range of -1.5 to -2.5. In our cloud distribution function (CDF) the cloud number drops too rapidly with increasing cloud radius. In addition, we find no clear scale break in the CDF. The same bias can be identified in the mass flux curve (Figure 2.9). The upper part of our mass flux curve decreases too rapidly compared with the LES data. There is a high number of small clouds but too few middle range clouds in the ensemble. The possible reason is that we have to run our model with column mean vertical profiles. This means that instability (Convective Available Potential Energy) is uniformly distributed in the whole grid area. In nature this would never be true! We would find a large fraction in the grid column with profiles which are less instable than the grid mean profile given by the GCM. On the other hand, we would find a small fraction in the grid column with a much more instable vertical situation (e.g. caused by local orographic structures or just by common inhomogeneity and turbulence). Since there is no way at the moment to extract this inhomogeneity, we cannot give a solution. This problem may arise from the fact that the interaction between the clouds is calculated by a matrix and not by a full tensor.
In spite of this bias it is obvious that out model can resolve the vertical structure of the convective mass flux much better than the standard convection scheme in ECHAM. In spite of all the mentioned deficits, the convective cloud field model does a good job in the ARM case.

Chapter 3

The Reduced Convective Cloud Field Model

Abstract A convective cloud field model (CCFM) is presented. This model is based on a cloud field model proposed and tested in the second part of this work. This reference model is formulated in the framework of population dynamics and self-organizing systems. In contrast, the model presented in this part renounces such a theoretical background and makes use of a more heuristical method. Both models determine a convective cloud state given by a discrete spectrum of different cloud types for spatial scales as needed in current AGCM's. Although the reference model (full model hereafter FCCFM) is satisfactory due to its more fundamental formulation, it has the drawback that it is much too time consuming to be used for global runs in an AGCM. This shortcoming has been overcome by the new model (reduced model hereafter RCCFM). Both models are compared in this section. The RCCFM in principle show the same structural behavior as the FCCFM. Beside the advantage of much less computer time demands, the RCCFM shows a stabler behavior caused by the fact that the numerical procedure is not as sensitive as in the FCCFM.

3.1 Introduction

Clouds play a crucial role in the global energy budget. The occurrence of clouds, as well as their special microphysical and dynamical structures, determine to a large degree the albedo of the Earth. Clouds are responsible for the different forms of precipitation formation and, therefore, are a key part of the hydrological cycle. Last but not least, clouds (especially convective clouds) provide, by latent heat release in precipitating convective systems and the vertical structure thereof, a strong forcing of the global circulation. Thus, clouds are a central part of the climate system. A physically based representation of clouds and cloud related processes is therefore one of the great challenges in numerical climate modeling. As already shown in the first chapter of this work, a great deficit in current convection schemes is the assumption of a single averaged cloud per GCM-column. This approach inhibits more detailed information about structures of cloud fields. The knowledge of these structures, which obviously appear in nature, would enable modelers to do much more sophisticated calculations of cloud related process (e.g. radiation, lightning; see also chapter 5.). To overcome this deficit at least to some degree, in the second chapter of this work we developed a cloud field model. This cloud field model is much more detailed than current convection schemes and it shows a quite good performance compared to LES model results. The main drawback of the model is its numerical sensitivity and its (compared to standard convection schemes) high computer time demand. Even though it would be possible to run a GCM including our model, it becomes very inconvenient. It can be used for time slice simulations at single grid columns. In this mode it can potentially advance to a very useful tool to study cloud field organization and structures.
However, our aim is to develop a model that is capable of being used for global GCM simulations. Therefore in this chapter we propose a computationally effective but simplified version of the model presented in chapter 2.

3.2 Model Description

The reduced model (RCCFM) is essentially based on the full model proposed in chapter 2. As shown in Figure 2.2, the CCFM basically consists of three parts:
a) definition of the cloud types by using a one dimensional cloud model
b) calculation of the interaction coefficients regarding the changes in the vertical energetic situation
c) calculation of the final cloud distribution function by using the Lotka-Volterra equation.

In the RCCFM point a) remains unchanged. In point b) the principal dependence on CAPE persists, while the detailed definition of the forcing vector F_i and the cloud-cloud interaction matrix K_{ij} is modified. Point c) is totally replaced by a different procedure to speed up the model sustainably. To elucidate the new procedure we again consider a situation with a neutral vertical situation at the last time step and an unstable one when the convection routine is activated.

Presuming that N different clouds form in this unstable environment, we can assume that these clouds have, regarding to their initial conditions, N different cloud tops. Let cloud type number N be the deepest, N-1 the second deepest, etc., and 1 the shallowest cloud type. While in the FCCFM we used a coupled system of N differential equations to determine the cloud distribution function, we choose now a much simpler way. Simpler and less mathematically founded! Whereas the FCCFM was based on the principles of population dynamics, the procedure in the RCCFM lacks such a theoretical background and needs a somewhat heuristic motivation:
The procedure starts with the deepest cloud type. Our assumption is now: The only reason for nature to enlist this cloud type to the actual cloud ensemble is that there is instability (created by all non convective processes in the current time step) that can only be removed by this cloud type and by no other. Thus, instability above all other cloud types! The contribution of cloud type N is chosen that this specific instability is totally removed. The further procedure is straightforward: Is there instability left that can only be removed by cloud N-1, etc. down to cloud type 1.
The mathematical formulation is given here:

$$CAPE_{cloud_i} = \int_{LNB_{cloud_{i+1}}}^{LNB_{cloud_i}} B_i dz \tag{3.1}$$

The definition of F_i and K_{ij} changes to:

$$F_i = \frac{CAPE_{cloud_i}(T) - CAPE_{cloud_i}(TM)}{CAPE_i(TM)\Delta t} \tag{3.2}$$

and

$$K_{ij} = \frac{CAPE_{cloud_i}(T_j) - CAPE_{cloud_i}(T)}{CAPE_i(T)\Delta t} \tag{3.3}$$

for $cloud \quad Top_j \geq \quad cloud \quad Top_i$ and

$$K_{ij} = 0 \tag{3.4}$$

for $cloud \quad Top_j > \quad cloud \quad Top_i$.
The mathematical procedure is given by the formula:

$$n_i = \frac{1}{K_{ii}}[F_i - \sum_{j=i+1}^{N} K_{ij}n_j] \tag{3.5}$$

3.3 Model Validation

3.3.1 Qualitative Validation

As discussed in chapter 2, the single column test of a new convection scheme can only by used as a soft test. It is redundant to give analogous examples for mass fluxes and CDF's as in chapter 2 for the RCCFM, since its principal ability to work as a convective scheme is obvious:
The changes from the FCCFM to the RCCFM, although of great importance for the numerical complexity of the model, are justified by a simplifying view on the physical process of self-organization. The overall model concept remains the same, only the procedure to determine the CDF is modified. Intuitively it seems to be obvious that both procedures lead to similar structures in the convective feedback. Therefore we skip the qualitative test. In contrast to the general feedback, the detailed behavior of both models (similarities and differences) not yet clear. To consider these details and to discuss both models, we proceed directly to the quantitative test.

3.3.2 Quantitative Validation and Comparison with the Full Model

The ARM-case setup is introduced and described in detail in chapter 2. Here we use exactly the same setup. The difference is of course that we use the RCCFM instead of the FCCFM as cloud model within the ECHAM single column setup. Everything else remains unchanged. In Figures 3.1 - 3.3 we present, analogous to chapter 2, cloud cover, LWP, and mass-fluxes. Additionally Figure 3.4 shows the CDF.

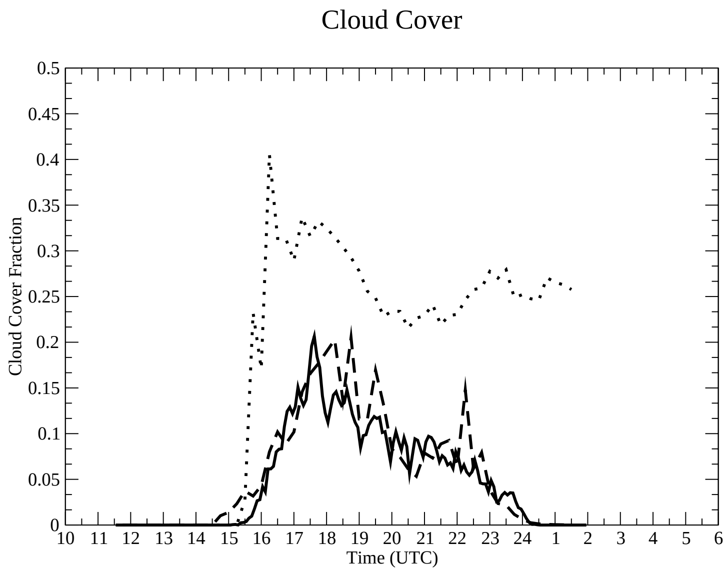

Figure 3.1 : Cloud cover for ARM-case; dotted line ECHAM5, solid line LES, dashed line RCCFM

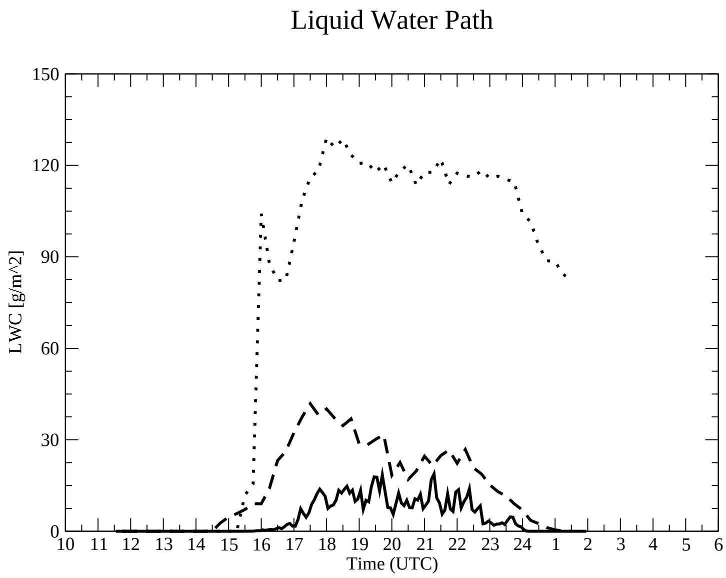

Figure 3.2 : Liquid water path for ARM-case; dotted line ECHAM5, solid line LES, dashed line RCCFM

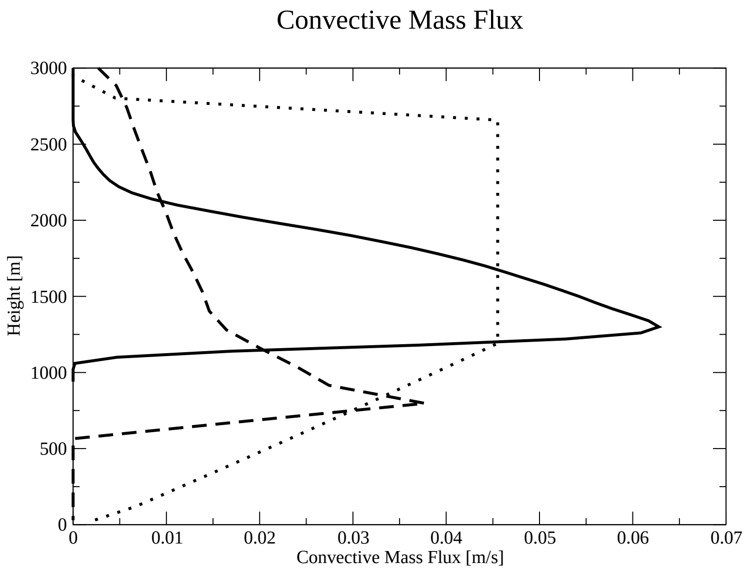

Figure 3.3 : Mass Flux ARM-case 20.00 UTC ; dotted line ECHAM5, solid line LES, dashed line RCCFM

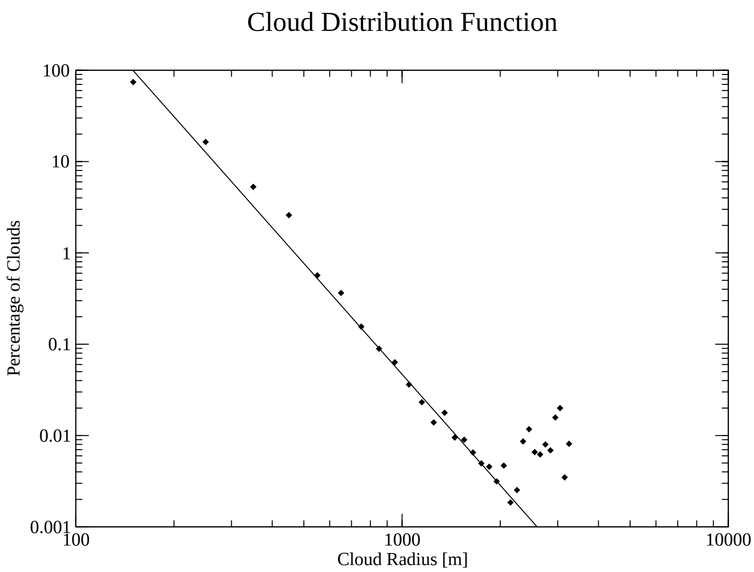

Figure 3.4 : Cloud distribution function from the RCCFM

Cloud cover is in a very good accordance to the LES data. The onset of the cloud field is even better simulated than in the FCCFM and the diurnal cycle is much smoother represented than in the FCCFM. The latter fact is probably due to the FCCFM model being much more sensitive and numerically unstable than the RCCFM because of the use of the Lotka-Volterra equation.

The liquid water path simulated by the RCCFM is still closer to LES data than the ECHAM standard convection. However, compared to LES and the FCCFM, it is too high.

The convective mass flux shown in Figure 3.3 does not fit perfectly to the LES data. Besides the too low cloud base, it is too weak and has a too small lapse rate with increasing height. The overall vertical structure is still better than in ECHAM. Finally, the CDF shows a power-law-like shape except for the cluster of large clouds with radii of about 3000m.
Our conclusion of this test is, that although the cloud cover of the RCCFM fits perfectly to LES data, there are some deficits related to LWP, mass-fluxes and the CDF. Nevertheless, the general convective feedback is represented better by the RCCFM than by the ECHAM standard convection.

We will now discuss in more detail the differences between the FCCFM and the RCCFM. Even though the ARM-case is just one example for a convective event there are some more coherences which can demand general validity.

In Figures 3.5-3.8 we confront the two models. Again we show cloud cover, mass-fluxes, LWP, and the CDF. The main difference between the two models is reflected in a consistent way by all these Figures:

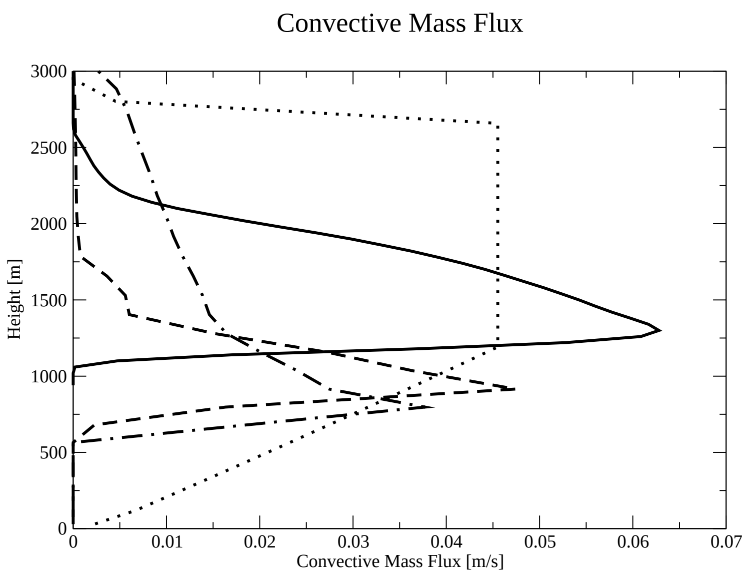

Figure 3.5 : Mass Flux ARM-case 20.00 UTC ; dotted line ECHAM standard, solid line LES, dashed line FCCFM, dashed dotted line RCCFM

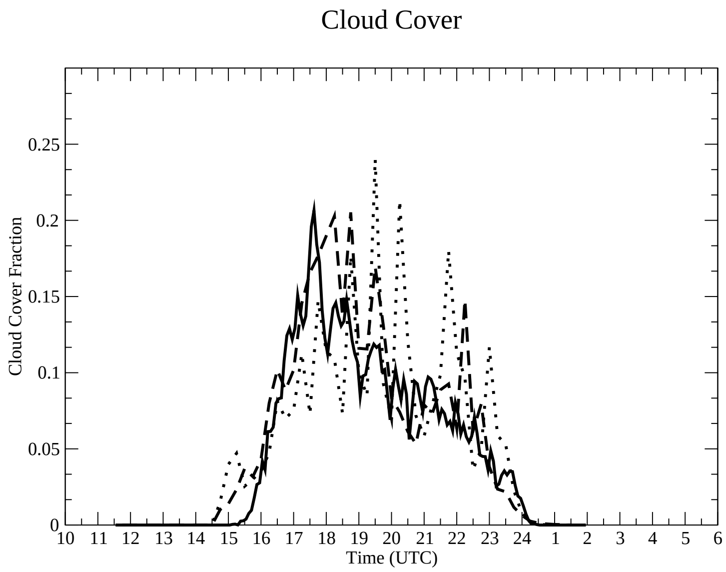

Figure 3.6 : Cloud cover ; solid line LES, dotted line FCCFM, dashed line RCCFM

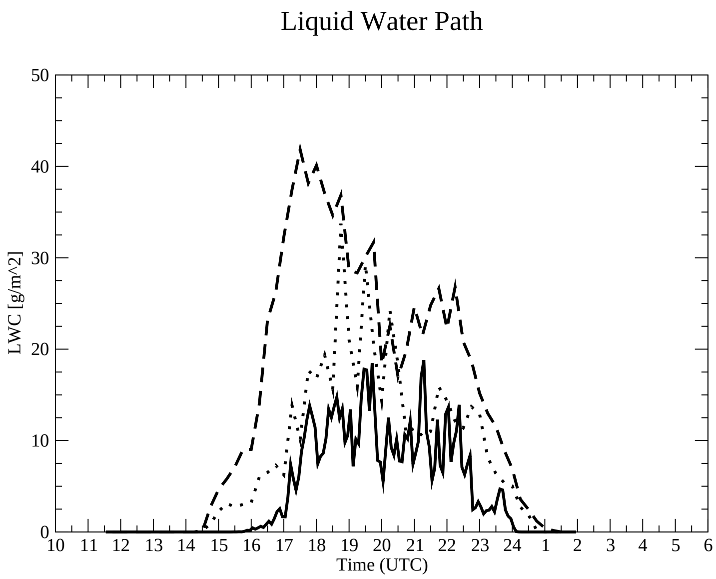

Figure 3.7 : Liquid Water Path ; solid line LES, dotted line FCCFM, dashed line RCCFM

In the FCCFM the CDF is determined interactively and the equilibrium solution is reached after a complex transient part during the iteration of the Lotka-Volterra equation. In the RCCFM the CDF is analytically constructed beginning with the deepest clouds. Therefore, in the RCCFM there is always a systematic tendency towards more higher clouds. This tendency (or bias) is directly shown in the CDF. It is also reflected in the shape of the mass flux. While the FCCFM mass flux shows a rapid decrease with height, the mass flux of the RCCFM decreases too slow caused by too many high clouds in the cloud spectrum. Finally, since deep clouds naturally show a higher LWP than thinner clouds, the overestimated LWP of the RCCFM is also probably caused by the "deep cloud"-bias.

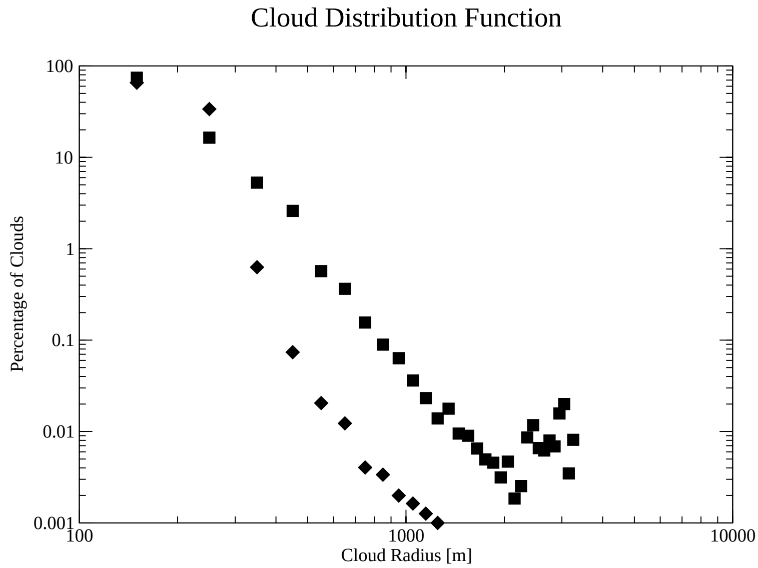

Figure 3.8 : Cloud Distribution Function: Diamonds FCCFM, Squares RCCFM

In spite of these differences, the basic features of both models are comparable. The FCCFM shows a better CDF, but at higher numerically instability and a much higher CPU-time demand. The RCCFM is much faster, numerically less fragile, and produces a smoother feedback. The stated "deep cloud" bias of the RCCFM shall be object of future improvements.

Chapter 4

The Reduced Model in a Global Mode

Abstract A convective cloud field model (CCFM) is used as convection parameterization within the ECHAM4 GCM. In this part we present first results of the performance of the reduced CCFM (RCCFM), introduced in chapter 3, when used in the global mode in a GCM. The model, which shows a quite good convective feedback in comparison to LES data for the ARM-case (chapter 3.) is now used for a global-GCM run. Two types of experiments are presented: First we test our model in a diagnostic procedure. This means we compute in addition to the standard ECHAM convection, which is still coupled to the GCM, our RCCFM. We diagnose the reaction of our model, but with no feedback to the GCM dynamics. In a second experiment we replace the ECHAM standard convection by the RCCFM. The results of both experiments show that the RCCFM gives reasonable precipitation and convective heating fields. In addition, we present statistical data of global cloud field patterns computed by the RCCFM.

4.1 Introduction

In chapters 2 and 3 we introduced two convective cloud field models. Both models were tested against LES data for a special convective episode (ARM-case). In this special case both models show a quite good performance close to LES simulations. In chapter 3 we discussed the differences in the convective feedback of both models. We had to compromise that the numerical efficiency of the reduced model (RCCFM) probably has caused a "deep cloud" bias. However, even with this bias the model shows a satisfactory performance in the "ARM-case".
Since our intention for developing the RCCFM was to get a model fast enough to be used in global mode in a GCM, we accept this "deep cloud" bias at this step and use the model as it is for first global tests. These tests cannot and shall not substitute

further detailed comparisons to cloud resolving LES model episodes.
However, they give a first assessment, whether the RCCFM is able to represent the great variability of convective events that appear in nature and in the model.

4.2 Experimental Setup

We present two experiments with slightly, but essentially different setups. As environmental GCM for our RCCFM we used the ECHAM4 model. To keep the experiments as simple and fast as possible we choose the coarsest available resolution (T21). Since the RCCFM is still some orders of magnitudes slower than other convection schemes we simulated only 10 days. This is sufficiently long to get a qualitative picture of the model performance but of course insufficient to give any statement about how the RCCFM will change the overall GCM performance.

In the first experiment we computed the convection twice:
a) the ECHAM standard convection with feedback to the model dynamics and
b) the RCCFM without this feedback, only for diagnostics

In the second experiment we switch off the standard convection and couple our model completely to the ECHAM model.

Why both these setups?

To answer this question we have to elucidate the "model world":
A global climate model is without any doubt a very complex and sensitive tool. It has to be carefully equilibrated. Therefore, all the physical parameterizations computed in the model, are in a sensitive balance to each other. Replacing one process parameterization by another, in particular such an important one like convection, can destroy the balance of the model without any preference whether the new parameterization is more realistic or physical than the old one or not. Thus, a first recommended test for each kind of parameterization is such a diagnostics test. The diagnostic test can only clarify the general behavior of the new parameterization. This can disclose obvious or hidden errors and point out the differences to the operational parameterization.
It cannot serve to analyze structures in the feedback! The climate system is a highly non-linear system. A change in crucial processes of this system can potentially cause effects of unexpected order and scale (see chapter 1). 10 days simulation time is a small period for the global scale. But even for this short time we find significant differences in both experiments. Therefore, to analyze structures in the convective feedback and to extract some statistical data about the cloud fields from our model,

the diagnostic mode (first experiment) is not sufficient. Since the ECHAM standard convection determines the model dynamics and the RCCFM is only allowed to react at each time step, the convective feedback of the RCCFM in the diagnostic mode is somewhat "virtual" and physically inconsistent. Thus, after having checked that the RCCFM shows a reasonable pattern in the first experiment, we change to the coupled mode.

4.2.1 Convective Feedback

The effects of convective clouds which are most important for the global weather and climate are precipitation and the release of latent heat in the free troposphere. There are of course a number of other effects of convection, but these two quantities (precipitation and heating rates) give a good overall picture of the performance of a convection scheme on the global scale. Figure 4.1 a-c shows 10 day means of convective precipitation, while Figure 4.2 a-c shows convective heating rates. There are three different data sets shown in each Figure. The first a) shows precipitation and heating rates from the ECHAM standard convection scheme. Since this is the operational scheme, it is no surprise that both pictures show realistic distributions. The data shown are a 10 day mean from a simulation in the beginning of January. Thus, the ITCZ is slightly shifted to the south. The regions with strong convective activity (Amazonia, Indonesia, the SPCZ (South Pazific Convergence Zone), the Kongo Basin, and the Indian Ocean) are well simulated. The heating rate pattern shows the strong convective heating over the tropics. This heating is essential for the global circulation since it is the most important energy source for the Hadley circulation. Both, convective heating and precipitation are in reasonable agreement to observations and re-analysis [*Roeckner et al.*, 1996].

The second set of pictures b) shows the convective feedback of the RCCFM in the diagnostic mode (first experiment). Some obvious errors appear. Precipitation gives a very unsatisfactory image. In contrast to the operational scheme, the RCCFM running in the diagnostic mode is neither able to simulate correctly the ITCZ nor at least one of the convective active regions. The ITCZ is only rudimentarily simulated. This is also reflected in the heating rates, which show a too weak vertical extension. In addition, there are some points on the globe [(60E,30S),(90E,30N),(130E,10N),(170W,35S),(160W,30N)] that show unrealistic high precipitation rates. At these points we have to suppose that the RCCFM crashes for, at the moment, unknown reasons. Concluding, the data shown in Figure 4.1 b) and 4.2 b) gives reason to trust in the principle ability of the RCCFM to work as convection scheme, but not more. The fields are far from showing a realistic convective feedback, but not as far that one has to reject the whole model.

Keeping in mind the unsatisfactory performance of the RCCFM in the first experiment, the second experiment in which we coupled the RCCFM completely to the ECHAM model gives an amazingly different image. Precipitation and convective heating rates in Figure 4.1 c) and 4.2 c) significantly better reflect the pattern expected from a convection scheme than pictures b) from the diagnostic run. The regions of high convective activity are simulated quite well. The global distribution of convection is somewhat broader, namely over the oceans. Precipitation rates along the ITCZ are a bit higher than in the operational scheme. Also the vertical expansion of the heating rates, which is an indication for the depth of deep convective towers, is much more realistic. Compared to the diagnostic simulation 4.2 b), the heating rates in the interactive simulation 4.2 c) give a reasonable general picture of the zonal mean convective activity. The convection reaches much higher altitudes and is more pronounced in the tropics (ITCZ). The differences between 4.2 b) and 4.2 c) show emphatically that the convection process, which is of outstanding importance for the model climate cannot be tested in a diagnostic mode. As already pointed out, we do not intend to analyze the convective feedback in too much detail. However, we would like to mention one difference between the standard configuration simulation 4.2 a) and the interactive simulation with our scheme 4.2 c):

While in 4.2 a) the convective heating is very homogeneously distributed from about 10S to 10N and from 900hPa up to 400hPa, this is not the case in 4.2 c). Here we find a pronounced vertical structure showing two well developed focal points of convective heating. Both are located over the tropics. The first one from about 900hPa to 800hPa can be easily identified with shallow convective clouds. The second one (600hPa - 350hPa) shows the more deep convective activity from the warm pools over the tropics.

There is no way to decide from these experiments alone whether the RCCFM does a better job than the operational scheme or not.

However, we particularly wish to point out that neitherin ECHAM nor in RCCFM any additional tuning happened.

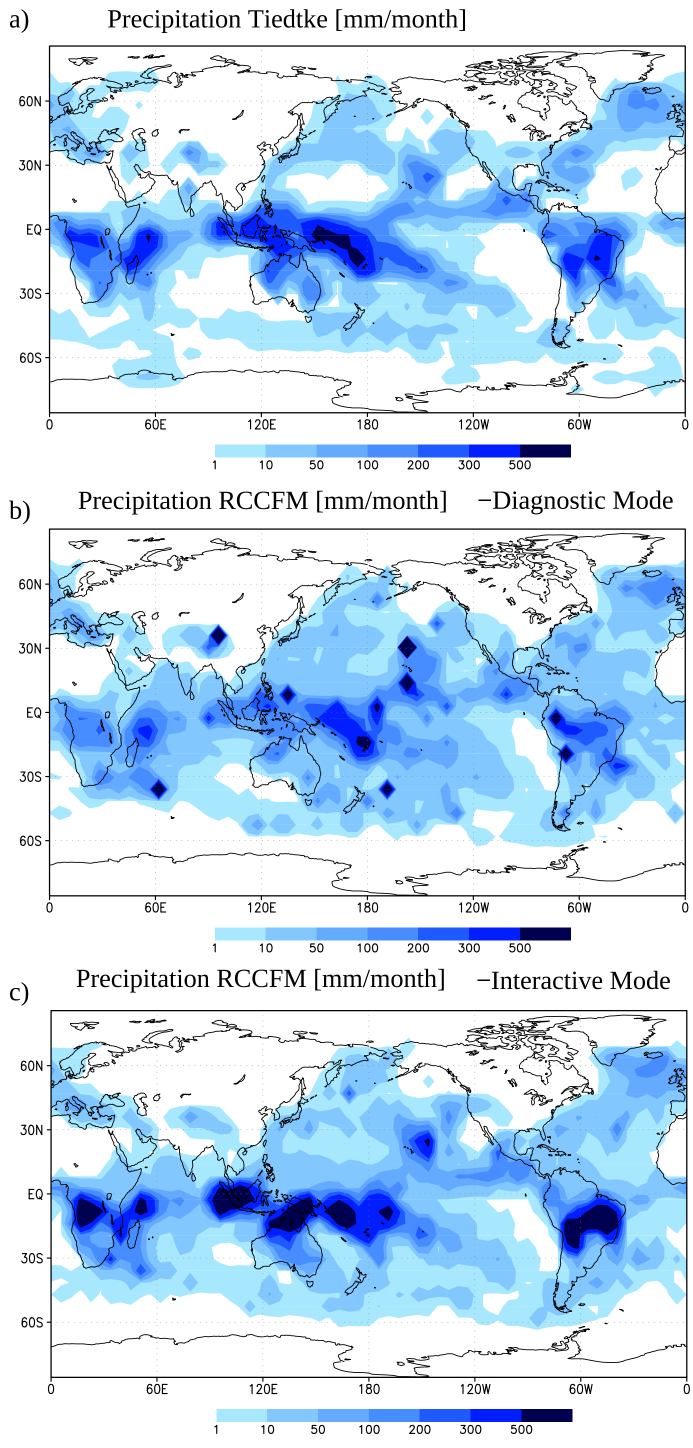

Figure 4.1 : Convective Precipitation

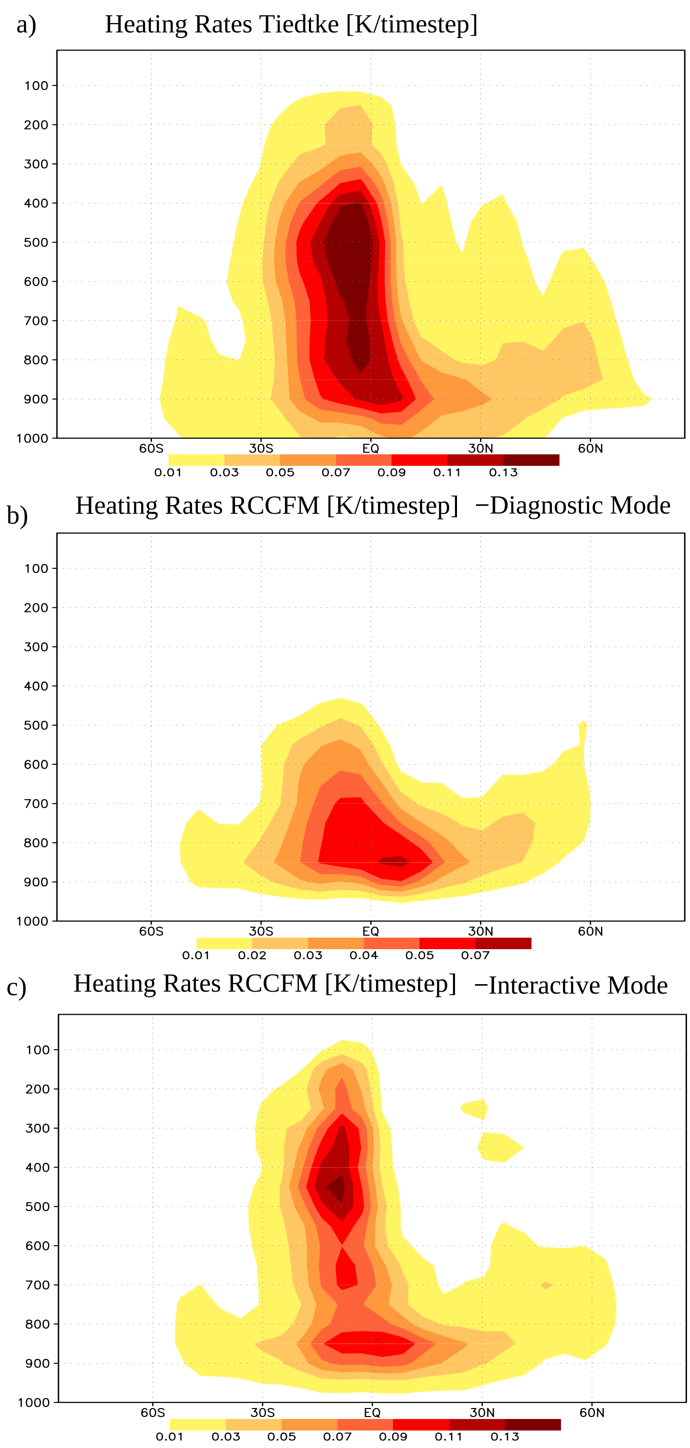

Figure 4.2 : Convective Heating Rates

4.2.2 Cloud Field Statistics

In the former section we considered only precipitation and heating rates. These are quantities that have to be provided by any convection scheme. In this section we would like to give some first examples of the statistics and more detailed data of the cloud fields computed by the RCCFM. Therefore, we show, for six consecutive time steps, three different data sets. This time step sequence was chosen arbitrarily. The first data set is a model orientated set (Figure 4.3). It shows the number of different cloud types that participate in the computed cloud distribution function (CDF). For this experiment we choose 20 different possible cloud types. Thus, the maximum value in these pictures is 20. How many of these 20 types finally participate in the cloud ensemble is determined by the RCCFM algorithm. The pictures give an impression how much variability there is in each cloud spectrum at each grid point:
We find more cloud types in regions with deep convection than in those with shallow convection. This is not too surprising. If the different cloud types in a grid column are too similar to each other, there is no reason for the RCCFM to use more cloud types than necessary to construct the cloud spectrum. On the other hand, for regions with deep convection it is apparent that the one dimensional cloud model produces probably 20 significant cloud types that can all participate in the cloud spectrum.
As a further, more detailed, insight into the cloud field structures we plotted in Figure 4.4 the maximum cloud depth, and in Figure 4.5 the difference of cloud depth of the deepest cloud and that of the shallowest. Both Figures show consistently that the general structures of the computed cloud fields are realistic. We find deep clouds in the regions of high convective activity, but also a high difference between the largest and the smallest cloud type in these regions. This indicates a high variability in the cloud spectrum. We have, therefore, a broad spectrum of different cloud types. Keeping in mind that the ECHAM GCM resolves the troposphere with about 10 layers, 5-15 different cloud types, depending on maximum cloud depth, in a grid column are a reasonable number and in the vertically discretized model world correspond to a continuous cloud spectrum. We get also the information, that the RCCFM is able to reproduce the shallow cumulus fields over large parts of the oceans. A lack in simulating these clouds is a deficit of many GCMs. Another remarkable feature, that can be extracted from the data sets 4.3 - 4.5, is the reasonable and consistent (when comparing 4.3 - 4.5 step by step) simulation of some deep convective events in the North Atlantic.
To conclude: The RCCFM provides useful information about cloud fields that cannot be provided by any other convection parameterization. Of course these data have to be checked against observations, but the RCCFM is the first model that enables such a check.

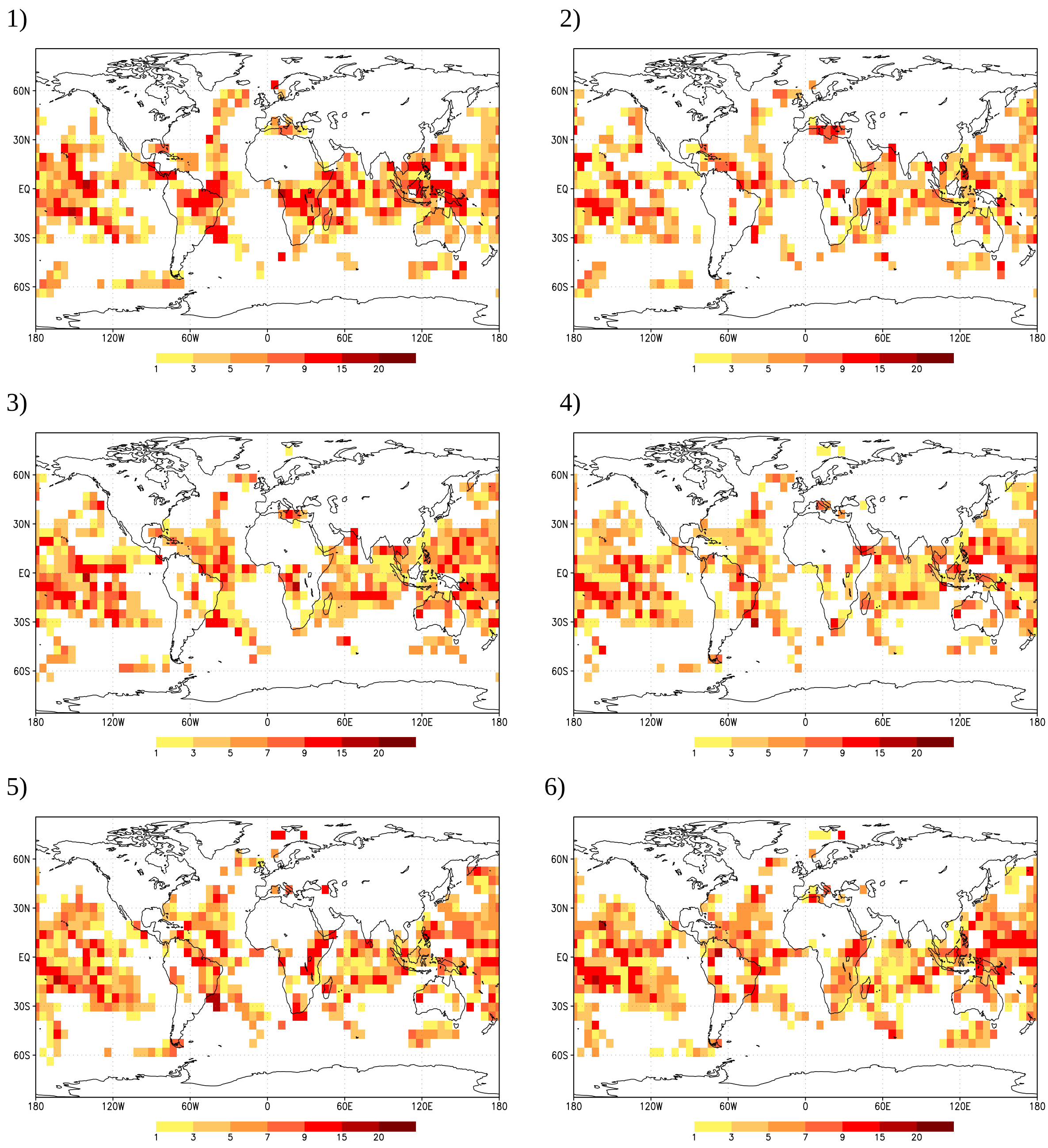

Figure 4.3 : Number of different cloud types that occur in each grid column

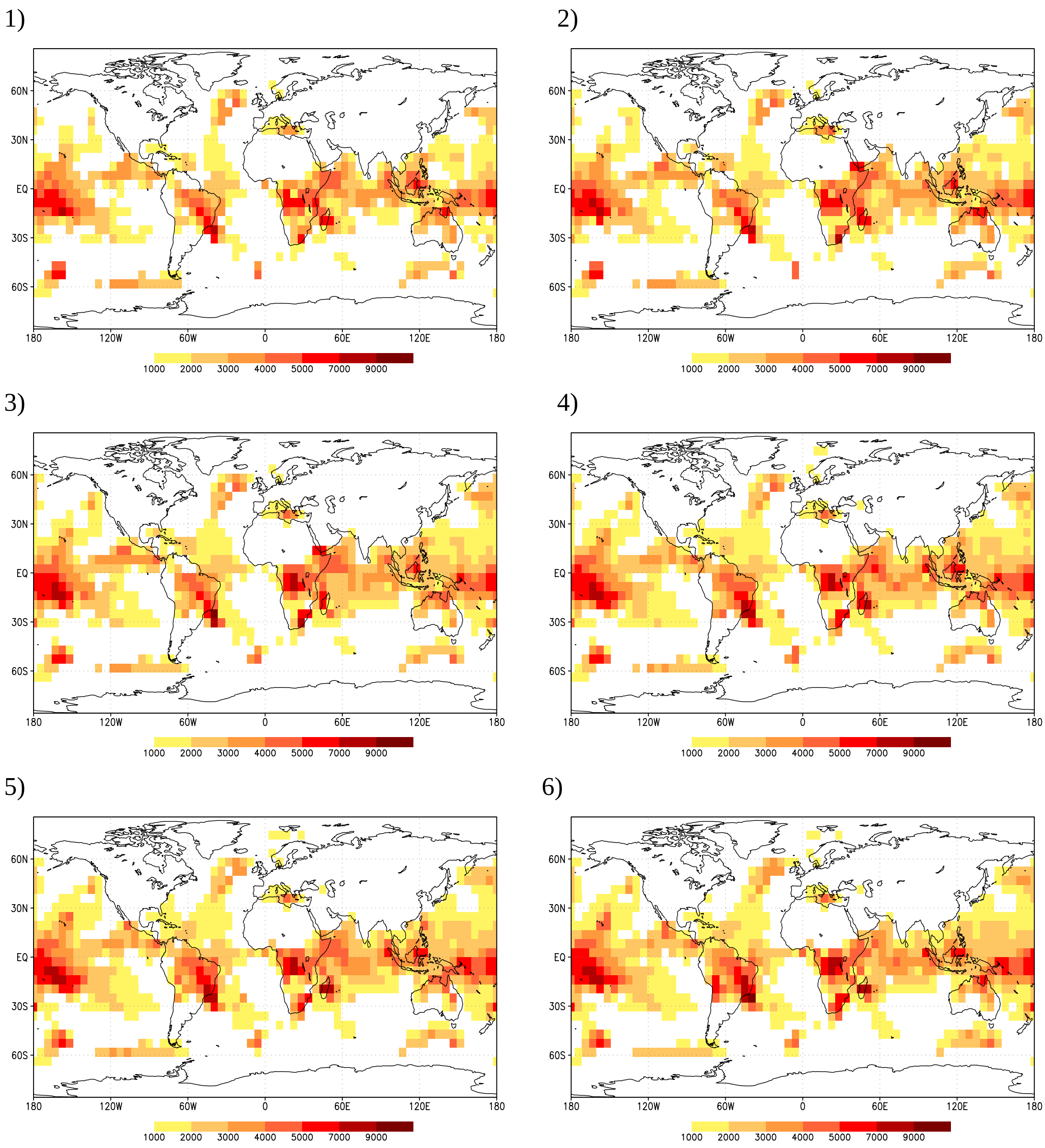

Figure 4.4 : Maximum Cloud Depth [m]

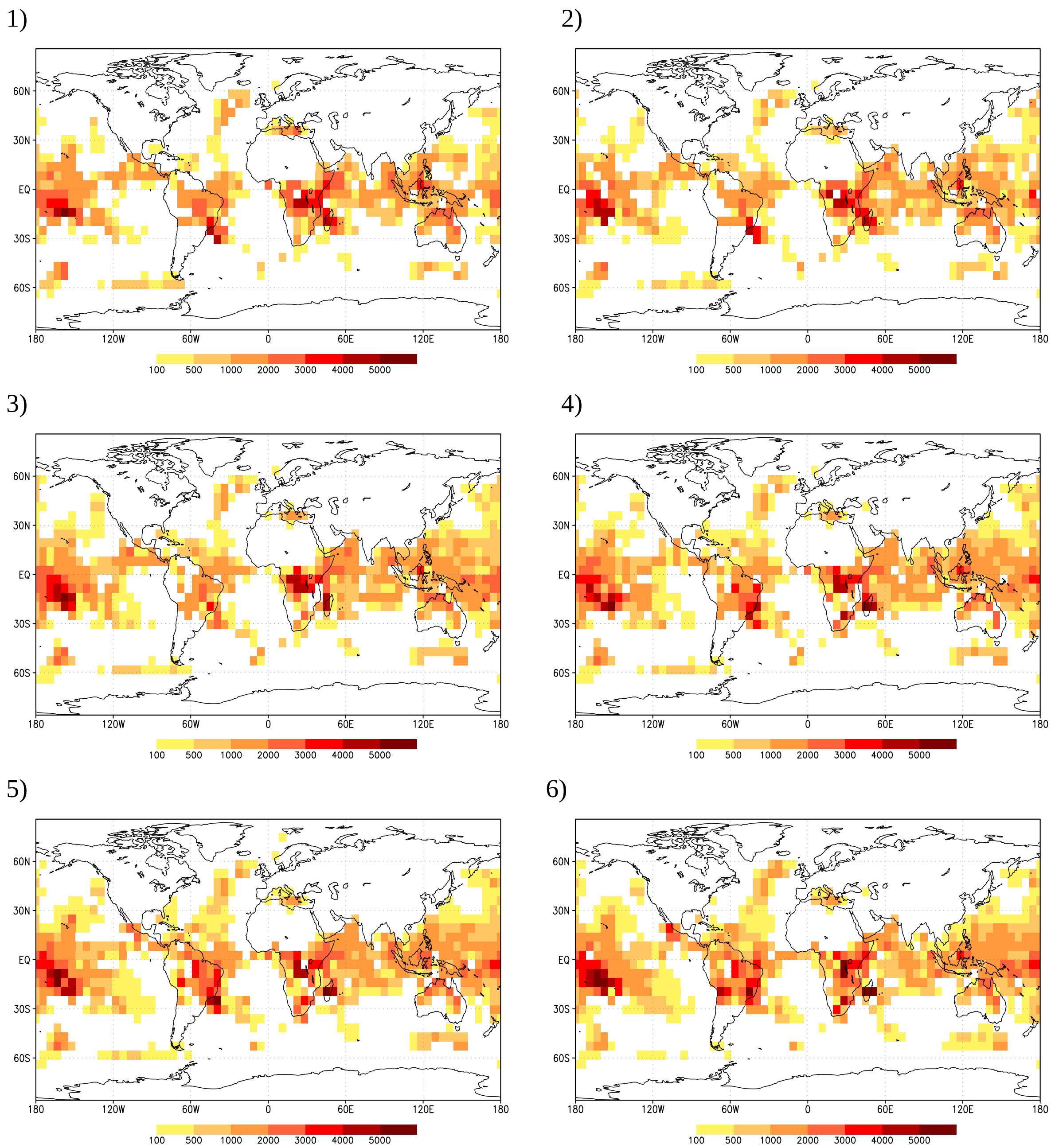

Figure 4.5 : Cloud depth (deepest cloud) - Cloud depth (shallowest cloud) [m]

Chapter 5

Concluding Remarks and Perspectives

The presented cloud field model is anything but in a final and complete state. Several questions remain open and many tests remain to be done. Conversely, there are quite a few topics and problems where the model potentially can help to push insights in numerical climate modelling. We wish to give only a short discussion of these issues. Additionally, this work has also disclosed some general shortcomings of current GCMs, beginning with convection parameterization, or, more general, cloud parameterization, up to requirements for the more general structure of global climate models. Keeping in mind that each modeler first sees his own topic we wish to propose a few changes in climate modelling philosophy. This may help also on other parameterization frontiers to identify the most promising methods to develop future Earth System Models.

5.1 Open Questions

Referring to Akio Arakawa [1] the entire cumulus cloud convection parameterization seems to be an open question. However, we parameterize it. And, in fact, the GCM models (which are all using parameterizations for convection) work.
In this work we tried to extend the quality of parameterization a bit. Trusting in the philosophy that a theoretically and physically based model can, at least to some degree, compensate the lack of information about the sub-grid state in a grid column, we developed a simple cloud field model to simulate some aspects of cloud field organization. The overall performance of this model is quite reasonable. Having in mind that the GCM used to run our model is tuned to work with a completely different cloud parameterization, our model produces a satisfactory cloud feedback.

[1] "To what extent is it possible to parameterize cumulus clouds?" [*Emanuel and Raymond*, 1993]

However, since our model is very time consuming and complex compared to other convection and cloud parameterizations, the main question is: "Is there any benefit due to the use of this cloud field model?" To answer this question, we have to look at the special features of our model. The strict and consequent cloud spectral approach as well as the use of a cloud model instead of a mass flux model, coupled with the higher internal vertical resolution of our model, promises a better simulation of vertical transport and vertical redistribution of e.g. humidity and tracers. Here remains much work to be done.
There is no doubt that the additional information about each cloud type is in fact helpful to include e.g. a higher level cloud microphysics and/or radiation.
However, the question remains whther the cloud spectrum shape diagnosed by our model that reflects the observed power law behavior at least in principle very good, is a realistic presentation of sub-grid variability. To answer this question there is a straightforward procedure to follow:
Beginning with the most coarse GCM resolution (T21) one has to calculate the cloud spectra for a certain region using finer and finer resolutions. The point of interest is then if the cloud spectrum, averaged over several finer grid columns reflects the structure of the spectra determined in the coarse resolution. Since our model always uses just grid mean profiles, this would be a real test to see if and how sub grid variability is really included in the model feedback.
Finally, one has to ask wheether our approach corresponds to the physics of cloud field organization. This answer is important since we want to use the model for further investigation: How do processes that originally affect only single clouds (e.g. microphysical or radiative effects related to aerosols) affect the organization of cloud fields?
To classify our cloud field model and to appraise it, it is certainly appropriate to compare it to other convection parameterizations. Since there are a couple of parameterizations that follow very similar strategies, we choose the most different ones (as well as the most prominent ones); namely the Tiedtke [*Tiedtke*, 1989] scheme, the Arakawa Schubert [*Arakawa and Schubert*, 1974] scheme, the Kreitzberg Perkey [*Kreitzberg and Perkey*, 1976, *Kreitzberg and Perkey*, 1977] scheme, and the Fritsch Chappel [*Kain and Fritsch*, 1990] scheme. While the first two are designed for global circulation models the latter two are developed for the special requirements of mesoscale models.
The Tiedtke scheme is the most idealized parameterization in this short list. One mass flux is calculated to represent a spectrum or ensemble of different convective clouds. The spectrum properties are included by using empirical parameters (e.g. for organized detrainment). The Tiedtke parameterization is very efficient and can be used even for long time climate simulations. Since the Tiedtke scheme is a mass-flux scheme, there is no explicit information about vertical velocity or cloud

cover available. Also the shape of the cloud spectrum that is calculated in our model for each meteorological situation separately (for each time step and each single grid column) is fixed in the Tiedtke model (prescribed by empirical constants). The closure procedure in the original Tiedtke scheme is based on moisture convergence. In a later version, used in the ECHAM4 model, this closure for deep convection was replaced by a closure based on CAPE.
The prominent Arakawa Schubert (AS) scheme is somewhat more complex. Beginning with this scheme, the idea of an explicit cloud spectrum was introduced in the field of convection parameterization. Therefore, it is (in a conceptual way) very similar to our model. However, there are two major differences to our model: The AS model introduces a spectrum of mass fluxes. So, again there is no detailed information about profiles of vertical velocity and cloud cover. Each of the single mass fluxes in the AS model is considered to represent one cloud type. The cloud ensemble (or better mass flux ensemble) is calculated using an equilibrium assumption with interaction coefficient very similar to our F_i and K_{ij}. The more important difference lies in the procedure to determine the final cloud ensemble: As reported [*Lord*, 1982, *Lord et al.*, 1982] this is a serious problem in the AS model. In our model (FCCFM) there is a more natural way to find the asymptotic state. Therefore, it is appropriate to define our model as a consequent upgrading of the AS model, or contrarivise, the AS model as a simplification of our model.

The comparison of our model to the Kreitzberg-Perkey (KP) scheme and the Fritsch-Chappel (FC) scheme is also very illuminative. Both schemes are conceived to be applied in higher resolution models (resolution on the order of 10 km instead of 100 km in the case of GCMs). For this order of resolution the statistical approach of a cloud spectrum is no longer as necessary as it is for GCMs. Consequently, these schemes assume the appearance of one cloud type per grid column. The cloud in both schemes (KP and FC) is represented by a one - dimensional cloud model very close to the one used here. Therefore, in both these schemes we find information about cloud cover and updraft velocity. And indeed this information is used in some mesoscale models to calculate the total cloud cover. The closure procedure is somewhat different in both schemes. However, it is finally based on CAPE similar to the closure in our model.
Therefore, in an idealized and conceptual way, we can consider our model as a meta model for the other parameterizations:
If we would use a very simplified mass flux model instead of the present one - dimensional cloud model we would end up with the "CAPE version" of Tiedtke assuming that we admit only one of the mass flux (cloud) types in our model.
If, we choose a simplified mass flux model to define our cloud types, still allowing for more than one cloud type, and if we simplify in addition the determination of the cloud

ensemble state, we are very close to the original AS model.
On the other hand, if we admit only one cloud type while keeping our relatively complex one-dimensional cloud model, our model is not too far from the KP and FC scheme.
In conclusion we would like to point out, that our model includes (at least to some degree) several other approaches. This is satisfying point, since we derived ours from the well known, and to a large degree successful, ideas of population dynamics. Maybe we took the most simple one in the field of self-organization and synergetics. Thus, the philosophy of our model opens the door for promising future research.

5.2 Chances and Perspectives of the Model

Vertical Transport:

To represent the vertical transport of chemical tracers is one of the most important tasks of convection parameterizations. A typical convective cloud can be described (in a very idealized way) a plume with entrainment of air (and therefore everything mixed with the air) at its base and detrainment of air at its top. Compared to the large scale lifting of air ($\sim 0.1 m/s$) the transport in convective clouds is very effective ($\sim 1 m/s to 10 m/s$ or even higher). The major point related to convective clouds is of course to determine the right source and the right ressource, which means to define cloud bases and cloud tops.
The cloud base is not the important point. In general, convection schemes determine the cloud base by lifting an air parcel from the ground to its condensation level. This level is called cloud base and it is the same for all clouds in one grid column.
The determination of cloud tops is more difficult. While it is common in nature that a cloud field with the spatial dimensions of a GCM grid cell has a uniform cloud base, it is almost impossible that all clouds on such a scale have the same tops. The distribution of cloud tops is essential in this case and it is equivalent with the distribution of different cloud types contributing to the cloud ensemble in a grid column.

Effects on Cloud Fields:

As discussed in the first part of this work (in the context of biomass burning), there are important microphysical processes related to aerosols that can affect a single cloud in a significant way. In our sensitivity study (chapter 1.) we parameterized this effect on the average cloud represented in the Tiedtke scheme by one mass-flux. However, since we have to deal with complex microphysical processes as well as with the strongly nonlinear process of cloud field organization, it is not yet clear how microphysical effects that affect single clouds influence the cloud field structure. While the general structure of cloud ensembles is fixed e.g. in the Tiedtke scheme, it is interactively determined in our model. Thus, using our model one can estimate the effect due to changes in the organization of structures.
There are other questions related to this issue:
What is the effect of increasing vertical resolution of the GCM (not just the internal vertical resolution in our model) on the structure of cloud fields? What is the effect of choosing a more complex cloud model to define the cloud types on this structure. Is there a cloud structure feedback from global warming? This is only a very incomplete list of questions. However, it shows the relevance of this topic.

Microphysics

Cloud microphysics is one of the hot topics of GCM improvement over the last

10 years (and probably will be for another 10 years), mainly due to the interest in chemistry and aerosol physics and their complexity. These topics are closely linked to cloud processes (e.g. chemical reactions, aerosol ageing, wet deposition). In turn, cloud processes like nucleation, precipitation formation etc., that finally determine the heating rates by clouds depend very strongly on e.g. the aerosol distribution. Thus, the improvement of cloud microphysics is one of the major points in earth system modelling. However, sophisticated microphysics should be coupled also to sophisticated cloud dynamics. Therefore it is inevitable to improve the whole cloud treatment.
To be clear: Just to increase the complexity of microphysics in a simple mass-flux model is both numerically inefficient and physically inconsistent!

New Cloud Parameterizations

As previously discussed, the traditional way of dividing cloud processes within a GCM into local convection and large scale condensation in stratiform clouds is at least questionable. The proposed cloud field model that shows a promising performance in the shallow cumulus ARM case should and probably can be expanded to be used as a unified cloud model. To get a better simulation of global cloud cover as well as a more physically based and transparent representation of cloud related processes would be the most important possible results of cloud field models.

5.3 Miscellaneous

Here we would like to mention some topics related to convective clouds that can obviously benefit from the consequent cloud spectrum approach.

Lightning:

Lightning is one of the major sources for NO_x [*Franzblau and Popp*, 1989]. Besides that, reliable information about lightning activity can help to locate and forecast natural vegetation fires as well as the related smoke hazards. Since the emissions of vegetation fires are of great relevance for atmospheric chemistry, these are two obvious reasons to consider lightning.
The parameterization of a convection dependent process (like lightning) can be just as good and physical as the parameterization of convection itself. Because this point shows very impressively how an improvement of the convection parameterization can potentially help to increase the physical consistency of climate models, we like to go into more detail:
The current way to parameterize lightning in global climate models is based on the top height of convective clouds. Using empirical relationships between cloud top height

and observed lightning rates [*Price and Rind*, 1992] derived a simple lightning parameterization. Although cloud top height is a good first guess, [*Price and Rind*, 1992] argued in their work that lightning activity is also strongly related to cloud dynamics as well as to the microphysical structure. These dependencies (high lightning rates in clouds with strong updrafts and vice versa, as well as high rates in clouds with a distinct ice phase) are used to explain the differences between continental cumulonimbus (more lightning) and maritime ones (far less lightning). The dynamical difference between continental and maritime thunderstorms has its origin in the large difference between the virtual temperature lapse rate within clouds (which is always moist adiabatic) and the lapse rate in the drier continental environment as compared to moist maritime environment.

Finally, a really physically based description of lightning (in contrast to an empirical relationship) needs much more than just some crude information about cloud vertical extent and dynamics. To calculate charge distributions and thus potential differences within clouds, one needs detailed microphysical information that cannot be provided by mass flux schemes. To be honest, it can not be provided by the cloud model used in this work. However, to replace the cloud model with a more complex one, is one of our next tasks.

In the long run it is very promising to develop a really coupled surface-cloud-aerosol-chemistry system:

Lightning can cause vegetation fires - change in surface properties - fire emission affects cloud microstructures and radiative effects - that may result in changes in precipitation - dryer or wetter surface - more or less fires due to lightning or other reasons.

Heavy Precipitation:

This part is related to physical improvements when land surface process models are coupled to a more sophisticated cloud model like the CCFM. It is well known that high, local precipitation rates (which are definitely sub-grid scale) in connection with deforestation or other land use types can lead to disastrous floodings. Again, in mass flux schemes there is no information available about the sub grid variability of convective precipitation since there is no information about cloud cover. In our model this information is available. Since we calculate distribution functions for cloud types and we know precipitation rates and cloud number (therefore cloud cover) for each type separately, we have detailed information about precipitation variability within the grid cell. Therefore, it is straightforward to describe whether the grid mean precipitation rate is widely distributed or strongly concentrated in a few percent of the cell surface.

Cloud Overshooting: Overshooting is a critical phenomenon in nature. The term describes the penetration of a convective updraft through the tropopause. Figure 2.3 in chapter 2 shows that the one dimensional cloud model is in principle able to describe the basic features of this process. It is important for radiation and chemistry, since overshooting clouds are mainly responsible for the water vapour (cloud liquid water/ice) injection into the stratosphere [*Brewer*, 1949, *Dobson*, 1956, *Forster and Shine*, 1999, *Kirk-Davidoff et al.*, 1999].

5.4 Next Steps and back to Microphysics

The convective cloud field model, that has been introduced in this work, provides several chances for future research.
In this section we wish to give a concrete example of ongoing work.
As already mentioned, the model is constructed in a strict modular way.
There are three components:
a) The cloud model
b) the definition of interactive coefficients
c) the master equation to find the actual cloud spectrum

Each of these components can be replaced by alternatives. In fact, the difference between the FCCFM (chapter 2.) and the RCCFM (chapter 3), is given by a simplification of point b) and point c). To think of improvements of each of these components will be one of the major tasks in our future research. If we want to change the strict energetic approach in point b) for the definition of the interaction coefficients we just have to replace this module. Do we wish to use a more complex model for the physics of self-organizing systems? We just have to change module c). However, the first step to expand the model is to work on the cloud model. Here we wish to resume the "aerosol" topic from the first chapter. The strategy to use our model to investigate this question is straightforward:
If we wish to include aerosol effects on clouds, in our scheme we have to choose an appropriate cloud model. Basically it is sufficient to change the microphysical component in our cloud model. Since at the beginning it is advisable to keep things simple we use a simple "aerosol connection". Currently we have included the simple Kessler microphysics [*Kessler*, 1969]. To account for aerosols our first choice will be an approach from [*Berry*, 1967] taking into account aerosol loading and size distribution.

Figure 5.1 shows the rain formation rate (which is a good indicator for latent heat release in the cloud) versus liquid water content. The solid line shows the Kessler results while the dashed curve shows a maritime cloud (clean air) from the Berry scheme and the dotted curve shows a continental cloud (polluted air). The different energy releases for the different cloud types in the Berry scheme compared to Kessler leads automatically to different interaction coefficients K_{ij} in our cloud field model. Finally, this will cause different cloud distribution functions. To investigate this effect (if and how this will affect the global circulation) will be our next task.

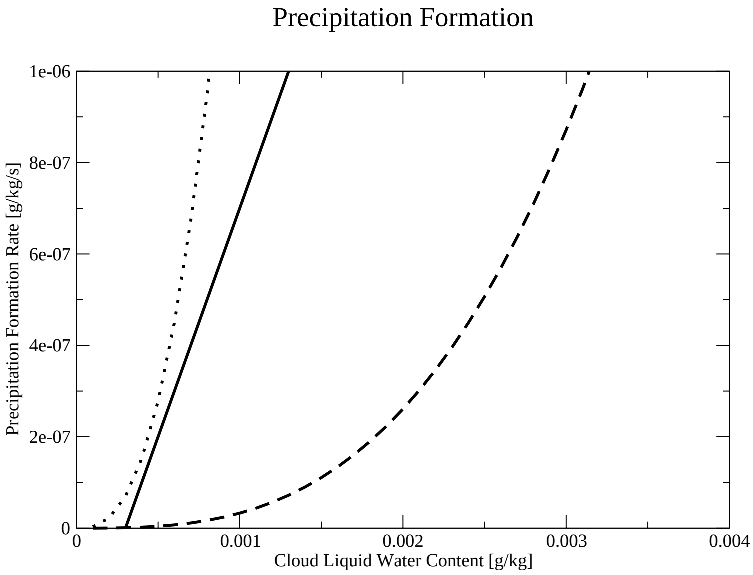

Figure 5.1 : Precipiation Formation Rate [g/kg/s]
solid line: Kessler; dotted line Berry (continental); dashed line Berry (maritime)

5.5 End

The topic of this work was to consider and to investigate an unsolvable problem. Can we hope to find a way to calculate an exact cloud distribution for grid columns as needed in global climate models? The answer is no. But we can improve and develop mathematical and physical models and tools to estimate and/or to predict the important statistical features of those cloud fields.
And there is need to do that!
Current GCMs have horizontal resolutions in the order of 100 km. Although the available computer power increases steadily, the global model that runs in a cloud resolving mode (order of 100 m) is far from being realizable in the next few years. Even if it would be possible to construct and run such a model, the investigation of cloud field organization would be an interesting challenge and a scientific question with its own relevance [*Haken* , 1977, *Haken* , 1983].
The CCFM, proposed in this work, is just a first step towards a new view on the cloud parameterization problem.
At the end of this work we wish to describe this strategy and the basic difference in the concepts and philosophies between current mass flux schemes and the CCFM:
Therefore we refer to the basic physics of thermodynamic systems. In this part of physics we have two different approaches:
The phenomenological and the statistical. Both terms are synonyms for the macroscopic and the microscopic treatment of a thermodynamical system. The phenomenological (macroscopic) thermodynamics describes a system with integrated, effective quantities (temperature, pressure, density). These quantities are only defined by the procedure to measure them, and (in the framework of this phenomenological approach) are not related to a microscopical structure of the considered system. In fact the term "microphysical state" is not defined in phenomenological thermodynamics.
The analogy to temperature, pressure, density are grid mean mass flux, heating rate, precipitation, etc. This analogy is not perfect but obvious. Of course one knows that a mass flux scheme describes a cloud ensemble. This is different to the phenomenological thermodynamics, where the considered system (gas, fluid) has no internal structure. Therefore, we know that a mass flux scheme describes the integrated effects of a cloud ensemble, but we have no chance to describe the internal structure on the basis of the knowledge of grid mean quantities. This is not a problem if we look for general structures and effects of clouds (heating, precipitation).
It becomes a serious problem when we look for other effects, like those are mentioned in section 5.2 and 5.3. In all these cases the knowledge of the averaged cloud ensemble quantities, as provided by a mass flux scheme, is insufficient. We need information about the "microscopic" cloud state. We need distribution functions for cloud structures. This is the analogy to the statistical thermodynamics. In this microscopic

theory one computes energy distributions for the single components of a macroscopic state (gas molecules, etc.). In the CCFM we have a numerical CDF. It gives us detailed information about the excitation of clouds. Do we have precipitation, ice formation, snow, lightning, etc. It is only up to the chosen one dimensional cloud model whether we include one of these effects or not.

Therefore, at the end of this work we cannot present a complete model ready to be used for operational climate studies, but a probably promising and interesting tool and concept for cloud science in the framework of climate system analysis.

Appendix A

List of Symbols and Abbreviations

A.1 Symbols

A, K_1, K_2, K_3	constants in the Kessler scheme
B	buoyancy
c	condensation rate
c_p	heat capacity at constant pressure
e	evaporation rate
g	acceleration of gravity
L	latent heat
q	specific humidity
q_l, Q_c	cloud liquid water
q_r, Q_h	rain water
q_s	saturation water vapour mixing ratio
Q_R	radiative heating
R	cloud radius
t	time coordinate
Δ t	time step
T	temperature
T_v	virtual temperature
T_p	cloud parcel temperature
$\underline{v}$	horizontal velocity (vector)
w	vertical velocity
z	vertical coordinate
x	horizontal coordinate
μ	dilution factor in the cloud model
ρ	density

A.2 Abbreviations

ACOH	Aerosol effect on COnvective Clouds
AGCM	Atmospheric General Circulation Model
ARM	Atmospheric Radiation Measurement program
AS	Arakawa Schubert scheme
CAPE	Convective Available Potential Energy
CCN	Cloud Condensation Nuclei
CDF	Cloud Distribution Function
CDNC	Cloud Droplet Number Concentration
CCFM	Convective Cloud Field Model
CTR	ConTRol simulation
CTR_s	ConTRol simulation Single time step
DJF	season: December, January, February
ECHAM	European Centre HAmburg Model
EUROCS	EUROpean Cloud Systems
EXP	EXPerimental simulation
EXP_s	EXPerimental simulation Single time step
FC	Fritsch Chappel scheme
FCCFM	Full Convective Cloud Field Model
GCM	General Circulation Model
ITCZ	Inter Tropical Convergence Zone
JJA	season: June, July, August
KP	Kreitzberg Perkey scheme
LES	Large Eddy Simulation
LNB	Level of Neutral Buoyancy
LWP	Liquid Water Path
MAM	season: May, April, March
RCCFM	Reduced Convective Cloud Field Model
SON	season: September, October, November
SPCZ	South Pacific Convergence Zone

Eine Wolke überhaupt ist nichts Fertiges, sie ist kein Product, sondern ein Process, sie besteht nur, indem sie entsteht und vergeht. Niemand wird die weisse Schaumstelle in einem hellen Gebirgsbach von der Höhe gesehn für etwas Festes auf dem Boden Liegendes halten. Und ist die Wolke, die den Gipfel des Berges umhüllt, etwas Anderes. Der Stein ist der Berg, der Bach die Luft, der Schaum die Wolke.

Heinrich Wilhelm Dove (1803-1879)
in "Meteorologische Untersuchungen"
Berlin, 1837.

Bibliography

[*Ackerman et al.*, 2000] Ackerman, A. S., O. B. Toon, D. E. Stevens, A. J. Heymsfield, V. Ramanathan, and E. J. Welton, Reduction of tropical cloudiness by soot, *Science*, **288**, 1042-1047, 2000.

[*Albrecht*, 1989] Albrecht, B.A., Aerosols, cloud microphysics, and fractional cloudiness, *Science*, **245**, 1227-1230, 1989.

[*Anthes*, 1977] Anthes, R. A., A cumulus parameterization scheme utilizing a one-dimensional cloud model. *Mon. Wea. Rev., 105*, 270-286, 1977.

[*Arakawa and Schubert*, 1974] Arakawa, A. and Schubert, W. H., 1974. Interaction of a cumulus ensemble with the large-scale environment, Part 1. *Journal of the Atmospheric Sciences*, **31**, 674-701.

[*ARM,EUROCS*] http://www.knmi.nl/samenw/eurocs/ARM/index.html

[*Benkovitz et al.*, 1994] Benkovitz, C.M., C.M. Berkowitz, R.C. Easter, S. Nemesure, R. Wagener and S. Schwartz, Sulfate over the north atlantic and adjacent continental regions: Evaluation for october and november 1986 using a three-dimensional model driven by observation-derivec meteorology, *J. Geophys. Res.*, **99**, 20725-20756,1994.

[*Benner and Curry*, 1998] Benner, T. C. and Curry, J. A., 1998. Characteristics of small tropical cumulus clouds and their impact on the environment. *Jounal of Geophysical Research*, **103**, 28753-28767.

[*Berry*, 1967] Berry, E. X., 1967. Cloud droplet growth by collection. *J. Atmos. Sciences*, **24**, 688-701.

[*Betts*, 1986] Betts, A. K., 1986. A new convective adjustment scheme. Part I: Observational and theoretical basis. *Quarterly Journal of the Royal Meteorological Society*, **112**, 677-691.

[*Betts and Miller*, 1986] Betts, A. K. and Miller, M. J., 1986. A new convective adjustment scheme. Part II: Single column tests using GATE wave, BOMEX, ATEX and arctic air-mass data sets. *Quarterly Journal of the Royal Meteorological Society*, **112**, 693-709.

[*Brewer*, 1949] Brewer, A. W., 1949. Evidence for a world circulation provided by the measurement of helium and water vapour distribution in the stratosphere. *Quarterly Journal of the Royal Meteorological Society*, **75**, 351 - 363.

[*Brown et al.*, 2001] Brown, A. R., et al. Large eddy simulations of the diurnal cycle of shallow cumulus convection over land. *Q. J. R. Meteorol. Soc.*, **127**, 2001.

[*Cahalan and Joseph*, 1989] Cahalan, R. F. and Joseph, J. H., 1989. Fractal statistics of cloud fields. *Monthly Weather Review*, **117**, 261-272.

[*Chlond and Müller]* Chlond. A., F. Müller, personal communication.

[*de Bort*, 1880] de Bort, D. Étude sur les causes qui de'terminant la circulation de l'atmosphere. *Ass. Franc. pur l'Ado. des Sci., Congress de Reims*, **44**, 1880.

[*Dobson*, 1956] Dobson, G. M. B., 1956. Origin and distribution of the polyatonic molecules in the atmosphere. *Proc. Roy. Soc. London*, **A236**, 187-193.

[*Emanuel et al.*, 1998] Emanuel, K. A., M. Zivkovic-Rothmann, Development and evaluation of a convection scheme for use in climate models, *J. of atmos. science*, **56**, 1766-1782, 1998.

[*Emanuel*, 1991] Emanuel, K. A., 1991. A scheme for representing cumulus convection in large-scale models. *Journal of the Atmospheric Sciences*, **48**, 2313-2335.

[*Emanuel*, 1994] Emanuel, K. A., 1994. Atmospheric Convection. *Oxford University Press.*

[*Emanuel and Raymond*, 1993] Emanuel, K. A., D. J. Raymond, 1993. The Representation of Cumulus Convection in Numerical Models. Meteorological Monographs. Published by the American Meteorological Society.

[*EUROCS]* http://www.cnrm.meteo.fr/gcss/EUROCS/EUROCS.html

[*Forster and Shine*, 1999] Forster, P. M. D., and K. P. Shine, 1999. Stratospheric water vapour changes as a possible cotributor to observed stratospheric cooling. *Geophys. Res/ Lett.*, **26**, 3309-3312.

[*Franzblau and Popp*, 1989] Franzblau, E., C. J. Popp, 1989. Nitrogen oxides produced from lightning. J. Geophys. Res., **94**, 11089-11104.

[*Gedney and Valdes*, 2000] Gedney, N., P. J. Valdes, 2000. The effect of Amazonian deforestation on the northern hemisphere circulation an climate. *Geophys. Res/ Lett.*, **27**, 3053-3056.

[*Guenther et al.*, 1995] Guenther, A., C.N. Hewitt, D. Erickson, R. Fall, et al., A global model of natural volatile organic compound emissions, *J. Geophys. Res.*, **100**, 8873-8892, 1995.

[*Graf et al.*, 1997] Graf, H.-F., J. Feichter, B. Langmann, Volcanic sulfur emissions: Estimates of source strength and its contribution to the global sulfate distribution, *J. Geophys. Res.*, **102**, 10727-10738, 1997.

[*Graf et al.*, 2001] Graf, H.-F., D. Rosenfeld, F. J. Nober, Sensitivity of global climate to the detrimental impact of smoke on rain clouds, *Max-Planck-Institute Report*, **315**, 2001.

[*Graf and Gräfe.*,1979] Graf, H.-F. and I. Gräfe, Precipitation distribution in the Berlin area depending on height weather and surface wind direction, *Z. Meteor.*, **29**, 56-64, 1979.

[*Kain and Fritsch*, 1990] Kain, J. S. and Fritsch, J. M., 1990. A one-dimensional entraining/detraining plume model and its application in convective parameterization. *Journal of the Atmospheric Sciences*, **47**, 2784-2802.

[*Kessler*, 1969] Kessler, E., 1969. On the distribution and concontinuity of water substance in atmospheric circulations. *Meteor Mono*, **32**.

[*Khain et al.*, 2001] Khain, A. P., D. Rosenfeld, A. Pokrovsky, Simulating convective clouds with sustained supercooled liquid water down to -37.5^{o}C using a spectral microphysics model, *Geophys. Res. Let. in press.*, 2001.

[*Kirk-Davidoff et al.*, 1999] Kirk-Davidoff, D. B., E. J. Hintsa, J. Anderson, and D. W. Keith, 1999. The effect of climate change on ozone depletion through changes in stratospheric water vapour. *Nature*, **402**, 399-401.

[*Lin and Neelin*, 2000] Lin, J. W., J. D. Neelin, 2000. Influence of a stochastic moist convective parameterization on tropical climate variability. *Geophys. Res. Let.*, **22**, 3691-3694.

[*Lotka*, 1925] Lotka, A. J., 1925. Elements of Physical Biology. Williams and Wilkins, Baltimore, 1925.

[*Mitchell*, 1999] Mitchell, J., 1999. Modeling cloud-climate feedbacks in predictions of human-induced climate change. Workshop on cloud processes and cloud feedbacks in large scale models, Reading.

[*Murray*, 1993] Murray, J. D., 1993. Mathematical Biology, Springer, Berlin, 1993.

[*Neggers et al.*, 2001] Neggers, R. A. J., H. J. J. Jonker, A. P. Siebesma, 2001. Size Statistics of Cumulus Cloud Properties in Large-Eddy Simulations. *J. Atm. Sciences*, in Press.

[*Haken* , 1977] Haken H., Synergetics, An Introduction, *Springer, Berlin, Heidelberg, New York*, 1977.

[*Haken* , 1983] Haken H., Advanced Synergetics, *Springer, Berlin, Heidelberg, New York*, 1983.

[*Hansen et al.*, 1997] Hansen, J., M.Sato, and R. Ruedy, Radiative forcing and climate response, *J. Geophys. Res.*, **102**, 6831-6864, 1997.

[*Hao et al.*, 1990] Hao, W. M., M. H. Liu, P.J. Crutzen, Estimates of annual and regional releases of co2 and other trace gases to the atmosphere from fires in the tropics, Springer Verlag, New York, 1990.

[*Hobbs et al.*, 1997] Hobbs, V. P., J. S. Reid, R. A. Kotchenruther, R. J. Ferek, R. Weiss, Direct radiative forcing by smoke from biomass burning, *Science*, **275**, 1777-1778, 1997.

[*Kettle et al.*, 1996] Kettle et al., A preliminary global data base of sea surface dimethyl sulfide measurments and a simple model to predict sea surface dimethyl sulfide as a function of latitude, longitude and month, *EOS*, **77**, 417, 1996.

[*Kuo*, 1965] Kuo, H. L., On formation and intensification of tropical cyclons through latent heat release by cumulus convection, *J. Atmos. Sci.*, **22**, 40-63, 1965.

[*Kuo*, 1974] Kuo, H. L., Further studies of the parameterization of the influence of cumulus convection on the large-scale flow. *J. Atmos. Sci.*, **31**, 1232-1240, 1974.

[*Kreitzberg and Perkey*, 1976] Kreitzberg, C. W., and D. Perkey, Release of potential instability. Part 1: A seqeuntial plume model within a hydrostatic primitive equation model. *J. Atmos. Sci.*, **33**, 456-475, 1976.

[*Kreitzberg and Perkey*, 1977] Kreitzberg, C. W., and D. Perkey, Release of potential instability. Part 2: The mechanism of convective /mesoscale interaction. *J. Atmos. Sci.*, **34**, 1569-1595, 1977.

[*Lahav and Rosenfeld*, 2000] Lahav, R., Rosenfeld, D., Microphysical characterization of the israel clouds from aircraft and satellites, 13^{th} *International Conference on Clouds and Precipitation, Proceedings, Volume 2*, 732, 2000.

[*Liousse et al.*, 1996] Liousse, C. , J. E. Penner, C. Chuang, J. J. Walton, H. Eddleman, H. Cachier, A global three-dimensional model study of carbonacceous aerosols, *J. Geophys. Res.*, **101**, 19411-19432, 1996.

[*Lohmann and Feichter*, 1997] Lohmann, U., J. Feichter, Impact of sulfate aerosols on albedo and lifetime of clouds, *J. Geophys. Res.*, **102**, 13685-13700, 1997.

[*Lohmann, et al.*, 1999] Lohmann, U., J. Feichter, C.C. Chuang, J.E. Penner, Predicting the number of cloud droplets in the ECHAM GCM, *J. Geophys. Res.*, **104**, 9169-9198, 1999.

[*Lohmann et al.*, 2000] Lohmann, U., J. Feichter, J.E. Penner and R.Leaitel, Indirect effects of sulfate and carbonaceous aerosols: A mechanistive treatment, *J. Geophys. Res.*, **105**, 13685-13700, 2000.

[*Lord*, 1982] Lord, S. J., Interaction of a cumulus ensemble with the large-scale environment. Part III: Semiprognostic test of the Arakawa Schuber cumulus parameterization. *J. Atmos. Sci.*, **39**, 88-103, 1982.

[*Lord et al.*, 1982] Lord, S. J., W. C. Chao, and A. Arakawa, Interaction of a cumulus ensemble with the large-scale environment. Part III: The discrete model. *J. Atmos. Sci.* **39**, 104-113, 1982.

[*Manabe and Strickler*, 1964] Manabe, S., and R. Strickler, Thermal equilibrium of the atmosphere with a convective adjustment. *J. Atmos. Sci.* **21**, 361-385, 1964.

[*Manabe et al.*, 1965] Manabe, S., J. Smagirinsky, and R. Strickler, Simulated climatology of a general circulation model with a hydrological cycle. *Mon. Wea. Rev.*, **93**, 769-798, 1965.

[*Mossop and Hallet*, 1974] Mossop, S.C., J.Hallet, *Science*, **186**, 632, 1974.

[*Nordeng*, 1994] Nordeng, T., Extended versions of the convective parameterisation scheme at ECMWF and their impact on the mean and transient activity of the model in the tropics. Tech Memo 206, 41 pp, Euro Cent for Medium Range Weather Forecasts, Reading, England.

[*Penner et al.*, 1998] Penner, J.E., C.C. Chuang and K. Grant, Climate forcing by carbonaceous and sulfate aerosols. *Climate Dyn.*, **14**, 839-851, 1998.

[*Price and Rind*, 1992] Price, C., D. Rind, 1992. A simple Lightning Parameterization for Calculating Global Lightning Distributions. *J. of Geophys. Res.*, **97**, 9919-9933.

[*Pruppacher and Klett*, 1997] Pruppacher, H. R. and J. D. Klett, Microphysics of clouds and precipitation, Kluwer Academic Publishers,2nd edn., 1997.

[*Rangno and Hobbs*, 1994] Rangno, A. and P.V. Hobbs, *Q. J. R. Met. Soc.*, **120**, 573, 1994.

[*Reynolds*, 1901] Reynolds, O., 1901. On the dynamical theory of incompressible viscous fluids and the determination of the criterion. *Cambridge University Press*, **2**, 535-577.

[*Roeckner et al.*, 1996] Reockner, E., et al., The atmospheric general circulation model ECHAM4: Model description and simulation of present day climate, *Max-Planck-Institut Report*, **218**, 1996.

[*Roelofs et al., 1998]* Roelofs, G.J., J. Lelieveld and L. Ganzeveld, Simulation of global sulfate distribution and the influence of effective cloud drop radii with a coupled photochemistry-sulfur cycle model, *Tellus*, **50B**, 224-242, 1998.

[*Rosenfeld and Lensky*, 1998] Rosenfeld, D., M.I. Lensky, Satellite-Based insights into precipitation formation processes in continental and maritime convective clouds, *Bull. of the Am. Meteor. Soc.*, **79**, 2457-2476, 1998.

[*Rosenfeld*, 1999] Rosenfeld, D., TRMM observed first direct evidence of smoke from forest fires inhibiting rainfall, *Geophys. Res. Let.*, **20**, 3105-3108, 1999.

[*Rosenfeld*, 2000 a] Rosenfeld, D., Suppression of rain and snow by urban and industrial air pollution, *Science*, **287**, 1793-1796, 2000.

[*Rosenfeld and Woodley*, 2000] Rosenfeld, D., and W. L. Woodley, Convective clouds with sustained highly supercooled liquid water down to -37.5^{0}C, *Nature*, **405**, 440-442, 2000.

[*Rotstayn et al.*, 2000] Rotstayn, L.D., B. F. Ryan, J. E. Penner, Precipitation changes in a GCM resulting from the indirect effect of anthropogenic aerosols, *Geophys. Res. Letters*, **27**, 3045-3048, 2000.

[*Spiro et al.*, 1992] Spiro, P.A., D.J. Jacob, J. A. Logan, Global inventory of sulfur emissions with 1 x 1 resolution, *J. Geophys. Res.*, **97**, 6023, 1992.

[*Tegen et al.*, 1996] Tegen, I, A.A. Lacis and I. Fung, The influence on climate forcing of mineral aerosols from disturbed soils, *Nature*, **380**, 419-422, 1996.

[*Textor et al.*, 2000] Textor, C., H.-F. Graf, A. P. Khain, Numerical simulation of the interaction of biomass burning aerosols and cloud microphysics, 13^{th} *International Conference on Clouds and Precipitation, Proceedings, Volume 2*, 905, 2000.

[*Tiedtke*, 1989] Tiedtke, M., A comprehensive mass flux scheme for cumulus cloud parameterisation in lagre-scale models. *Quart. J. Roy. Meteor. Soc.*, **117**, 1779-1800, 1989.

[*Twomey*, 1977] Twomey, S., The influence of pollution on the shortwave albedo of clouds, *J. Atmos. Sci.*, **34**, 1149-1152, 1977.

[*Volterra*, 1931] Volterra, V., 1931. Lecons sur la Theorie Mathematique de la Lutte pour la Vie. Gauthier Villars, Paris.

[*Warner*, 1968] Warner, J., A reduction in rainfall associated with smoke from sugarcane fires - An inadvertent weather modification, *J. Appl. Meteorl.*, **7**, 247-251, 1968.

[*Walker*, 1924] Walker, G., Correlations in seasonal variations of weather IX. *India. Meteor. Dept. Memoirs*, **24**, 275-332, 1924.

[*Weinstein and MacCready*, 1969] Weinstein, A. I., P. B. MacCready, 1969. An isolated cumulus cloud modification project. *J. of Appl. Met.*, **8**, 936-947.

[*Weger et al.*, 1992] Weger, R. C., J. Lee, T. Zhu, and R. M. Welch, Clustering, Randomness and Regularity in Cloud Fields: 1. Theoretical Considerations. *J. Geophys. Res.*, **97**, 20519-20536, 1992.

[*Weger et al.*, 1993] Weger, R. C., J. Lee, and R. M. Welch, Clustering, Randomness and Regularity in Cloud Fields: 3. The Nature and Distributions of Clusters. *J. Geophys. Res.*, **98**, 18449-18463, 1993.

[*Zhu et al.*, 1992] Zhu, T., J. Lee, R. C. Weger, and R. M. Welch, Clustering, Randomness and Regularity in Cloud Fields: 2. Cumulus Cloud Fields. *J. Geophys. Res.*, **97**, 20537-20558, 1992.